


# Therapeutic Targeting of Histone H3 Lysine 36 Trimethylation-Deficient Cancers

DPhil thesis supervised by
Dr. Timothy Humphrey

Kirsten Anne Lopez
St. Anne's College

Department of Oncology
University of Oxford
Trinity Term 2019



# Abstract

## Therapeutic Targeting of Histone H3 Lysine 36 Trimethylation-Deficient Cancers

Kirsten Anne Lopez
St. Anne's College
Department of Oncology

Doctor of Philosophy
University of Oxford
Trinity Term 2019

Histone modifications play diverse and essential roles in the maintenance of genome integrity, as evidenced by the frequency at which different histone marks are dysregulated during tumourigenesis. The trimethylation of histone H3 at lysine 36 (H3K36me3) and SETD2, the enzyme solely responsible for this histone mark, are important in many cellular processes and have been reported to be lost or mutated in cancers. Targeting cells that are deficient in H3K36me3 or SETD2 is therefore an attractive therapeutic strategy for specifically killing tumour cells with minimal effect on normal tissue using the concept of synthetic lethality.

Using a previously reported synthetic lethal interaction between SETD2 and the WEE1 kinase as a starting point, a high-throughput small-molecule compound screen was performed in cells in which SETD2 had been deleted using CRISPR-Cas9 technology. The aim of this screen was to identify two categories of hits: (1) those that enhance the SETD2-WEE1 synthetic lethality (synergy hits) and (2) those that target SETD2-CRISPR cells on their own (novel synthetic lethality hits).

Analysis of the synergy hits focused on histone deacetylases (HDACs), which revealed that the Class I HDACs HDAC1 and HDAC2 had differential effects on the SETD2-WEE1 synthetic lethality. Furthermore, depletion of both HDACs individually led to a significant loss of viability specifically in SETD2-CRISPR cells. The results suggest a putative synthetic lethality between SETD2 and HDAC2 that bears certain similarities to the relationship between SETD2 and WEE1.

The most potent among the novel synthetic lethality hits was a compound called RITA, which demonstrated the ability to target SETD2 deficiency in the form of CRISPR knockout, siRNA knockdown, and naturally occurring mutations. This was accompanied by a striking upregulation and activation of the p53 tumour suppressor, activation of the DNA damage response, cell cycle arrest, and apoptosis. These phenotypes were further associated with increased levels of replication stress markers and reduced replication fork velocity. The potential mechanism of action of this compound was investigated via a number of strategies based on current knowledge of SETD2 and RITA, as well as more exploratory approaches. Overall, the data indicate that perturbations in the G1/S transition and replication stress play key roles in mediating RITA's cytotoxicity in the context of SETD2 loss.

# Acknowledgements

First, I would like to thank my supervisor Dr. Timothy Humphrey for giving me the opportunity to work in his lab and on this project, as well as his unwavering support and encouragement throughout my PhD. I would also like to thank the members of the Humphrey Group: our incredibly patient and helpful postdocs Dr. Sovan Sarkar, Dr. Chen-Chun Pai, Dr. Fiona Okonjo, and Dr. Sam Durley; and my fellow PhD students Lee Armfield and Linda van Bijsterveldt. They have been an indispensable part of my life here in Oxford and I am fortunate to have met and worked with them. I am also very grateful to Dr. Hongbin Yang (from the D'Angiolella Group) and Dr. Juri Na (from the Kiltie Group) for their technical assistance, scientific advice, and moral support. In addition, I would like to thank Urology Cancer Research (UCARE) for providing me with a study grant for my living expenses.

This project relied heavily on collaborations with other groups both within Oxford and in other parts of the UK. My sincere thanks to Dr. Daniel Ebner and Ms. Elena Seraia from the Target Discovery Institute for their assistance with the high-throughput screen. Thank you to Dr. Deborah Sneddon, Dr. Bart Cornelissen, and Prof. Stuart Conway for their invaluable contributions to the chemical modification of RITA and for providing a chemist's perspective on this investigation. I would also like to thank Prof. George D. Jones, Mr. Christian Cooper, and Mr. Michalis Challoumas from the University of Leicester for performing the comet assays, as well as Prof. Peter McHugh for his suggestions and insights on the crosslinking aspects of the RITA chapter.

Finally, I would like to dedicate this thesis to my family, especially to my parents who inspired and continue to inspire me to pursue scientific knowledge and provided the financial and emotional support I need to be here in the first place.

# Declaration

I declare:

The work presented in this thesis is my own, with the exception of:

- The modified comet assay, which was done by Mr. Christian Cooper and Mr. Michalis Challoumas from Prof. George D. Jones's group at the University of Leicester
- The synthesis of the RITA variants, which was done by Dr. Deborah Sneddon from Dr. Bart Cornelissen's group at the University of Oxford
- The RNA sequencing experiment, which was done by Novogene Co. Ltd.

No portion of this work has been previously submitted for another qualification at this, or any other university.

Signed .....

Kirsten Anne Lopez

# Nomenclature

Mammalian

Genes are denoted by capital letters in italics, e.g. *SETD2*. Homozygous knockouts are shown as (-/-) respectively e.g. SETD2(-/-). Protein names are denoted by capital letters in non-italics, e.g. SETD2.

*Schizosaccharomyces pombe*

Genes are denoted by lower-case letters in italics, e.g. *set2*. Protein names are given an initial capital letter followed by lower-case letters in non-italics, e.g. Set2.

# Abbreviations

| | |
|---|---|
| °C | degree Celsius |
| µg | microgram |
| µl | microlitre |
| µM | micromolar |
| 53BP1 | p53-binding protein 1 |
| ac | acetyl |
| Alt-EJ | alternative end joining |
| ATP | adenosine triphosphate |
| bp | base pair |
| BrdU | 5-bromo-2'-deoxyuridine |
| BSA | bovine serum albumin |
| CDK | cyclin-dependent kinase |
| CldU | 5-chloro-2'-deoxyuridine |
| DDR | DNA damage response |
| DMEM | Dulbecco's modified minimal essential medium |
| DMSO | dimethyl sulphoxide |
| DNA | deoxyribonucleic acid |
| dATP | deoxyadenosine triophosphate |
| dNDP | deoxynucleoside diphosphate |
| dNTP | deoxyribonucleotide triphosphate |

| | |
|---|---|
| DSB | DNA double-strand break |
| DTT | dithiothreitol |
| dTTP | deoxythymidine triphosphate |
| dUTP | deoxyuridine triphosphate |
| E1 | ubiquitin-activating enzyme |
| E2 | ubiquitin-conjugating enzyme |
| E3 | ubiquitin-ligating enzyme |
| EDTA | ethylenediaminetetraacetic acid |
| FACS | fluorescence-activated cell sorting |
| FBS | foetal bovine serum |
| g | gram |
| *g* | relative centrifugal force |
| GO | gene ontology |
| Gy | gray |
| H3K36 | histone H3 lysine 36 |
| HAT | histone acetyltransferase |
| HCl | hydrochloric acid |
| HDAC | histone deacetylase |
| HMT | histone methyltransferase |
| HR | homologous recombination |
| HRP | horseradish peroxidase |
| IdU | 5-iodo-2′-deoxyuridine |
| IR | ionising radiation |
| kDa | kilodalton |
| LB | Luria-Bertani medium |
| LOH | loss of heterozygosity |
| M | molar |
| me1 | monomethyl |
| me2 | dimethyl |
| me3 | trimethyl |
| mg | milligrams |
| ml | millilitres |
| mM | millimolar |
| MMEJ | microhomology-mediated end joining |
| NaCl | sodium chloride |
| ng | nanograms |
| nM | nanomolar |
| NHEJ | non-homologous end joining |
| nM | nanomolar |

| | |
|---|---|
| NTP | ribonucleotide triphosphate |
| OD | optical density |
| p | p-value for Student's t-test |
| PBS | phosphate buffered saline |
| PCR | polymerase chain reaction |
| pg | picograms |
| qPCR | quantitative polymerase chain reaction |
| RNA | ribonucleic acid |
| RNase | ribonuclease |
| RNR | ribonucleotide reductase |
| RPA | replication protein A |
| RRM2 | ribonucleotide reductase regulatory subunit M2 |
| *S. cerevisiae* | *Saccharomyces cerevisiae* |
| *S. pombe* | *Schizosaccharomyces pombe* |
| SAGA | Spt-Ada-Gcn5 acetyltransferase |
| SD | standard deviation |
| SDS | sodium lauryl sulphate |
| SDS-PAGE | sodium lauryl sulphate-polyacrylamide gel electrophoresis |
| SET | Su3-9, Enhancer-of-zeste and Trithorax |
| SETD2 | SET Domain Containing 2 |
| SSB | single-strand break |
| ssDNA | single-stranded DNA |
| su | sumo |
| Tris | tris (hydroxymethyl) methylamine |
| U | units |
| ub | ubiquitin |
| UV | ultraviolet |
| V | volts |
| w/v | weight per volume |

Contents

Abstract ..... i

Acknowledgements ..... ii

Declaration ..... iii

Nomenclature ..... iv

Abbreviations ..... iv

1. Introduction ..... 1

1.1 Cancer biology and its hallmarks ..... 1

1.2 The eukaryotic cell cycle ..... 2

1.3 DNA damage repair pathways ..... 6

1.4 Cancer therapeutics: from DNA-damaging agents to targeted therapy ..... 10

1.5 Synthetic lethality and cancer ..... 14

1.6 Epigenetics ..... 19

1.7 SETD2 ..... 21

1.8 Synthetic lethality of SETD2 and WEE1 ..... 25

1.9 Thesis aims ..... 26

2. Materials and Methods ..... 29

2.1 Cell Culture ..... 29

2.2 Cell Lines ..... 29

2.3 High-throughput Compound Screening ..... 30

2.4 Statistical Analysis of Screening Results ..... 31

2.5 Validation of Positive Hits ..... 31

2.6 Drugs and Inhibitors ..... 32

2.7 Resazurin Assay for Cell Viability ..... 32

2.8 Clonogenic Survival Assay ..... 33

2.9 Apoptosis Detection Assay ..... 33

2.10 siRNA Transfection ..... 34
2.11 Bacterial Transformation ..... 34
2.12 Plasmid Purification ..... 35
2.13 Plasmid Transfection ..... 36
2.14 Histone Extraction ..... 36
2.15 Western Blotting ..... 37
2.16 Cell Cycle Analysis by BrdU Incorporation ..... 38
2.17 Immunofluorescence Staining of Foci ..... 39
2.18 DNA Fibre Assay ..... 40
2.19 RNA Sequencing ..... 41
2.20 Modified Single-Cell Gel Electrophoresis (Comet) Assay ..... 42
3. Therapeutic targeting of SETD2 deficiency and modulation of the SETD2-WEE1 synthetic lethality ..... 45
3.1 High-throughput compound screening ..... 46
3.2 Histone deacetylase inhibition enhances the cytotoxic effects of WEE1 inhibition regardless of SETD2 status ..... 48
3.3 Class I HDACs HDAC1 and HDAC2 mediate distinct effects on the SETD2-WEE1 synthetic lethality ..... 52
3.4 HDAC2 displays putative synthetic lethality with SETD2 and leads to RRM2 downregulation without any cell cycle defects ..... 55
3.5 Dual HDAC1/2 inhibitor romidepsin selectively targets SETD2-deficient cells and induces more rapid G1 arrest in the absence of SETD2 ..... 60
3.6 Chapter Discussion ..... 64
4. Therapeutic targeting of SETD2 loss with novel synthetic lethal interactions ..... 69
4.1. Identification and validation of putative synthetic lethal hits ..... 70
4.2. RITA induces p53 upregulation and activation, as well as apoptotic cell death, specifically in SETD2-deficient cancer cells ..... 74

4.3. RITA induces cell cycle arrest and activates the DNA damage response specifically in SETD2-deficient cancer cells ..... 80

4.4. RITA induces replication stress specifically in SETD2-deficient cancer cells ..... 85

4.5. Chapter Discussion ..... 88

5. Molecular mechanisms of the p53 reactivator RITA in the context of SETD2 loss .....91

5.1. RITA sensitivity is not dependent on homologous recombination proficiency, dNTP supply, or CDK activation ..... 92

5.2. RITA sensitivity is enhanced by SETD2 loss in the presence or absence of p53.... 99

5.3. RITA is able to target cells deficient in the crosslink repair protein XPF but does not lead to increased DNA-DNA crosslink formation in the absence of SETD2.....102

5.4. RITA sensitivity in the absence of SETD2 is associated with altered expression of genes involved in DNA replication and the G1/S transition .....107

5.5. Modification of RITA's terminal hydroxyls and ring groups modulates its potency against SETD2-deficient cells .....113

5.6. Chapter Discussion .....118

6. Discussion.....124

6.1 Epigenetic modifiers as targets in cancer therapy .....124

6.2 Targeting the loss of epigenetic regulators via synthetic lethality .....127

6.3 Past and current attempts to target p53 in human cancers .....129

6.4 Future work.....134

7. Bibliography .....136

8. Appendix.....161

8.1 List of Top 100 Hits for New Synthetic Lethal Compounds (0.1 μM) .....161

8.2 List of Top 100 Hits for Synergistic Compounds (0.1 μM) .....165

# 1. Introduction

## 1.1 Cancer biology and its hallmarks

Cancer is a disease of abnormal, dysregulated cell division that can affect almost every organ in the human body. It is further subdivided based on the cell type and tissue of origin, with each subtype and individual patient having unique molecular and physiological characteristics. A set of overarching features or hallmarks that define cancer as a whole has been proposed and serves to guide the scientific understanding of the complexities of tumourigenesis. These six acquired capabilities of cancer, which are cellular adaptations necessary for malignant transformation, are: self-sufficiency in growth signals, insensitivity to anti-growth signals, evading apoptosis, tissue invasion and metastasis, sustained angiogenesis, and limitless replicative potential (Hanahan and Weinberg, 2000). These were further refined and expanded upon in a subsequent review by the same authors in 2011 (Fig. 1.1), where two emerging hallmarks and two enabling characteristics were added: deregulating cellular energetics, avoiding immune destruction, genome instability and mutation, and tumour-promoting inflammation (Hanahan and Weinberg, 2011). In particular, the acquisition and accumulation of mutations and chromosomal aberrations over successive rounds of cell division is a key factor in the development of other oncological features in both hereditary and sporadic cancers (Negrini et al., 2010).

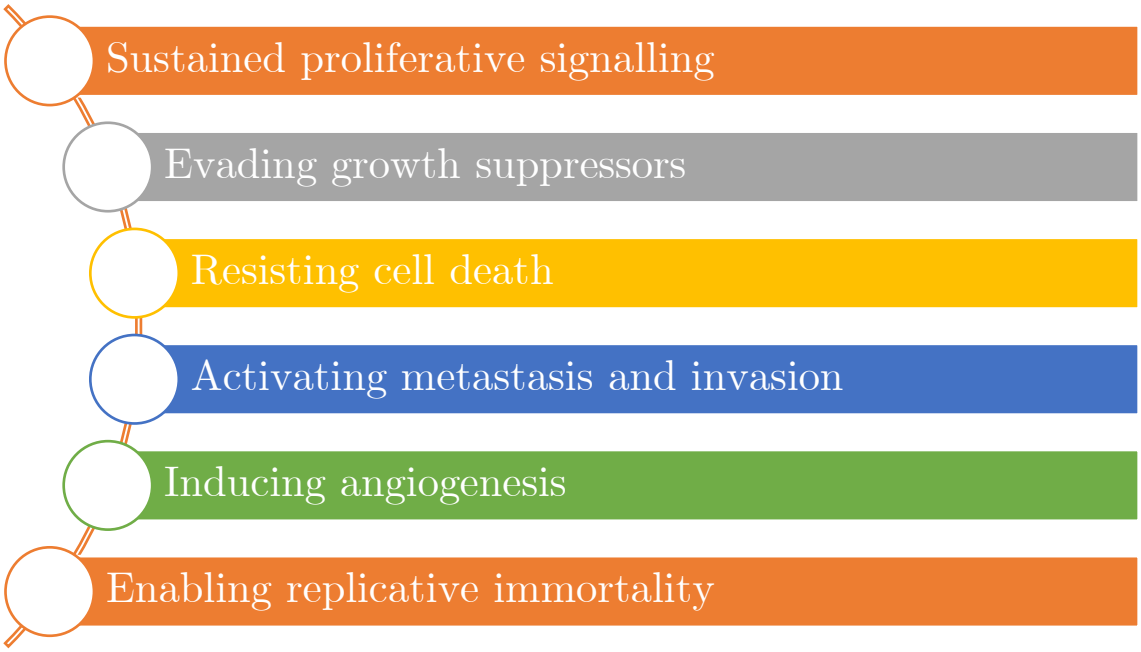



Figure 1.1. Hallmarks of cancer, refined and updated in 2011 by Hanahan and Weinberg.

## 1.2 The eukaryotic cell cycle

Cell division is a tightly regulated, multistep procedure that coordinates cell growth, genome duplication, and segregation of cell components into two daughter cells. It is divided into four main phases, each characterised by distinct molecular and biochemical events (Fig. 1.2). Non-dividing or quiescent cells are said to be in G0, a transient state triggered by either the absence of growth factor signalling or the presence of growth inhibitory stimuli (Coller et al., 2006). Upon re-entry into the cell cycle, cells begin in G1 phase and make the necessary preparations for the main event of the next phase: DNA replication. S phase is spent on the critical task of ensuring the entirety of the cell's genome is completely and accurately copied. Subsequently, the cell enters G2 phase in preparation for the final stage: cell division. Finally, mitosis

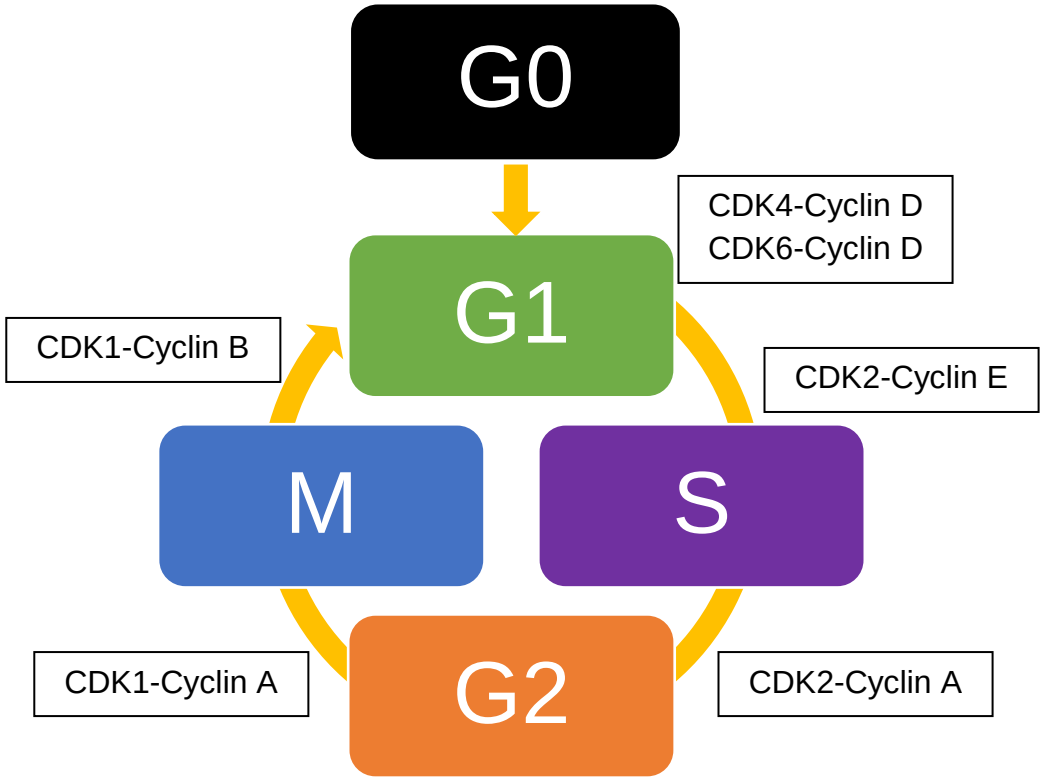



Figure 1.2. Diagram of the eukaryotic cell cycle, including the CDK-cyclin complexes that act predominantly at each phase or transition. Adapted from (Vermeulen et al., 2003).

itself is subdivided into several phases during which the cell divides its organelles and genetic material into two equal portions and reforms into two new cells (Vermeulen et al., 2003). The key regulators of the orderly progression through the cell cycle are cyclin-dependent kinases (CDKs) and their co-activator cyclins (Evans et al., 1983; Nurse et al., 1976). CDKs are expressed constitutively but remain inactive until bound by their partner cyclins, after which they proceed to phosphorylate a plethora of downstream targets and mediate the activation or inactivation of cell cycle components (Morgan, 1995; Pines, 1995). In contrast, most cyclins are present only at specific points in the cell cycle, thereby activating CDK activity only when necessary (Fig. 1.2) (Evans et al., 1983; Pines, 1991).

At the boundary between each cell cycle phase is a checkpoint that ensures the appropriate conditions are met prior to entering the next phase (Hartwell and Weinert, 1989). During G1, the restriction point determines whether to fully commit to cell cycle progression or to return to G0 (Pardee, 1974). Immediately before S phase, the G1/S checkpoint is responsible for detecting whether preparations for DNA replication have been completed, as well as the presence of damaged DNA. S phase entry can be delayed via either accelerated degradation of the phosphatase CDC25A (Mailand et al., 2000), which dephosphorylates and activates the CDK2-cyclin E complex (Blomberg and Hoffmann, 1999; Sexl et al., 1999), or activation of the tumour suppressor p53 and its downstream effector, the CDK inhibitor p21 (Harper et al., 1995).

Once the cell successfully enters S phase, the intra-S checkpoint is in charge of sensing any mishaps that arise from or could interfere with the process of DNA

replication. This is predominantly mediated by two serine/threonine kinases: Ataxia Telangiectasia Mutated (ATM) and ATM and Rad3-related (ATR) and their respective downstream pathways, which also coordinate the DNA damage response (DDR) in other cell cycle phases. As demonstrated by the disease after which it is named, ATM and its effector kinase CHK2 are mainly involved in the detection and repair of double-strand breaks (DSBs) (McKinnon, 2012). On the other hand, ATR responds to a wider variety of DNA lesions because of its ability to detect single-stranded DNA (ssDNA) bound by the ssDNA-binding protein Replication Protein A (RPA) (Zou and Elledge, 2003). Since disruptions to the replication machinery usually lead to the formation of ssDNA due to the uncoupling of the DNA polymerase and helicase, ATR and its downstream effector kinase CHK1 are the dominant mediators of the replication stress response (Zeman and Cimprich, 2014).

Another DNA damage checkpoint is present at the G2/M transition and is critical to prevent damaged or incompletely replicated DNA from being passed on to subsequent generations. As with G1/S checkpoint, cell cycle arrest at the G2/M boundary can be mediated by the p53 pathway via CDK inhibitors such as p21 (Bunz et al., 1998) or via dissociation of CDK1-cyclin B complexes by GADD45 (Zhan et al., 1999). There are also p53-independent mechanisms of G2/M arrest, including the inhibitory phosphorylation of CDK1 by the WEE1 kinase, which attenuates the activity of CDK1-cyclin B (Parker and Piwnica-Worms, 1992). Furthermore, nuclear CDK1 can be maintained in its phosphorylated state via CHK1/CHK2-mediated

phosphorylation of CDC25, which promotes its binding to 14-3-3 proteins and subsequent sequestration in the cytoplasm (Peng et al., 1997).

The importance of the G1/S and G2/M checkpoints is readily apparent in mitosis, where the DDR is inactivated at multiple levels. ATM signalling is still triggered by DSBs, but activation of CHK2 is attenuated by the mitotic kinase PLK1 (van Vugt et al., 2010). Components of DSB repair pathways, such as the ubiquitin ligase RNF8 and the DSB sensor 53BP1, are also phosphorylated to prevent their association with damaged DNA (Lee et al., 2014; Orthwein et al., 2014). A complete DDR is delayed until the subsequent G1 phase, which means that mitotic cells display a higher sensitivity to DNA damage (Giunta et al., 2010). Incongruously, this suppression of the damage response was revealed to be critical for the maintenance of genome stability via the prevention of repair-induced telomere fusions during mitosis (Orthwein et al., 2014).

## 1.3 DNA damage repair pathways

DNA replication is a highly accurate process with error rates estimated between 1 per $10^6$ and 1 per $10^{11}$ bases for DNA polymerases with proofreading capability (Drake et al., 1998; Kunkel, 2004). Despite this, mutations and DNA damage from endogenous and exogenous sources can accumulate over a cell's lifetime and must be dealt with before the cell divides and passes on its genome. Eukaryotes have evolved a sophisticated network of molecular pathways to detect and repair various types of lesions, from single nucleotide mismatches to highly toxic DSBs (Table 1.1). Each

Table 1.1. Types of DNA damage and their corresponding repair pathways. Adapted from (Torgovnick and Schumacher, 2015)

| Type of DNA Damage | DNA Repair Pathway |
|---|---|
| O-methylated bases ($O^6$-methylguanine) | Direct repair by $O^6$-methylguanine-DNA methyltransferase (MGMT) |
| N-methylated bases, abasic sites, single-strand nicks or breaks (SSBs) | Base excision repair (BER) |
| Base mismatches, small insertions/deletions | Mismatch repair (MMR) |
| Intrastrand crosslinks, bulky DNA adducts | Nucleotide excision repair (NER) |
| Single-strand breaks (SSBs) | Single-strand break repair (SSBR) |
| Double-strand breaks (DSBs) | Nonhomologous end-joining (NHEJ)<br>Homologous recombination (HR)<br>Alternative end-joining (Alt-EJ) |
| Interstrand crosslinks (ICLs) | Fanconi anaemia (FA) pathway |

pathway includes factors that identify the type of damage, recruit downstream factors, and catalyse the removal and/or repair of the lesion.

DNA bases can be modified by alkylation, oxidation, reduction, or fragmentation due to the presence of reactive oxygen species from normal cellular metabolism or exogenous factors (e.g. ionising/UV radiation, alkylating agents). $O^6$-methylguanine, for example, is produced by purine alkylation and is highly mutagenic (Green et al., 1984; Loechler et al., 1984). The enzyme $O^6$-methylguanine-DNA methyltransferase (MGMT), as its name suggests, recognises and binds directly to $O^6$-methylguanine and repairs it by transferring the methyl group to one of its own cysteine residues (Pegg, 1990). Damaged bases are also dealt with by the base excision repair (BER) pathway, which uses several DNA glycosylases and the APE1 endonuclease to remove the damaged base, followed by DNA polymerases and ligases to fill in the gap left behind

(Krokan and Bjoras, 2013). In addition, modified bases and errors during DNA replication can lead to base mispairing and, subsequently, point mutations; these are dealt with by the mismatch repair (MMR) pathway, which involves the recognition of the mismatch by the MutSα complex followed by the excision of the incorrect base by MutLα and gap filling by polymerases (Kunkel and Erie, 2015). Bulkier DNA lesions, such as intrastrand crosslinks, are detected and repaired by the nucleotide excision repair (NER) pathway, which either scans the entire genome (GG-NER) or is alerted by stalled transcriptional machinery (TC-NER) (Marteijn et al., 2014). Both NER pathways are comprised of proteins in the Xeroderma Pigmentosum (XP) family of proteins, named after the photosensitivity syndrome associated with XP gene mutations (Cleaver, 1968).

Another form of DNA damage can occur in the form of breaks in one or both strands of the DNA double helix. Single-strand breaks (SSBs) are quickly bound by poly(ADP-ribose) polymerase (PARP), which promotes the recruitment of other enzymes necessary for end processing, gap filling, and ligation (Caldecott, 2008). Double-strand breaks (DSBs) are more dangerous lesions with several repair mechanisms that are applied in a cell cycle-dependent and location-dependent manner. In mammalian cells, the dominant DSB repair pathway is classical non-homologous end joining (c-NHEJ), which efficiently re-ligates most DSBs with minimal end processing (Beucher et al., 2009). However, since most DSB ends need to be processed to remove a few nucleotides prior to ligation, c-NHEJ often leads to short insertions or deletions and is considered an error-prone form of repair. In contrast, DSB repair by

homologous recombination (HR), as its name indicates, requires a homologous template to fill in the break; as such, HR is only available in cells that have completed S-phase and therefore have homologous chromosomes. HR is a complex multi-step process that involves DSB end resection, homology search, strand invasion, and DNA synthesis (Wright et al., 2018). In situations where these two major DSB repair pathways are impaired or inhibited, cells can switch to alternative end joining (alt-EJ), which is also known as microhomology-mediated end joining (MMEJ) because it involves short regions of complementarity (microhomologies) annealing together and the subsequent overhangs being cleaved, leading to larger insertions/deletions compared to c-NHEJ (Sfeir and Symington, 2015).

Interstrand crosslinks (ICLs) are toxic lesions that prevent the unwinding of the DNA double helix, thus impeding both replication and transcription and potentially leading to DSBs after the collapse of the replication fork (Bessho, 2003; McHugh et al., 2000). ICL repair involves the coordination of multiple repair mechanisms, which is accomplished by the Fanconi Anaemia (FA) pathway (Deans and West, 2011). FA genes have all been implicated in the disease that is their namesake, which is characterised by genomic instability and increased cancer risk (Fanconi, 1967), and play key roles in the resolution of ICLs (Niedernhofer et al., 2005). The FA pathway includes members of the NER pathway that are required for the critical "unhooking" step that creates incisions on either side of the ICL (Niedernhofer et al., 2004), as well as the HR pathway to resolve the DSB that is generated as part of the repair process (Niedzwiedz et al., 2004).

## 1.4 Cancer therapeutics: from DNA-damaging agents to targeted therapy

The treatment of cancer has been the goal and ambition of scientists and clinicians for centuries. Prior to the 1950s, therapeutic options for dealing with malignancies were limited by an incomplete understanding of the intricacies of cancer biology and, in most cases, surgery was the only effective tool. This began to change with the discovery of the anti-tumour effects of nitrogen mustard and related compounds (Gilman and Philips, 1946; Goodman et al., 1946). In addition, the observation that folic acid promotes leukemic cell proliferation led to the successful application of folate analogues such as aminopterin and methotrexate in cancer therapy (Farber and Diamond, 1948; Li et al., 1958). The efficacy of these agents against tumour cells was eventually revealed to be due to their shared ability to induce DNA damage, paving the way for the development of more effective DNA-targeting compounds.

Different classes of DNA-damaging agents react with DNA in different ways (Table 1.2). These range from single modified bases, such as the N-methylated or O-methylated purines generated by nitrogen mustards (Brookes and Lawley, 1961; Osborne et al., 1995), to the multitude of lesions that result from ionising radiation and radiomimetics, the majority of which are produced by reactive oxygen species (Ward, 1988). Over time, to improve therapeutic efficacy and combat the persistent phenomenon of drug resistance, combination therapies were devised where multiple classes of chemotherapy were administered in a single treatment regimen; the earliest success was the combination of nitrogen mustard, vincristine (a microtubule inhibitor), procarbazine (another alkylating agent), and prednisone (an anti-inflammatory steroid)

Table 1.2. Classes of chemotherapy agents and the types of DNA damage produced

| Class | Examples | Type of DNA Damage |
|---|---|---|
| Alkylating agents | Nitrogen mustard and its derivatives (e.g. chlorambucil, cyclophosphamide) | N-methylation or O-methylation adducts at purines |
| Crosslinking agents | Platinum agents (e.g. cisplatin), mitomycin C | Intra/interstrand crosslinks |
| Antimetabolites | Folate inhibitors (e.g. methotrexate), base analogues (e.g. 5-fluorouracil, gemcitabine) | Inhibition of DNA synthesis |
| Topoisomerase poisons | Camptothecin, doxorubicin | Topoisomerase-DNA adducts |
| Radiation and radiomimetics | Ionising radiation, bleomycin | SSBs, DSBs |

for the treatment of Hodgkin's lymphoma (Devita et al., 1970; Moxley et al., 1967). This further led to the study and application of adjuvant therapy, where a chemotherapy agent is given in addition to the primary therapeutic regimen (either surgery, radiotherapy, or combination chemotherapy) to boost its efficacy. One of the earliest examples was in breast cancer, where the administration of an alkylating agent post-mastectomy resulted in a significant reduction in the rate of tumour recurrence (Fisher et al., 1968). These initial successes triggered a wave of discoveries that culminated in the widespread acceptance of combination therapies as the clinical norm for cancer treatment.

As chemotherapeutic agents improved and more efficacious regimens were developed, the limitations of this therapeutic strategy became increasingly apparent. Drug resistance was observed early on during the study of nitrogen mustards (Goodman et al., 1946) and subsequent investigations have uncovered multiple ways through

which tumours can evolve to survive a particular treatment. One mode of resistance involves changes in drug metabolism, wherein the uptake, detoxification, and/or efflux of the compound(s) are modified to render them ineffectual; for example, overexpression of the ATP-binding cassette (ABC) family of membrane transport proteins has been linked to multi-drug resistance in various tumour types by facilitating the diffusion of drugs out of the cell (Stavrovskaya and Stromskaya, 2008). In addition, sensitivity to antimetabolites such as nucleoside analogues is associated with the expression of specific membrane transporters that allow the compounds to enter the cell (Lang et al., 2001; Mackey et al., 1998; Mata et al., 2001), as well as enzymes that convert prodrugs into their active forms (Bhalla et al., 1984; Verhoef et al., 1981). The issue of off-target toxicity also became an increasing concern, and the effects of chemotherapy on normal tissues limited the number of drugs that could be combined as well as the dosage that could be safely administered. The higher efficacy of chemotherapeutic drugs on rapidly dividing cells meant that sites of active proliferation such as the gastrointestinal tract and bone marrow are also vulnerable. Furthermore, quiescent cells are not immune to DNA damage; platinum agents often induce nephrotoxicity, hearing loss, and other neuropathies (Wang and Lippard, 2005; Yao et al., 2007), while doxorubicin frequently leads to cardiomyopathy and congestive heart failure (Minotti et al., 2004; Olson and Mushlin, 1990).

With advances in genetic and molecular biology techniques, many of the signalling pathways that are perturbed in cancer cells were discovered and investigated. Small-molecule inhibitors of key components of these pathways were developed as part and

parcel of the ongoing attempts to understand their roles in cancer biology and were tested for their anti-tumour effects. The hallmarks of cancer (Hanahan and Weinberg, 2000) described previously guided much of the progress into this new era of targeted therapy and the development of high-throughput screening techniques allowed thousands of compounds to be assessed quickly and efficiently. One of the prominent pioneers of this revolution is the compound imatinib mesylate (Gleevec), which targets the BCR-ABL oncoprotein produced by chromosomal fusion in a subset of chronic myeloid leukaemia patients (Druker et al., 2001). In addition to small chemical inhibitors, larger biological molecules such as peptides and antibodies have also successfully demonstrated clinical efficacy against specific targets. One of the earliest examples of monoclonal antibody therapy in cancer is the human epidermal growth factor receptor 2 (HER2)-specific antibody trastuzumab (Herceptin), which has proven effective in a substantial proportion of breast cancers that overexpress HER2 (Slamon et al., 2001).

An unfortunate reality is that many of the limitations of chemotherapy still apply to targeted therapies, particularly the issues of drug resistance and toxicity. Due to the very nature of targeted therapy, cancer cells can often adapt by accumulating mutations or reducing the expression of the molecular target. Imatinib resistance has been observed in CML populations that have acquired mutations in the ABL kinase catalytic domain that retain enzymatic activity but abrogate imatinib binding (Gorre et al., 2001; Shah et al., 2002). A similar situation arose in non-small cell lung cancers treated with epithelial growth factor receptor (EGFR) inhibitors, with a resistant

subpopulation gaining a T790M mutation that altered the EGFR protein just enough to prevent its recognition by first-generation inhibitors (Yu et al., 2013). Several strategies have been applied in an attempt to work around the problem of drug resistance. Regimens combining traditional chemotherapy and targeted therapies have been successful in some cases, such as the combination of rituximab (an anti-CD20 monoclonal antibody) and cyclophosphamide, doxorubicin, vincristine, and prednisone in the treatment of B-cell lymphoma (Coiffier et al., 2002). Another tactic is to target other proteins in the same pathway or in parallel pathways to pre-empt potential modes of resistance; for example, a dual SRC/ABL kinase inhibitor was able to bypass imatinib resistance (Shah et al., 2004). Inhibitors of the DDR (e.g. ATM, ATR, CHK1) have been shown to synergise with DNA-damaging agents such as ionising radiation, topoisomerase poisons, platinum drugs, and antimetabolites (reviewed by (Brandsma et al., 2017)), providing further evidence that traditional chemotherapy and radiotherapy can coexist with and enhance the anti-tumour efficacy of newer, more specific compounds.

## 1.5 Synthetic lethality and cancer

A key challenge in the treatment of cancer is achieving sufficient anti-tumour activity while limiting any negative impact on the patient. Maximising a drug's therapeutic index, defined as the ratio between the dose that induces toxicity and the dose needed for therapeutic efficacy (Kaelin, 2005), is a problem that still plagues researchers and clinicians alike. This has led to increased efforts to discover tumour-specific therapies that can complement or even replace existing chemotherapies, which

can induce severe side effects (Druker, 2002). A promising tool for achieving tumour specificity is the concept of synthetic lethality, a biological interaction in which two genes or pathways independently regulate the same cellular process (Hartman et al., 2001). If a pair of genes has a synthetic lethal interaction, the loss or inhibition of either one leaves the cell viable because the alternative pathway remains functional, whereas loss of both leads to cell death (Fig. 1.3).

One of the earliest synthetic lethal interactions to be discovered in the context of cancer treatment is the relationship between poly (ADP-ribose) polymerase (PARP) inhibition and BRCA1/2 mutations. Two independent groups (Bryant et al., 2005; Farmer et al., 2005) revealed that BRCA-null or mutant cells are acutely sensitive to PARP depletion or inhibition. A phase I clinical trial of olaparib (Lynparza) in BRCA-mutant patients with breast, ovarian, and prostate cancer confirmed the clinical value of the synthetic lethal interaction, with promising response rates and lower toxicity compared to conventional chemotherapy (Fong et al., 2009). Subsequently, a phase II trial continued to demonstrate positive results and revealed that breast tumours responded to olaparib regardless of their estrogen receptor (ER) status, implying that BRCA mutations could predict therapeutic response across different breast cancer subtypes (Tutt et al., 2010). Other PARP inhibitors have also been developed and have displayed at least some activity against BRCA-mutant tumours in clinical trials (Lord et al., 2015), as well as other tumour types that are not necessarily linked to BRCA mutations (Sandhu et al., 2013). Indeed, additional synthetic lethal interactions with PARP have been investigated, including other components of the DDR and HR repair

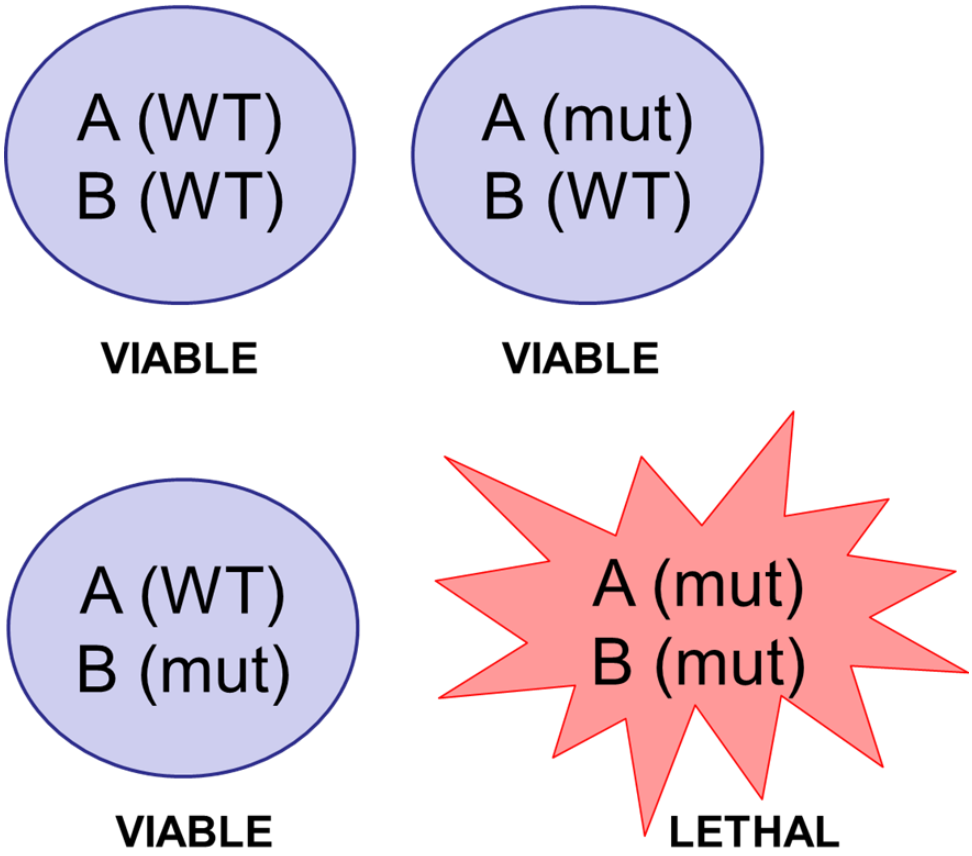



Figure 1.3. Concept of synthetic lethality. Gene A and Gene B are synthetic lethal if one functional copy of A or B is sufficient for viability but simultaneous inactivation of both genes leads to cell death. Adapted from (Chan and Giaccia, 2011).

pathways (McCabe et al., 2006) and the tumour suppressor PTEN (Mendes-Pereira et al., 2009; Minami et al., 2013). In addition, certain cancer-related gene translocations, such as TMPRSS2-ERG in prostate cancer (Brenner et al., 2011) and EWSR1-FLI1 in Ewing's sarcoma (Brenner et al., 2012), have been associated with increased sensitivity to PARP inhibition. It is clear that despite, or perhaps because of, its prominent clinical success, the PARP-BRCA synthetic lethality still continues to inform and guide further research in this field.

Synthetic lethal interactions with potential clinical utility in cancer therapy were initially discovered via genetic screens in model organisms such as yeast (Hartwell et al., 1997). If relevant homologues were available, candidates were further tested in human cell lines and animal models. In many cases, there were no direct equivalents to the genes involved in the synthetic lethality, but cross-species conservation could still be established by investigating functionally similar pathways and gene interaction networks (Dixon et al., 2009; Roguev et al., 2008). One such prediction was made from the observation that cohesin family members and replication fork components were synthetic lethal in yeast, which led to the discovery of a similar interaction between cohesin and PARP in mammalian cells despite the absence of a yeast homologue for PARP genes (Bailey et al., 2014; McLellan et al., 2012). The need for species conservation was bypassed by the discovery of gene knockdowns via RNA interference (RNAi), which facilitated the expansion of synthetic lethality screens into human cell lines (Cheung et al., 2011; Paddison et al., 2004; Vizeacoumar et al., 2013). More recently, the CRISPR-Cas9 system has been applied with increasing frequency to the

task of identifying every possible synthetic lethal interaction in the human genome (Behan et al., 2019; Hart et al., 2015; Wang et al., 2015), boasting a supposedly higher degree of target specificity and the advantages of permanent, irreversible gene deletion (Shalem et al., 2015). Both techniques have their flaws and limitations, including issues with off-target effects and poor reproducibility (Bhinder and Djaballah, 2013; Jackson et al., 2003; Munoz et al., 2016), but improvements are constantly being made as these technologies mature.

Other than genetic techniques, drug libraries can also be utilised for synthetic lethality screens. As with RNAi or CRISPR screens, chemical screens can be either forward or reverse. Forward screens aim to identify a set of essential genes in a collection of cell lines that have mutations in the gene of interest. In contrast, reverse screens begin with an isogenic pair of cell lines where the gene of interest has been mutated and identify the genes required for cell viability in the mutant but not the wild-type. The forward approach has the benefit of being closer to physiological conditions but is subject to cell line heterogeneity, whereas the reverse approach provides greater confidence that any genetic interactions observed are real while needing to use artificially engineered cell lines that may not recapitulate true cancer physiology. Forward screens have been the source of much data regarding cell line sensitivity to a wide variety of drugs (Shoemaker, 2006); however, the significant hurdle posed by the heterogeneous nature of cell lines and the lack of robust controls have led to reverse chemical screens becoming more prevalent over the years. One of the earliest such screens tested 30,000 compounds in isogenic DLD-1 cell lines where the mutant

*K-Ras* allele had been deleted (Torrance et al., 2001). Another study leveraged the phenomenon of synthetic dosage lethality, wherein overexpression of one gene is lethal when combined with the loss of another gene (Kroll et al., 1996), and screened more than 20,000 compounds in normal cells engineered to overexpress a number of oncogenes (Dolma et al., 2003). More recently, genetic and chemical methods have been combined in drug discovery; for example, a CRISPR library comprised of approximately 4000 genes was used to identify determinants of MEK inhibitor sensitivity in pancreatic ductal adenocarcinoma (Szlachta et al., 2018). Combinational drug screens have also seen some success, with both approved and experimental compounds tested for synergistic interactions that could be taken forward into the clinic (Licciardello et al., 2017; Wali et al., 2017).

## 1.6 Epigenetics

From as early as the 1940s, scientists had observed that phenotypes could arise in the absence of genotypic alterations and these events were broadly classified under the new field of epigenetics (Waddington, 1942). Soon after, modifications in DNA that did not change the actual nucleotide sequence were discovered in the form of DNA methylation (Hotchkiss, 1948) and were eventually postulated to play a role in the regulation of gene expression (Holliday and Pugh, 1975). The discovery that DNA is bound by histones, a family of evolutionarily conserved proteins that wrap around DNA and package it into nucleosomes (Kornberg, 1974), provided further insight into how genes could be affected by factors other than DNA itself. Nucleosomes are comprised of two copies of each core histone H2A, H2B, H3, and H4 to form an octamer around

Table 1.3. The human histone code and the relevant enzymes involved in each modification. Adapted from (Zhao and Garcia, 2015).

| Histone Modification | Writer/Eraser | Examples |
|---|---|---|
| Acetylation | Acetyltransferase<br>Deacetylase | H4K16ac |
| Methylation | Methyltransferase<br>Demethylase | H3K36me3 |
| Phosphorylation | Kinase<br>Phosphatase | γH2AX (H2AX phospho-Ser139) |
| Ubiquitination | Ubiquitin E1/E2/E3 ligase<br>Deubiquitinase | H2BK120ub |
| SUMOylation | SUMO E1/E2/E3 ligase<br>DeSUMOylase | H4K59su |

which 145-147 base pairs of DNA are wound (Luger et al., 1997). Histones have N-terminal tail domains that are the substrates of a wide array of post-translational modifications that comprise the so-called "histone code" (Strahl and Allis, 2000). The first to be discovered was acetylation and methylation, which were also found to be involved in controlling gene expression (Allfrey et al., 1964). Over the years, many more types of histone modifications were identified (Table 1.3) and their roles in replication, transcription, repair, and genome stability remain an active area of research.

## 1.7 SETD2

After the discovery of histone methylation in the 1960s (Allfrey et al., 1964), it took more than 30 years for the first histone methyltransferase (HMT), SUV39H1, to be characterised (Rea et al., 2000). Its structure, particularly the presence of a SET (Su(var)3–9, Enhancer of Zeste, and Trithorax) domain, facilitated the identification of other putative HMTs (Dillon et al., 2005). Set2 is one such SET domain protein that was found to be responsible for mono-, di-, and trimethylation of histone H3 at lysine 36 (H3K36me1, me2, and me3) in *Saccharomyces cerevisiae* (Strahl et al., 2002). Its human homologue SETD2 had been identified earlier on as an interaction partner for huntingtin, a protein linked to Huntington's Disease (Faber et al., 1998), and it was subsequently discovered to possess methyltransferase activity (Sun et al., 2005). In contrast to budding yeast, mammalian cells have a more complex system of H3K36 methylation, with multiple distinct methyltransferases that catalyse mono- and dimethylation, while in somatic cells SETD2 is the sole enzyme responsible for H3K36 trimethylation (Fig. 1.4) (Edmunds et al., 2008). In other contexts, such as during meiosis, other HMTs have been found to catalyse H3K36me3 (Powers et al., 2016).

Set2/SETD2 catalyses histone methylation co-transcriptionally by binding to the phosphorylated C-terminal domain of RNA polymerase II (Gerber and Shilatifard, 2003; Krogan et al., 2003; Li et al., 2002; Yoh et al., 2008). Indeed, deleting or mutating Set2's SRI (Set2 Rpb1 Interacting) domain not only abrogates its interaction with RNA Pol II but also impairs H3K6 methylation (Kizer et al., 2005; Li et al., 2003). Consistently, H3K36me3 has been linked to transcription-related cellular processes.

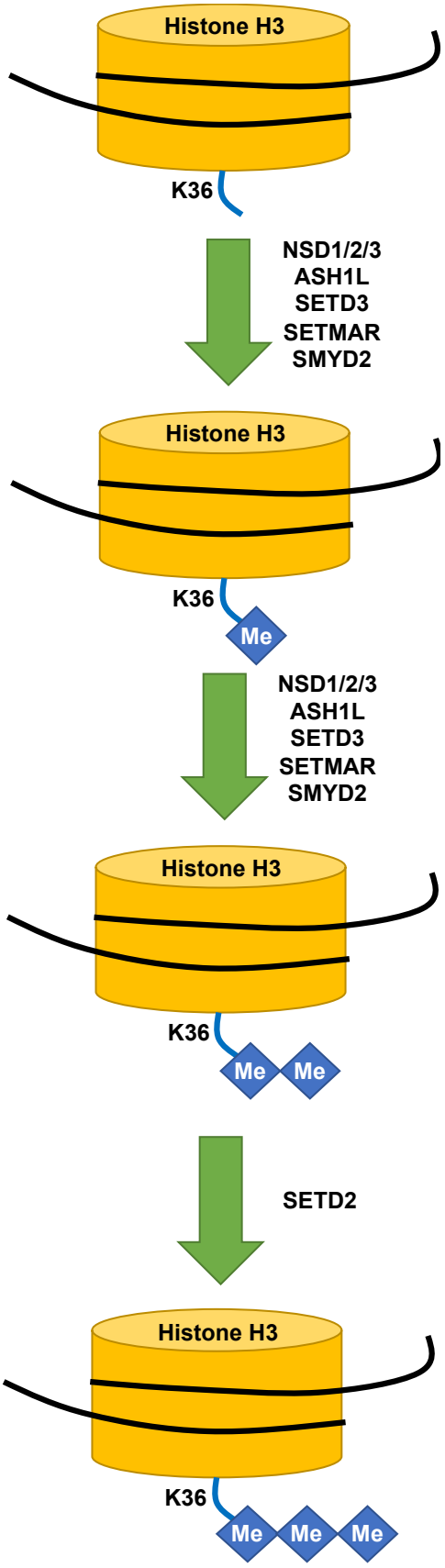



Figure 1.4. Methylation of histone H3 lysine 36 (K36) in mammalian cells. Adapted from (Wagner and Carpenter, 2012).

Alternative splicing of the human fibroblast growth factor receptor 2 (FGFR2) gene was shown to be determined by the levels of H3K36me3 (Luco et al., 2010). Loss of this histone mark has been associated with the increased occurrence of cryptic intragenic transcription due to the impaired recruitment of the FACT (FAcilitates Chromatin Transcription) complex, leading to dysregulated chromatin remodelling during gene transcription (Carvalho et al., 2013). In addition to its roles in transcription, H3K36me3 is also important for the maintenance of genome stability. Components of the MMR pathway such as the hMutSα complex have been shown to be recruited in an H3K36me3-dependent manner (Li et al., 2013). Furthermore, this histone mark is involved in the repair of DSBs via HR by promoting the recruitment of LEDGF (Lens Epithelium-Derived Growth Factor), which is necessary for the early resection steps of the recombination process (Pfister et al., 2014).

SETD2's contributions to essential genomic processes is consistent with its role as a tumour suppressor in various cancer types. SETD2 mutations occur relatively frequently in certain cancers, particularly in renal cancer, colorectal cancer, and paediatric high-grade gliomas (Fig. 1.5). SETD2 deletions and mutations were detected in a substantial number of clear cell renal cell carcinoma (ccRCC) clinical samples (Dalgliesh et al., 2010) and cell lines (Duns et al., 2012). SETD2's location on chromosome 3p makes it one of the most frequent examples of loss of heterozygosity (LOH) in ccRCC (Zbar et al., 1987). Mutations in SETD2 are associated with lower cancer-specific survival in renal cell carcinoma (Hakimi et al., 2013); consistently, analysis of H3K36me3 levels via immunohistochemistry revealed a progressive decline

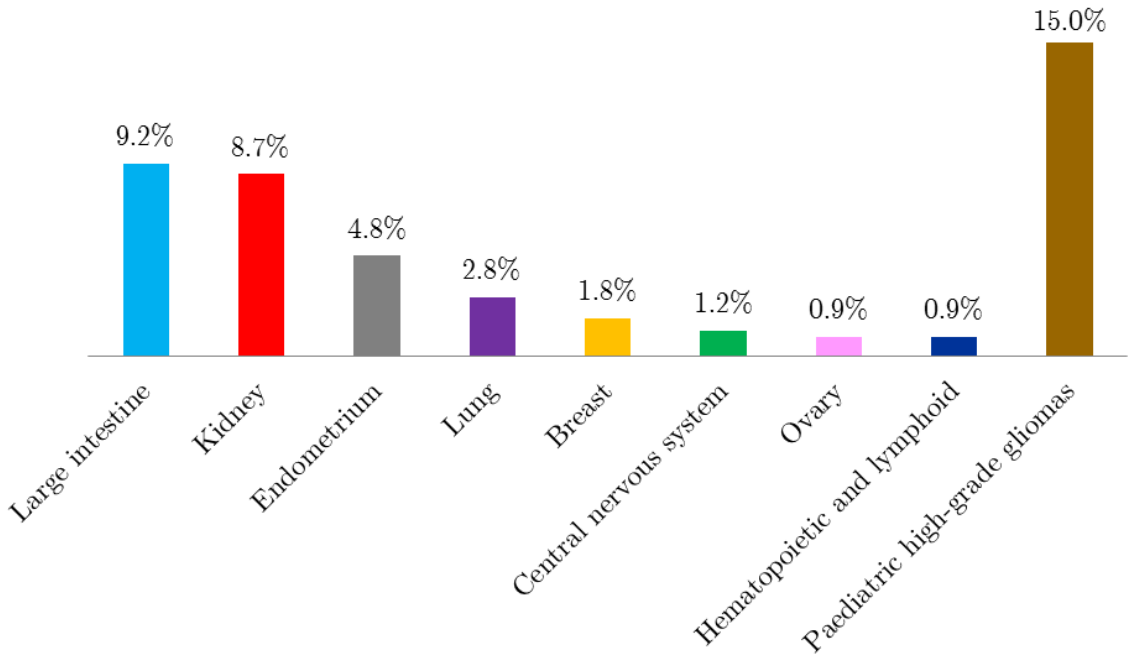



Figure 1.5 SETD2 mutation frequency in selected cancer types. Source: COSMIC database and (Fontebasso et al., 2013).

in staining intensity from primary tumour to metastases in renal cell carcinoma patients, culminating in an approximately 60% reduction in positive nuclei compared to uninvolved renal tissue (Ho et al., 2016). Missense or truncating mutations that inactivate the methyltransferase activity of SETD2 were also observed in 15% of paediatric and 8% of adult high-grade gliomas, with no mutations observed in tumours of Grade II and below (Fontebasso et al., 2013). Comparison of SETD2 expression between breast tumour samples and adjacent normal tissue revealed a marked reduction in SETD2 transcript and protein levels in breast cancer (Newbold and Mokbel, 2010).

## 1.8 Synthetic lethality of SETD2 and WEE1

An evolutionarily conserved synthetic lethal interaction between SETD2 and the cell cycle regulator WEE1 was discovered in *Schizosaccharomyces pombe* (Pai et al., 2019) and human cells (Pfister et al., 2015). The Wee1 kinase was first characterised in *S. pombe* and was shown to phosphorylate the cyclin-dependent kinase Cdc2 at Thr14 and Tyr15, which is critical to prevent premature entry into mitosis (Nurse and Thuriaux, 1980). The human homologue of Wee1 (WEE1) has a similar function in regulating the activity of CDK1 and CDK2, although it was discovered to be a tyrosine-specific kinase (Parker and Piwnica-Worms, 1992). WEE1 protein levels and activity reach their peak during the S and G2 phases of the cell cycle, after which it is hyperphosphorylated and degraded during mitosis (Watanabe et al., 1995). The WEE1 inhibitor AZD1775 was found to selectively target cancer cell lines that are SETD2-deficient (either naturally, after siRNA depletion, or after CRISPR/Cas9-mediated

deletion) (Pfister et al., 2015). The combined loss of SETD2 and WEE1 led to a striking phenotype of S-phase arrest and impaired DNA replication, which were found to coincide with downregulation of RRM2, a subunit of the enzyme ribonucleotide reductase (RNR) (Fig. 1.6). RNR is responsible for the rate-limiting step of *de novo* deoxyribonucleotide (dNTP) synthesis (Wright et al., 1990), and cellular levels of its RRM2 subunit are strictly controlled in a cell cycle-dependent manner (Chabes et al., 2004). After the successful completion of DNA replication and S-phase, RRM2 is targeted by the CDK/$SCF^{CyclinF}$ complex, leading to its degradation via ubiquitin-mediated proteolysis (D'Angiolella et al., 2012). Inhibition of WEE1 results in hyperactivation of CDK1/2, thereby drastically shortening the half-life of the RRM2 protein and impairing the cell's ability to replenish its dNTP supply (Pfister et al., 2015). In addition, excessive CDK activity has been found to cause dysregulated and inappropriate firing of replication origins, further contributing to the shortage of cellular dNTPs (Beck et al., 2012).

## 1.9 Thesis aims

*In vivo* experiments in mouse xenograft models have shown that the WEE1 inhibitor AZD1775 is capable of inhibiting the growth of SETD2-deficient renal cancer cell lines and regressing tumour size by approximately 50% (Pfister et al., 2015). In order to improve the potency of AZD1775 and further our understanding of the molecular mechanisms by which it exerts its anti-tumour effects in the absence of SETD2, a high-throughput small-molecule compound screen was conducted in collaboration with the Target Discovery Institute (TDI). More than 2000 compounds,

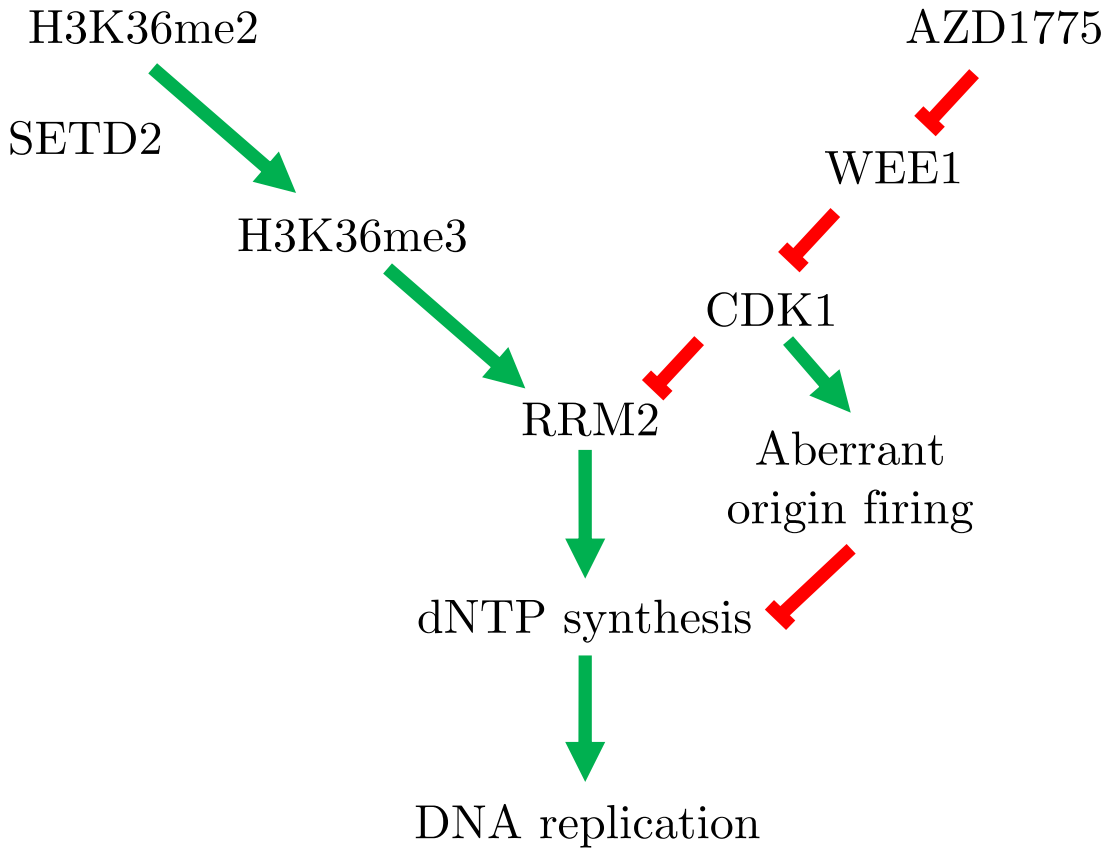



Figure 1.6. Proposed mechanism underlying the synthetic lethality between loss of SETD2/H3K36me3 and inhibition of WEE1. Diagram adapted from (Pfister et al., 2015).

either alone or in combination with AZD1775, from TDI's drug libraries were tested on U2OS osteosarcoma cells in which the SETD2 gene has been deleted using the CRISPR/Cas9 system, as well as on isogenic parental U2OS cells. The aim of this screen is to identify compounds that fall into one of two categories: (a) those that enhance sensitivity to AZD1775 (synergy hits) or (b) those that specifically target SETD2-deleted cells in the absence of AZD1775 (new synthetic lethal hits). After validation of promising hits, the molecular mechanisms underlying the interaction of these compounds with SETD2 and WEE1 or SETD2 alone will be investigated, with the ultimate goal of proposing novel therapeutic modalities for the treatment of H3K36me3-deficient tumours.

The first chapter of this thesis will focus on the first category of the compound screen, namely the synergy hits. The most promising candidate will be discussed in further depth, with the aim of understanding the relationship of its target with SETD2 and WEE1. The second chapter will look into the second category, namely the new synthetic lethal hits. The phenotypes generated by the top candidate will be investigated in detail, guided by existing scientific knowledge on the compound itself and SETD2's biological functions. Finally, the third chapter will continue exploring the novel putative synthetic lethality from the previous chapter, with emphasis on uncovering its mechanisms of action in the context of SETD2 loss.

# 2. Materials and Methods

## 2.1 Cell Culture

All cell lines except LB996 were maintained in complete medium consisting of Dulbecco's modified minimal essential medium (DMEM, Life Technologies) supplemented with 10% foetal bovine serum (FBS, Sigma), 100 U penicillin (Sigma), and 0.1 mg/ml streptomycin (Sigma). LB996 cells were cultured in Iscove's Modified Dulbecco's Medium (IMDM, Life Technologies) with 10% FBS, 100 U penicillin, 0.1 mg/ml streptomycin, and G5 supplement (Life Technologies). All cells were grown at 37°C in a humidified incubator with 5% carbon dioxide. Cells were subcultured every 3-4 days as follows: cells were washed with phosphate buffered saline (PBS, Life Technologies) and then incubated with trypsin (Life Technologies) at 37°C until most cells had detached. Trypsinised cells were re-suspended in complete medium, centrifuged at 300 *g* for 3 minutes, and re-plated at the appropriate dilution.

## 2.2 Cell Lines

The cell lines used in this study are described below:

The U2OS cell line was derived from human osteosarcoma and obtained from ATCC (ATCC number HTB-96). The U2OS SETD2-deleted cell lines #19, #30, and #37 were generated by our own group using the CRISPR-Cas9 technology (Pfister et al., 2015).

The 786-O, A498, and LB996 cell lines were derived from human clear cell renal cell carcinomas. 786-O was obtained from the lab of Dr. Valentine Macaulay at the

Department of Oncology, University of Oxford. A498 was obtained from ATCC (HTB-44). LB996 was obtained from the lab of Prof. Benoit van den Eynde at the Oxford Ludwig Institute.

The MCF7 p53 wild-type and p53-CRISPR cell lines were obtained from the lab of Dr. Ross Chapman at the Wellcome Centre for Human Genetics.

The U2OS XPF wild-type and XPF-CRISPR cell lines were obtained from the lab of Prof. Peter McHugh at the Weatherall Institute of Molecular Medicine.

## 2.3 High-throughput Compound Screening

The compound screen was performed at the Target Discovery Institute (TDI) in collaboration with Dr. Daniel Ebner and Ms. Elena Seraia.

Parental and SETD2-deleted U2OS cells were seeded into 384-well plates (600 cells per well) using the Janus Liquid Handling Workstation (Perkin Elmer) and incubated at 37°C overnight. Subsequently, the compound libraries (TDI Expanded Oncology Drug Set and SelleckChem Bioactive Compound Library) were thawed at room temperature and diluted into dimethyl sulphoxide (DMSO) or complete medium using the Echo Acoustic Liquid Handler (Labcyte). The diluted compounds (or DMSO as a negative control) were added to the cells using the Janus workstation and incubated for 24 hours. The following day, the WEE1 inhibitor AZD1775 was diluted and added to the cells using the same procedure as the compound libraries and incubated for 72 hours. Subsequently, cell viability was measured using the resazurin assay.

## 2.4 Statistical Analysis of Screening Results

Statistical analysis of the compound screening results was performed using the HTScape software, which was developed in-house by Dr. Francesca Buffa's group. The raw data (.csv) files obtained from the resazurin assay and annotation files for the compound libraries were uploaded onto the HTScape software and Z-scores were calculated. Comparison between different cell lines and conditions was carried out by subtracting their respective Z-scores and calculating a false-positive discovery rate (PFP). Hits with PFP $< 0.05$ were defined as statistically significant.

## 2.5 Validation of Positive Hits

Positive hits were selected for validation based on several criteria. These are listed as follows:

- Statistical significance (PFP $< 0.05$)
- FDA approval status (compounds that are approved for clinical use or are currently in trials)
- Relevance of target pathway/function

Cells were seeded into a 96-well plate (2000 cells per well) overnight before drug/inhibitor treatment. DMSO (solvent for the inhibitors) was used as a negative control.

For validation of putative new synthetic lethal hits, cells were first treated with either DMSO or 2 μM RO3306, a CDK1 inhibitor, for 24 hours. This was followed by the addition of increasing concentrations (from a maximum of 20 μM serially diluted in increments of 2) of the compound to be validated on top of the existing medium,

after which the cells were incubated for another 48 hours prior to measurement of cell viability via the resazurin assay.

For validation of putative synergy hits, cells were first treated with increasing concentrations (from a maximum of 20 μM serially diluted in increments of 2) of the compound to be validated for 24 hours. Subsequently, 150 nM AZD1775 or DMSO was added on top of the existing medium and incubated for 48 hours prior to measurement of cell viability via the resazurin assay.

## 2.6 Drugs and Inhibitors

All inhibitors were dissolved in DMSO and stored at -80°C per the manufacturer's instructions. Compounds/inhibitors used are listed below:

WEE1 inhibitor: AZD1775 (Selleck Chemicals)

HDAC inhibitor: Panobinostat (from the lab of Prof. Anne Kiltie)

HDAC1/2 inhibitor: Romidepsin (from the lab of Prof. Anne Kiltie)

All compounds used for the validation of the high-throughput screen were obtained from Selleck Chemicals.

## 2.7 Resazurin Assay for Cell Viability

At the desired time point after treatment, culture medium was removed and fresh complete medium without phenol red and containing 10 μg/ml resazurin (Sigma) was added to each well. Resazurin is a nonfluorescent dye that can be converted via a redox reaction to a red fluorescent compound, resorufin, by living cells. The fluorescent signal is proportional to the number of living cells and was measured by a fluorescence plate

reader (BMG Labtech) after 2 hours of incubation at 37°C. For drug treatment experiments, IC50 is defined as the concentration of drug that reduces viability by 50%.

## 2.8 Clonogenic Survival Assay

Prior to drug treatment, cells were seeded into 6-well plates at low densities and incubated overnight at 37°C. Culture media was subsequently replaced with media containing DMSO or the appropriate concentration of drug and incubated for 10 days at 37°C. Each well was then washed with PBS and stained with Brilliant Blue R Concentrate (Sigma) for 1 hour with gentle shaking. Plating efficiency (PE) and Surviving Fraction (SF) were calculated according to the published protocol (Franken et al., 2006)

## 2.9 Apoptosis Detection Assay

Apoptotic cell death was measured in a 96-well format using the RealTime-Glo™ Annexin V Apoptosis and Necrosis Assay (Promega) per the manufacturer's instructions. In brief, cells were seeded at 3000 cells/well in 96-well plates overnight. The following day, the media was replaced with 100 µl/well of media containing the compound to be tested. Immediately afterwards, another 100 µl/well containing the 2X Detection Reagent (which consists of Annexin NanoBiT® Substrate, $CaCl_2$, Necrosis Detection Reagent, Annexin V-SmBiT, and Annexin V-LgBiT) was added. The luminescence signal is proportional to the number of apoptotic cells and was measured by a plate reader (BMG Labtech) 30 hours after incubation at 37°C.

## 2.10 siRNA Transfection

All siRNAs (10-20 nM final concentration) were delivered to the cells by Lipofectamine RNAiMAX (Life Technologies) per the manufacturer's instructions. Cells were incubated with siRNA-Lipofectamine mix in suspension (reverse transfection) in complete medium without penicillin and streptomycin. The medium was replaced 16 hours after transfection. Cells were analysed or further treated at least 48 hours after transfection. Western blotting was performed to determine knockdown efficiency.

The sequences of the siRNAs are listed below:

siHDAC1 (Ambion): GCCGGUCAUGUCCAAAGU

siHDAC2 (Ambion): GGAUUACAUCAUGCUAAG

siSETD2 (pooled) (Dharmacon): GAAACCGUCUCCAGUCUGU,

UAAAGGAGGUAUAUCGAAU

siRAD51 (pooled) (Qiagen): AAGGGAAUUAGUGAAGCCAAA,

CAGGAUAAAGCUUCCGGGAAA, CACUUCUAAAUUAAUGGUAAA,

CACGGUUAGAGCAGUGUGGCA

siBRCA1 (Dharmacon): AAUGCCAAAGUAGCUAAUGUAUUUU

siRB1 (Dharmacon): ON-TARGETplus SMARTpool L-003296 (proprietary sequences)

## 2.11 Bacterial Transformation

Chemically competent *Escherichia coli* DH5α cells (produced in-house by Carol Walker) were used for plasmid amplication. 1-5 μl of plasmid DNA (1 pg-100 ng) was added to 50 μl of bacterial cell suspension. The mixture was incubated on ice for 30

minutes, heat-shocked at 42°C for 30 seconds, left on ice for 5 minutes, and allowed to recover in 1 ml Luria-Bertani (LB, Sigma) broth for 1 hour at 37°C with shaking. 50-100 µl of the mixture was plated onto an LB plate with the appropriate antibiotic for selection and incubated overnight at 37°C. Depending on the plasmid backbone, selection of the plasmid-carrying bacteria clones was achieved by adding either 100 µg/ml ampicillin or 50 µg/ml kanamycin to the LB agar plates.

## 2.12 Plasmid Purification

Plasmid purification from bacterial cultures was performed using QIAprep spin miniprep kits (Qiagen) according to the manufacturer's instructions. The QIAprep columns contain a silica membrane that binds DNA in the presence of a high concentration of chaotropic salt and allows DNA elution in low-salt buffer or water.

In brief, individual colonies were grown overnight at 37°C with shaking in 2 ml of LB broth containing the appropriate antibiotic for selection in a 10 ml tube. Samples were transferred to 2 ml microcentrifuge tubes and harvested by centrifugation at 8,000 *g* for 3 minutes. The pellet was resuspended in 250 µl P1 buffer (containing RNase A), lysed by addition of 250 µl P2 buffer, and mixed by inverting the tubes. The P2 lysis buffer was neutralised by adding 350 µl of P3 buffer. The precipitated cell debris and genomic DNA were separated from the solution by centrifugation at 17,000 *g* for 10 minutes at room temperature. The supernatant (containing plasmid DNA) was transferred into a QIAprep spin column and centrifuged for 1 minute at 17,000 *g* and the flow-through was discarded. The plasmid DNA bound to the silica membrane was washed with 0.75 ml PE buffer to remove impurities. The plasmid DNA was eluted by

incubating 50 µl Milli-Q water in the column for 1 minute before centrifugation into a collection tube.

## 2.13 Plasmid Transfection

Plasmid DNA (5 µg) was delivered to the cells by Lipofectamine 2000 (Life Technologies) per the manufacturer's instructions. Cells were seeded in a 6-well plate ($4 \times 10^5$ per well) overnight prior to transfection. The plasmid DNA-Lipofectamine mix was added into each well containing complete medium without penicillin and streptomycin. The medium was replaced 16 hours after transfection and the cells were allowed to recover for another 24 hours. Transfected cells were then subjected to antibiotic selection using geneticin (G418, Life Technologies).

The plasmids used in this study are listed below:

pcDNA3.1-RRM2 (T33A) (from the lab of Dr. Vincenzo D'Angiolella)

## 2.14 Histone Extraction

This protocol was adapted with modifications from Dr. Junjie Chen's laboratory (Huang et al., 2009) by Dr. Raul Mostoslavsky's group.

In brief, cells were lysed in buffer containing 10 mM HEPES pH 7.4, 10 mM KCl, and 0.05% NP-40 supplemented with protease and phosphatase inhibitors for 20 minutes on ice. The lysate was centrifuged for 10 minutes at 17,000 *g* at 4°C. The supernatant, which contains the cytoplasmic proteins, was removed and stored separately. The pellet, which contains the nuclear fraction, was washed once with lysis buffer and centrifuged for 10 minutes at 17,000 *g* at 4°C. The supernatant was discarded

and the pellet was resuspended in 0.2 N HCl and incubated for 20 minutes on ice. The solution was centrifuged for 10 minutes at 17,000 *g* at 4°C. The supernatant, which contains histone proteins, was transferred to a fresh tube and protein concentration was measured using the Bradford assay.

## 2.15 Western Blotting

For preparation of whole cell lysate, cells were lysed in lysis buffer (50 mM Tris-HCl pH 7.5, 150 mM NaCl, 1% Triton X-100, supplemented with protease and phosphatase inhibitors) for 30 minutes on ice. The lysate was centrifuged for 10 minutes at 17,000 *g* at 4°C to pellet cellular debris. The supernatant was transferred to a fresh tube and protein concentration was measured using the Bradford assay.

25 µg of protein was mixed with the NuPAGE LDS loading buffer (Life Technologies) containing the reducing agent dithiothreitol (DTT) and denatured by boiling at 95°C for 10 minutes. All samples and 10 µl of molecular weight ladder (Fermentas) were loaded onto pre-cast NuPAGE gels (Life Technologies) and electrophoresis was performed at 150 V. Proteins were transferred onto a PVDF membrane (0.45 µm pore size, Life Technologies) or a nitrocellulose membrane (0.2 µm pore size, Bio-Rad) in a transfer cassette (Life Technologies) at 30 V for 2 hours at 4°C.

The membrane was blocked in blocking buffer (PBS + 0.1% Tween-20+ 5% skimmed milk) for 1 hour at room temperature before incubating with the primary antibody diluted in the blocking buffer at 4°C overnight. After washing three times with PBS-T (PBS + 0.1% Tween-20), the membrane was then incubated with a

horseradish peroxidase (HRP)-conjugated secondary antibody diluted in blocking buffer for 1 hour at room temperature. After washing three times with PBS-T, the proteins on the membrane were visualised with the ECL chemiluminescence substrate (Thermo Scientific) per the manufacturer's instructions.

Primary antibodies used for Western blotting are listed here: H3K36me3 (Abcam), histone H3 (Abcam), HDAC1 (Cell Signaling Technology), HDAC2 (Cell Signaling Technology), RRM2 (Santa Cruz Biotechnology), Flag tag (Sigma), cleaved caspase-3 (Abcam), caspase-3 (Abcam), p53 (Santa Cruz Biotechnology), phospho-p53 Ser15 (Cell Signaling Technology), phospho-CHK1 (Ser345) (Cell Signaling Technology), CHK1 (Cell Signaling Technology), phospho-CHK2 (Thr68) (Cell Signaling Technology), CHK2 (Cell Signaling Technology), p21 (Cell Signaling Technology), RAD51 (Santa Cruz Biotechnology), BRCA1 (Calbiochem), RB (Cell Signaling Technology), α-tubulin (Santa Cruz Biotechnology), and GAPDH (Novus).

## 2.16 Cell Cycle Analysis by BrdU Incorporation

Immediately prior to harvesting, cells were incubated in media containing 20 μM bromodeoxyuridine (BrdU) for 30 minutes at 37°C while protected from light. Cells were collected by trypsinisation and fixed in ice-cold 70% ethanol for at least 30 minutes. Since the anti-BrdU antibody recognises single-stranded DNA, cells were incubated for 20 minutes at room temperature in 2 M hydrochloric acid (which denatures double-stranded DNA). Cells were washed once in PBS, followed by once in PBS + 0.5% Tween-20 + 0.5% FBS.

Cells were then incubated in blocking buffer (PBS with 2% FBS) containing an anti-BrdU monoclonal antibody (BD Biosciences) (1:100 dilution) for 90 minutes at room temperature or overnight at 4°C. Cells were washed twice with PBS and then incubated in blocking buffer containing the Alexa Fluor 488 secondary antibody (Life Technologies) (1:200 dilution) for 60 minutes at room temperature in the dark. Cells were then washed in PBS, resuspended in PBS + 0.1 mg/ml propidium iodide, and analysed using the FACScan flow cytometer (Becton Dickinson).

## 2.17 Immunofluorescence Staining of Foci

Cells were seeded onto glass coverslips overnight. At the desired time point after treatment, pre-extraction buffer (10 mM PIPES pH 6.8, 300 mM sucrose, 100 mM NaCl, 1.5 mM $MgCl_2$, and 0.5% Triton X-100) was added for 2 minutes on ice. The cells were then fixed in 4% paraformaldehyde in PBS for 10 minutes at room temperature. Coverslips were washed 3 times in PBS and incubated in blocking buffer (PBS + 0.1% Triton X-100 + 1% BSA + 1% FBS) for 1 hour. Coverslips were then incubated with primary antibody in PBS + 1% BSA + 1% FBS overnight at 4℃. Unbound primary antibody was removed by washing 3 times for 5 minutes in PBS at room temperature, followed by incubation with the indicated secondary antibody for 60 minutes at room temperature in the dark. Slides were then washed twice for 5 minutes in PBS and once in PBS with Hoechst 33342 (1:1000, Molecular Probes) before mounting with VECTASHIELD® Antifade Mounting Media (Vector Laboratories). Slides were imaged using the Zeiss 710 confocal microscope with a 63X oil objective.

The primary antibodies used for immunofluorescence are: phospho-RPA (Ser33) (Bethyl Laboratories), 53BP1 (GeneTex), and γH2AX (Novus).

## 2.18 DNA Fibre Assay

Cells were seeded overnight such that they reached approximately 20% confluency the following day. Cells were labelled with 30 mM CldU (Sigma-Aldrich) for 30 min, washed twice with PBS, and labelled with 250 mM IdU in the presence of 150 nM RITA or DMSO for another 30 min. Following pulse labelling, cells were quickly trypsinized and resuspended in PBS at 2.5 x $10^5$ cells/ml. Labelled cells were diluted 1:8 with unlabelled cells, and 2.5 µl of cells were mixed with 7.5 µl of lysis buffer (200 mM Tris-HCl, pH 7.5, 50 mM EDTA, and 0.5% (w/v) SDS) on a glass slide. After 9 min, the slides were tilted at 15°–45°, and the resulting DNA spreads were air-dried and fixed in 3:1 methanol/acetic acid overnight at 4℃. The DNA fibers were denatured with 2.5 M HCl for 1 hr, washed with PBS, and blocked with 2% (w/v) BSA in PBS + 0.2% Tween-20 for 40 min. The CldU and IdU tracts were labelled (for 2.5 hr in the dark, at RT) with anti-BrdU antibodies recognizing CldU (rat; Abcam) and IdU (mouse; BD), respectively. After washing for 5 x 3 min in 0.2% (v/v) PBS-T, the following secondary antibodies were used (1 hr incubation, in the dark, at RT): anti–mouse Alexa Fluor 488 (Molecular Probes) and anti–rat Cy3 (Jackson ImmunoResearch Laboratories, Inc.). After washing for 5 x 3 min in PBS-T (0.2% (v/v)), the slides were air dried completely, mounted with 20 ml/slide ProLong® Gold Antifade Mountant (Life Technologies), and sealed to a coverslip with transparent nail polish.

Microscopy was performed with a fluorescence microscope (Nikon Ni-E; 100X oil objective) and the images were processed with the Fiji software. At least 200 fibres were measured per condition.

## 2.19 RNA Sequencing

Library preparation and Illumina sequencing was performed by technical staff at Novogene Co. Ltd. Duplicate samples of wildtype and SETD2-CRISPR isogenic U2OS treated were treated with either DMSO or 15 nM RITA for 48 hours. A total amount of 3 µg RNA per sample was used as input material for the RNA sample preparations. Ribosomal RNA was removed using the Epicentre Ribo-zero$^{TM}$ rRNA Removal Kit (Epicentre, USA) according to the manufacturer's instructions, and rRNA free residue was cleaned up by ethanol precipitation. Subsequently, sequencing libraries were generated using the rRNA-depleted RNA by NEBNext® UltraTM Directional RNA Library Prep Kit for Illumina® (NEB, USA) following manufacturer's recommendations. Briefly, fragmentation was carried out using divalent cations under elevated temperature in NEBNext First Strand Synthesis Reaction Buffer (5X). First strand cDNA was synthesized using random hexamer primer and M-MuLV Reverse Transcriptase (RNaseH-). Second strand cDNA synthesis was subsequently performed using DNA Polymerase I and RNase H. In the reaction buffer, dNTPs with dTTP were replaced by dUTP. Remaining overhangs were converted into blunt ends via exonuclease/polymerase activities. After adenylation of 3' ends of DNA fragments, NEBNext Adaptor with hairpin loop structure were ligated to prepare for hybridization. In order to select cDNA fragments of preferentially 150~200 bp in length,

the library fragments were purified with AMPure XP system (Beckman Coulter, Beverly, USA). Then 3 µl USER Enzyme (NEB, USA) was used with size-selected, adaptor-ligated cDNA at 37°C for 15 min followed by 5 min at 95°C before PCR. Then PCR was performed with Phusion High-Fidelity DNA polymerase, Universal PCR primers and Index (X) Primer. Finally, products were purified (AMPure XP system) and library quality was assessed on the Agilent Bioanalyzer 2100 system. Clustering of the index-coded samples was performed on a cBot Cluster Generation System using HiSeq PE Cluster Kit cBot-HS (Illumina) according to the manufacturer's instructions. After cluster generation, the library preparations were sequenced on an Illumina HiSeq platform and paired-end reads were generated.

## 2.20 Modified Single-Cell Gel Electrophoresis (Comet) Assay

This assay was performed by Mr. Christian Cooper and Mr. Michalis Challoumas from Prof. George D. Jones's group in the University of Leicester according to a published protocol (Spanswick et al., 2010). Cells were seeded at 100,000 cells/well in 6-well plates and incubated overnight. The following day, the cells were treated with DMSO, RITA, or mitomycin C for 1 hour at 37°C. All samples were then harvested by trypsinisation and aliquoted into separate tubes with 20,000-25,000 cells each, resuspended in freezing medium (complete DMEM + 10% DMSO), and frozen at -80°C for at least 24 hours.

Meanwhile, microscope slides were precoated with 1% type 1-A agarose in water by pipetting 1 ml of molten agarose onto the centre of the slide. A coverslip was placed on top and the slides were allowed to set before removing the coverslip. The slides were

then allowed to dry overnight at room temperature. The samples are then thawed and resuspended in complete culture medium. With the exception of the unirradiated controls, the samples were irradiated on ice at 5 Gy. 0.5 mL of resuspended cells was then placed in a 24-well plate on ice. Subsequently, 1 ml of molten 1% LGT agarose was added to water cooled to 40°C and mixed. Then, 1ml was pipetted onto the centre of the slide on ice and a coverslip was placed on top. After the agarose has set, the coverslip was removed and placed in a tray on ice. The slides were covered with ice cold lysis buffer containing 1% Triton X-100 and incubated on ice for 1 hour in the dark. The lysis buffer was carefully removed and replaced with ice cold double-distilled water, followed by incubation for 15 minutes in the dark. This step was repeated a further three times before the slides were carefully removed and transferred to an electrophoresis tank. The slides were covered with ice cold alkali buffer and incubated for 45 minutes in the dark. Electrophoresis was performed for 25 minutes at 18 V (0.6 V/cm), 250 mA in the dark. The slides were then carefully removed from the buffer and placed on a horizontal slide rack. Each slide was flooded twice with 1 ml neutralisation buffer and incubated for 10 minutes, followed by rinsing twice with 1 mL PBS for 10 minutes. Excess liquid was removed and the slides were dried overnight at room temperature.

To stain the slides for visualisation, the slides were re-hydrated in double-distilled water for 30 minutes. Each slide was then flooded twice with 1 ml of 2.5 μg/ml propidium iodide solution and incubated for at least 30 minutes at room temperature in the dark. The slides were rinsed twice with double-distilled water for 10 minutes and

once for 30 minutes then dried at 40$^{o}$C in the dark. Once dry, a few drops of distilled water were added to each slide and covered with a coverslip. Individual cells and comets were examined at 20X magnification, with 100 comets counted per slide.

# 3. Therapeutic targeting of SETD2 deficiency and modulation of the SETD2-WEE1 synthetic lethality

*In vivo* experiments in mouse xenograft models have shown that the WEE1 inhibitor AZD1775 is capable of inhibiting the growth of SETD2-deficient renal cancer cell lines and regressing tumour size by approximately 50% (Pfister et al., 2015). In order to improve the potency of AZD1775 and further our understanding of the molecular mechanisms by which it exerts its anti-tumour effects in the absence of SETD2, a high-throughput small-molecule compound screen was conducted in collaboration with the Target Discovery Institute (TDI). More than 2000 compounds, either alone or in combination with AZD1775, from TDI's drug libraries were tested on U2OS osteosarcoma cells in which the SETD2 gene has been deleted using the CRISPR/Cas9 system, as well as on isogenic parental U2OS cells. The aim of this screen is to identify compounds that fall into one of two categories: (a) those that enhance sensitivity to AZD1775 (synergy hits) or (b) those that specifically target SETD2-deleted cells in the absence of AZD1775 (new synthetic lethal hits).

## 3.1 High-throughput compound screening

In order to identify compounds that fall under the categories previously enumerated, a high-throughput screen was conducted. The experimental design is described in Fig. 3.1A. The compounds used were provided by the TDI in two libraries: the Expanded Oncology Drug Library (ODL) and the SelleckChem Bioactive Compound Library (Selleck). The ODL is composed of 298 different compounds that are specifically oncology-related, whereas the Selleck library has 1902 different compounds with a wide variety of therapeutic applications; there is an overlap of 165 compounds between these 2 libraries (Fig. 3.1B). All assays were conducted in a 384-well format and both cells and compounds were added using automated liquid handling systems to ensure accuracy and precision. The endpoint of the screen was cell viability, as measured by the resazurin assay 96 hours after addition of the compound libraries (Fig. 3.1C). For statistical analysis of the raw viability data, the HTScape software developed by Dr. Francesca Buffa's group was used. This software can calculate Z-scores for each sample and incorporate the results with user-inputted information on plate layouts, treatment regimens, and compound names. Based on the difference between Z-scores of desired groups of interest (e.g. AZD1775-treated wells vs. wells without AZD1775) and false-positive discovery rates (PFP), a list of the top 100 hits for each of the aforementioned categories was obtained. To select hits for further validation, three criteria were applied: (a) PFP $< 0.05$, (b) currently FDA-approved or undergoing clinical trials, and (c) relevance to pathways of interest. For synergy

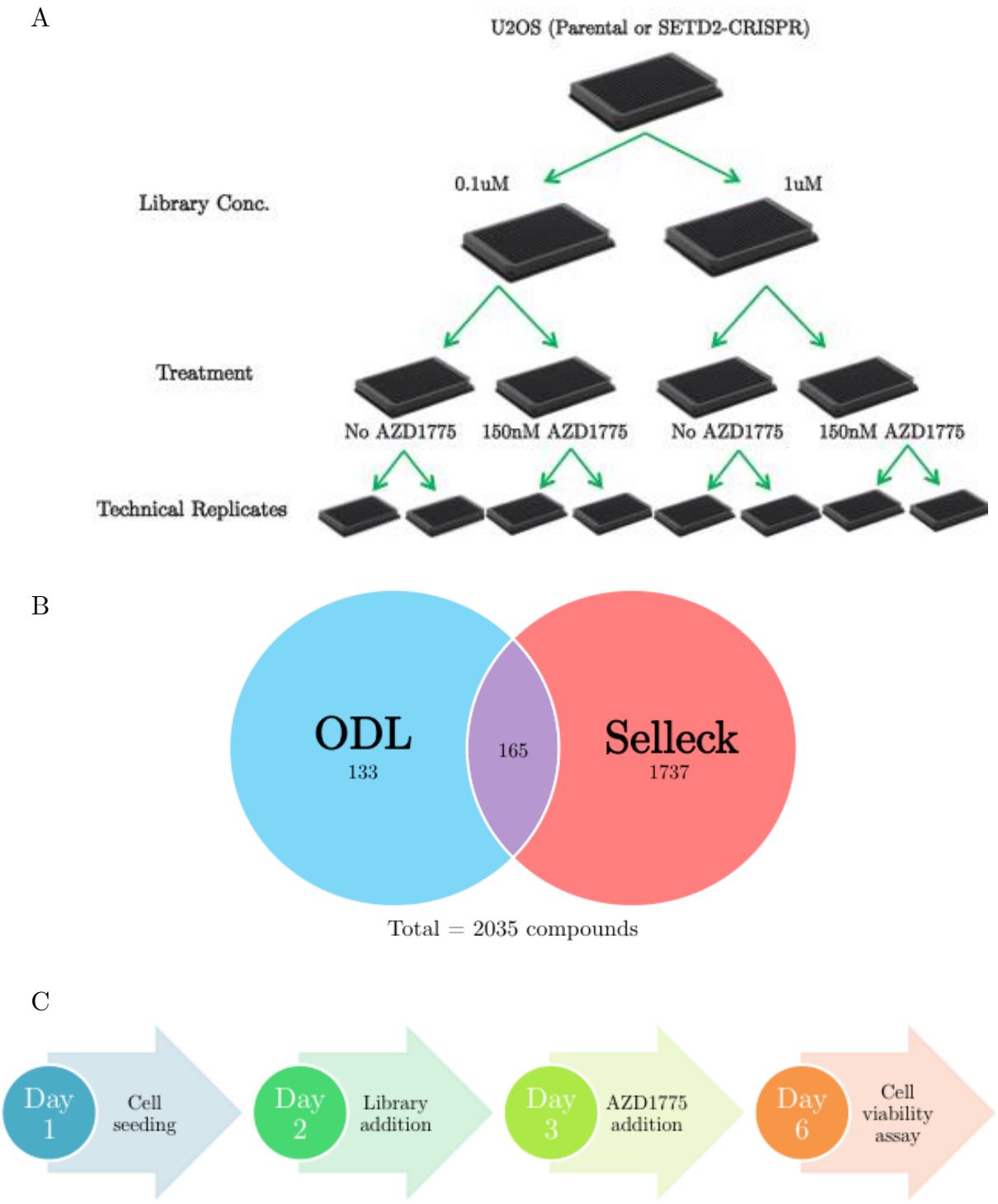



Figure 3.1 High-throughput screen setup. A. Assay conditions and variables selected for testing. For each drug library plate, 16 seeded plates were required (2 cell lines x 2 library conc. x 2 treatments x 2 replicates). B. Venn diagram showing the number of compounds in each library and the overlap between them. A total of 7 library plates with 2035 different compounds were tested. C. Day-by-day protocol for each step of the screen.

hits, an additional criterion was included: the compound must not be toxic as a single agent at the lowest dose (0.1 μM) as, due to the nature of the statistical analysis, fluctuations in fluorescence readings have a greater risk of creating false-positive results in samples with low fluorescence signal. Based on these criteria, the compounds listed in Table 3.1 were taken forward for validation experiments.

## 3.2 Histone deacetylase inhibition enhances the cytotoxic effects of WEE1 inhibition regardless of SETD2 status

After statistical analysis, the hits were ranked by Z-score and, encouragingly, two of the most highly ranked compounds were CHK1 inhibitors. Several groups have reported synergy between WEE1 and CHK1 inhibitors (Carrassa et al., 2012; Chila et al., 2015; Russell et al., 2013), which suggests that CHK1 can be considered a positive control for the reliability of our screen. Looking at the top 20 compounds from this list, it was observed that three of the top hits are histone deacetylase (HDAC inhibitors). The dynamics of histone acetylation is one of a plethora of epigenetic events that determine chromatin structure and gene expression. The addition of acetyl groups to histones converts the positive charge on lysine residues to a neutral charge, which nullifies their attraction to the negatively charged phosphate backbone on DNA and leads to a more relaxed, less compact conformation (Norton et al., 1990). Conversely, the deacetylation of histones reverts them to their positively charged state and increases their affinity for DNA, leading to chromatin compaction (Ruthenburg et al., 2007). Whether chromatin is in a relaxed or compacted state significantly affects its

Table 3.1. List of compound hits selected for validation. "Synergy" hits are those that enhance sensitivity to AZD1775, whereas "New SL" hits are those that specifically target SETD2(-/-) cells.

| Category | Drug | Target | Mean ΔZ-scores | Approved/Clinical Trial? |
|---|---|---|---|---|
| Synergy | Panobinostat | HDAC | -7.86 | Approved for multiple myeloma |
| Synergy | Nutlin-3 | E3 Ligase, Mdm2 | -5.23 | Completed Phase 1 as RG7112 (optimised version) |
| Synergy | Sorafenib Tosylate | PDGFR, Raf, VEGFR | -4.78 | Approved |
| Synergy | Decitabine | DNA Methyltransferase | -4.94 | Approved for myelodysplastic syndromes (MDS) |
| New SL | RITA (NSC 652287) | E3 Ligase, p53 | -14.95 | No information |
| New SL | MK-8776 (SCH 900776) | Chk1 | -4.70 | Phase 2 |
| New SL | ABT-263 (Navitoclax) | Bcl-2 | -5.00 | Phase 2 |
| New SL | GSK1838705A | IGF-1R, ALK | -3.72 | No information |
| New SL | Tranylcypromine (2-PCPA) HCl | KDM1A, monoamine oxidase | -3.60 | Approved for depression, Phase 2 for cancer |

accessibility to various proteins and protein complexes, including the transcriptional machinery (Lee et al., 1993). HDACs are comprised of 18 proteins divided into five structurally distinct classes: Class I (HDAC1, 2, 3, 8), Class IIa (HDAC4, 5, 7, 9), Class IIb (HDAC6, 10), Class III (SIRT1-7), and Class IV (HDAC11). The development of HDAC inhibitors as anticancer therapies began with compound screens to identify molecules with the ability to induce tumour cell differentiation (Leder and Leder, 1975; Riggs et al., 1977). This eventually led to the synthesis of more potent pan-HDAC inhibitors, as well as compounds that target a specific class of HDACs, and several of these inhibitors have attained FDA approval.

To validate the screen results, the FDA-approved pan-HDAC inhibitor panobinostat was selected and a dose-response curve was constructed (Fig. 3.2A), which showed that the inhibitor works potently on both cell lines. Combination experiments with AZD1775 were performed using a dose of panobinostat slightly below the IC50 (5 nM) and confirmed that HDAC inhibition does sensitise U2OS cells to the WEE1 inhibitor (Fig. 3.2B). Published results from our group indicate that the ribonucleotide reductase subunit RRM2 plays a key role in the SETD2-WEE1 synthetic lethality (Pfister et al., 2015); thus, the effect of HDAC inhibition on RRM2 expression was investigated. Western blot analysis showed that panobinostat treatment by itself did not lead to obvious changes in RRM2 protein levels (Fig. 3.2C), whereas AZD1775 treatment reduced RRM2 levels with or without panobinostat. The inhibitor also did not affect levels of Class I HDACs HDAC1 and HDAC2, indicating that its effects are not mediated by changes in HDAC protein expression. These results suggest that the

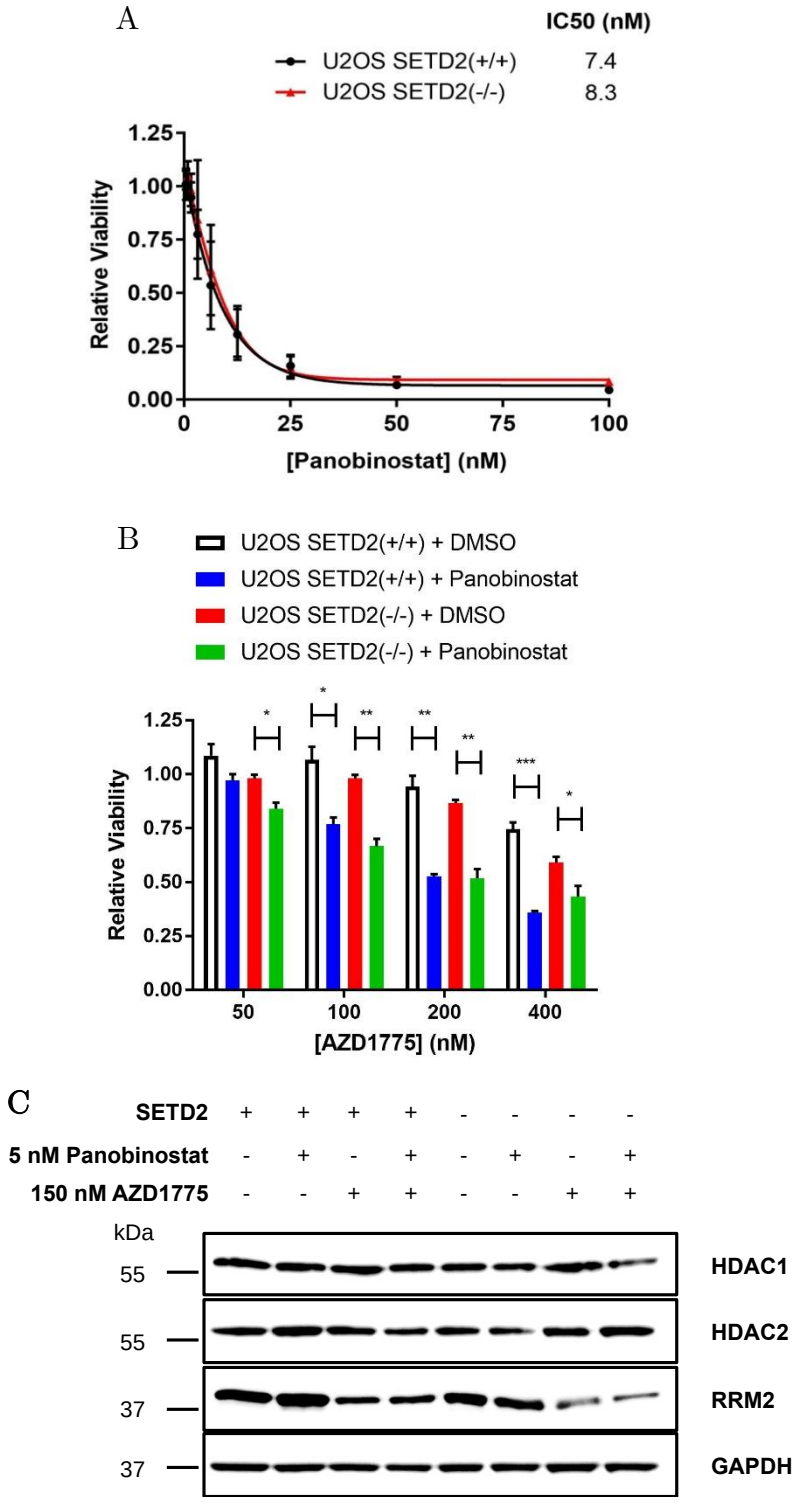
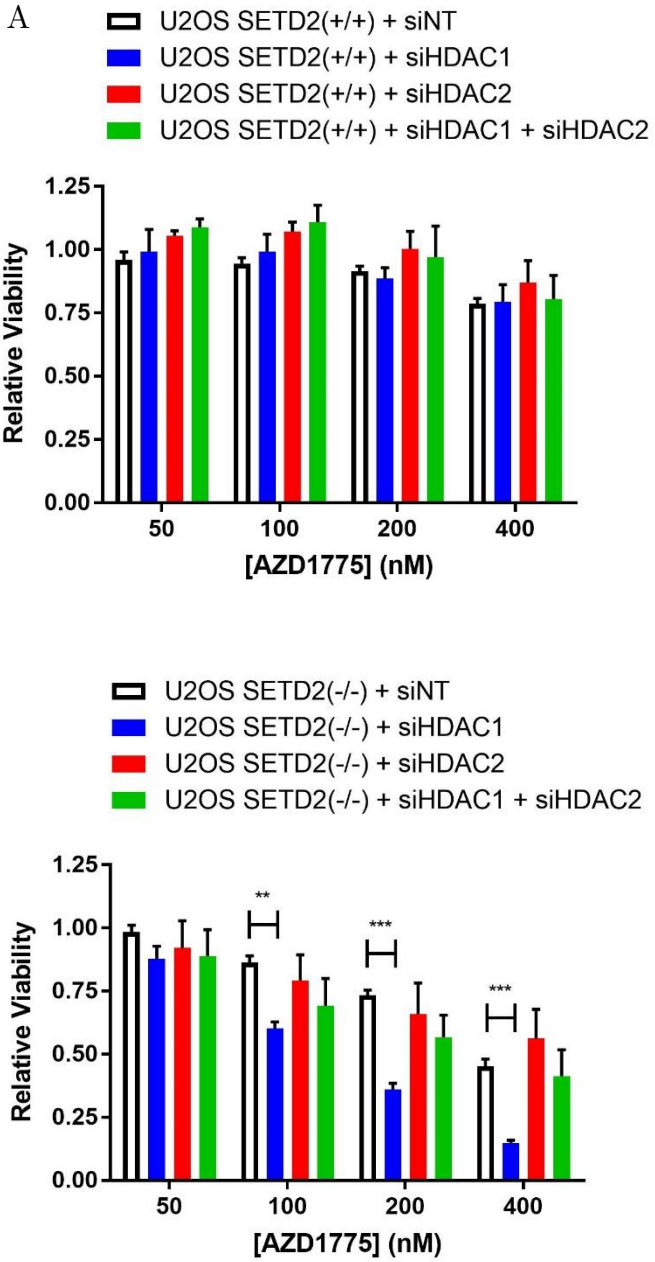


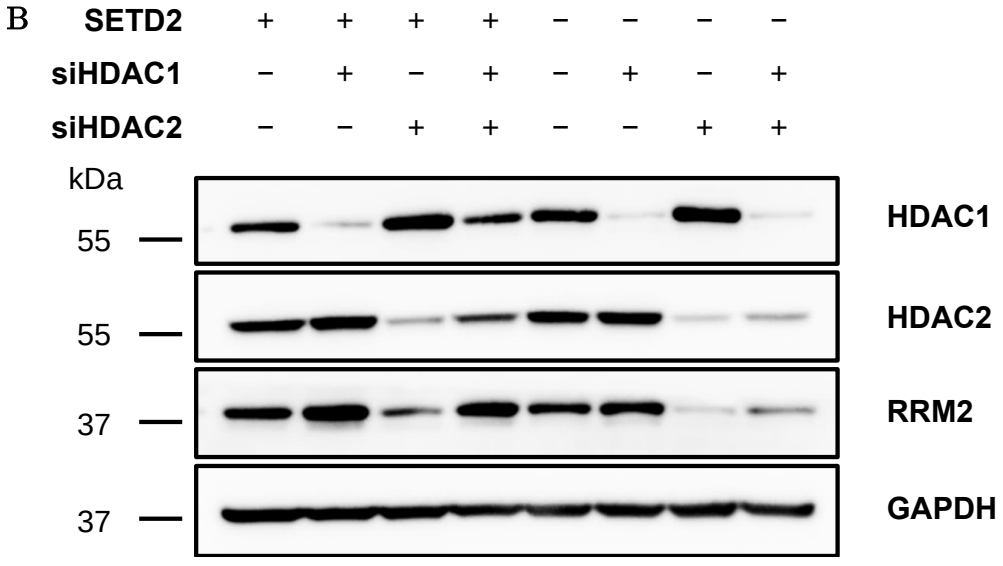

Figure 3.2. A. Dose-response viability curves for panobinostat in parental and SETD2-CRISPR U2OS cells. Data are shown as mean ± SD (n = 3). IC50 values were calculated via nonlinear regression (4-parameter curve fitting). B. Cell viability assay of parental and SETD2-CRISPR U2OS cells treated with increasing doses of AZD1775 with or without panobinostat (5 nM). Viability was calculated relative to samples without AZD1775. Data are shown as mean ± SD (n = 3). P-values were calculated using the Student's two-tailed t-test. * $p < 0.05$, ** $p < 0.01$, *** $p < 0.001$. C. Western blot of HDAC1, HDAC2, and RRM2 after panobinostat treatment of parental and SETD2-CRISPR U2OS cells.

increase in AZD1775 sensitivity after panobinostat treatment is not due to any further depletion of the RRM2 protein, which is consistent with a true synergistic interaction wherein HDAC inhibition affects an independent pathway through which the consequences of WEE1 inhibition are exacerbated.

## 3.3 Class I HDACs HDAC1 and HDAC2 mediate distinct effects on the SETD2-WEE1 synthetic lethality

In *Saccharomyces cerevisiae*, recruitment of the HDAC Rpd3S is mediated by binding of the Eaf3 chromodomain to methylated H3K36, and this acts as a form of "transcriptional memory" that reverts chromatin to its pre-transcription state via histone deacetylation (Carrozza et al., 2005; Joshi and Struhl, 2005). Given this potential link between HDACs and SETD2, the mammalian orthologues of Rpd3S, HDAC1 and HDAC2, were investigated. When combined with AZD1775 treatment, depletion of HDAC1 but not HDAC2 had a sensitising effect that was observed only in SETD2-CRISPR cells (Fig. 3.3A). Published literature on the physiological functions of HDAC1 and HDAC2 has indicated that these enzymes play both redundant (Montgomery et al., 2007; Montgomery et al., 2009; Senese et al., 2007; Yamaguchi et al., 2010) and unique (Bicaku et al., 2008; Fritsche et al., 2009; Lagger et al., 2002; Marchion et al., 2009; Zupkovitz et al., 2010) roles in essential biological processes; when their activities diverge, HDAC1 appears to be involved in promoting cell proliferation whereas HDAC2 negatively regulates apoptosis (Jurkin et al., 2011).


A
U2OS SETD2(+/+) + siNT
U2OS SETD2(+/+) + siHDAC1
U2OS SETD2(+/+) + siHDAC2
U2OS SETD2(+/+) + siHDAC1 + siHDAC2
Relative Viability
1.25
1.00
0.75
0.50
0.25
0.00
50
100
200
400
[AZD1775] (nM)
U2OS SETD2(-/-) + siNT
U2OS SETD2(-/-) + siHDAC1
U2OS SETD2(-/-) + siHDAC2
U2OS SETD2(-/-) + siHDAC1 + siHDAC2
Relative Viability
**
***
***
[AZD1775] (nM)


B
SETD2
siHDAC1
siHDAC2
kDa
55
55
37
37
HDAC1
HDAC2
RRM2
GAPDH

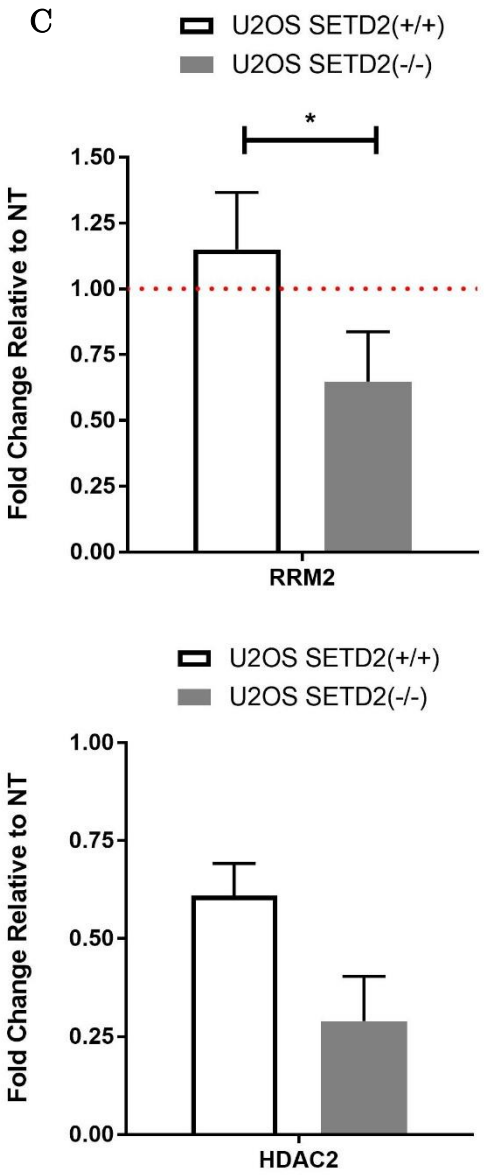
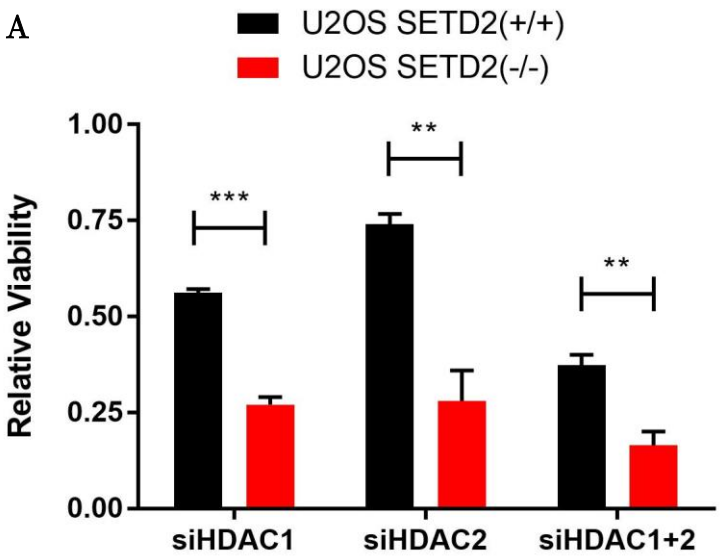


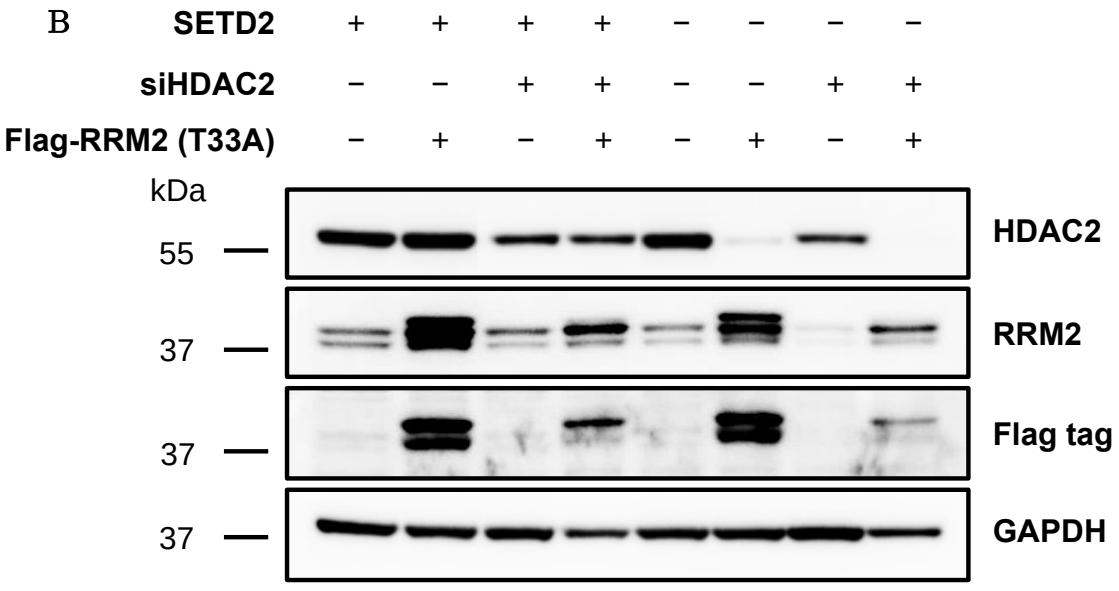

Figure 3.3. A. Cell viability assay after AZD1775 treatment combined with siRNA depletion of HDAC1, HDAC2, or both in parental and SETD2-CRISPR U2OS. Viability was calculated relative to cells incubated with non-targeting siRNA. Data are shown as mean ± SD (n = 3). P-values were calculated using the Student's two-tailed t-test. *** $p < 0.01$. B. Western blot of HDAC1, HDAC2, and RRM2 after siRNA depletion of HDAC1, HDAC2, or both in parental and SETD2-CRISPR U2OS. C. Quantitative RT-PCR analysis of RRM2 mRNA levels after siRNA depletion of HDAC2. siRNA efficiency was confirmed by measuring HDAC2 mRNA levels. Samples were normalised to the housekeeping gene GAPDH. Fold change was calculated relative to samples treated with non-targeting siRNA. Data are shown as mean ± SD (n = 3).

To further investigate the apparent link between HDAC depletion, SETD2 loss, and WEE1 inhibition, Western blot analysis was performed to determine RRM2 levels under these conditions. siRNA depletion of HDAC2, but not HDAC1, led to a dramatic downregulation of RRM2 protein, particularly in SETD2-CRISPR cells (Fig. 3.3C) even in the absence of AZD1775. In addition, RRM2 transcription was also revealed to be reduced more drastically in the absence of SETD2 after HDAC2 knockdown, as measured by quantitative RT-PCR (Fig. 3.3D). Although this initially seems to be at odds with the viability results (Fig. 3.3A), in which loss of HDAC1 but not HDAC2 sensitised SETD2-CRISPR cells to AZD1775, these results may be evidence of epistasis between HDAC2, SETD2, and WEE1 in the context of RRM2 regulation. Because combined loss of SETD2 and WEE1 already leads to critically low levels of RRM2, any further depletion mediated by HDAC2 loss would not be expected to enhance this synthetic lethality.

## 3.4 HDAC2 displays putative synthetic lethality with SETD2 and leads to RRM2 downregulation without any cell cycle defects

One unexpected observation arose after siRNA depletion of HDAC1/2 on their own (without WEE1 inhibition): a striking loss of viability that was significantly greater in SETD2-CRISPR compared to parental cells (Fig. 3.4A). In particular, the reduced viability after HDAC2 depletion appears to be more specific to SETD2-deleted cells, which is consistent with a putative role for HDAC2 in the maintenance of RRM2


A
U2OS SETD2(+/+)
U2OS SETD2(-/-)
Relative Viability
1.00
0.75
0.50
0.25
0.00
***
**
**
siHDAC1
siHDAC2
siHDAC1+2


B
SETD2 + + + + − − − −
siHDAC2 − − + + − − + +
Flag-RRM2 (T33A) − + − + − + − +
kDa
55
37
37
37
HDAC2
RRM2
Flag tag
GAPDH

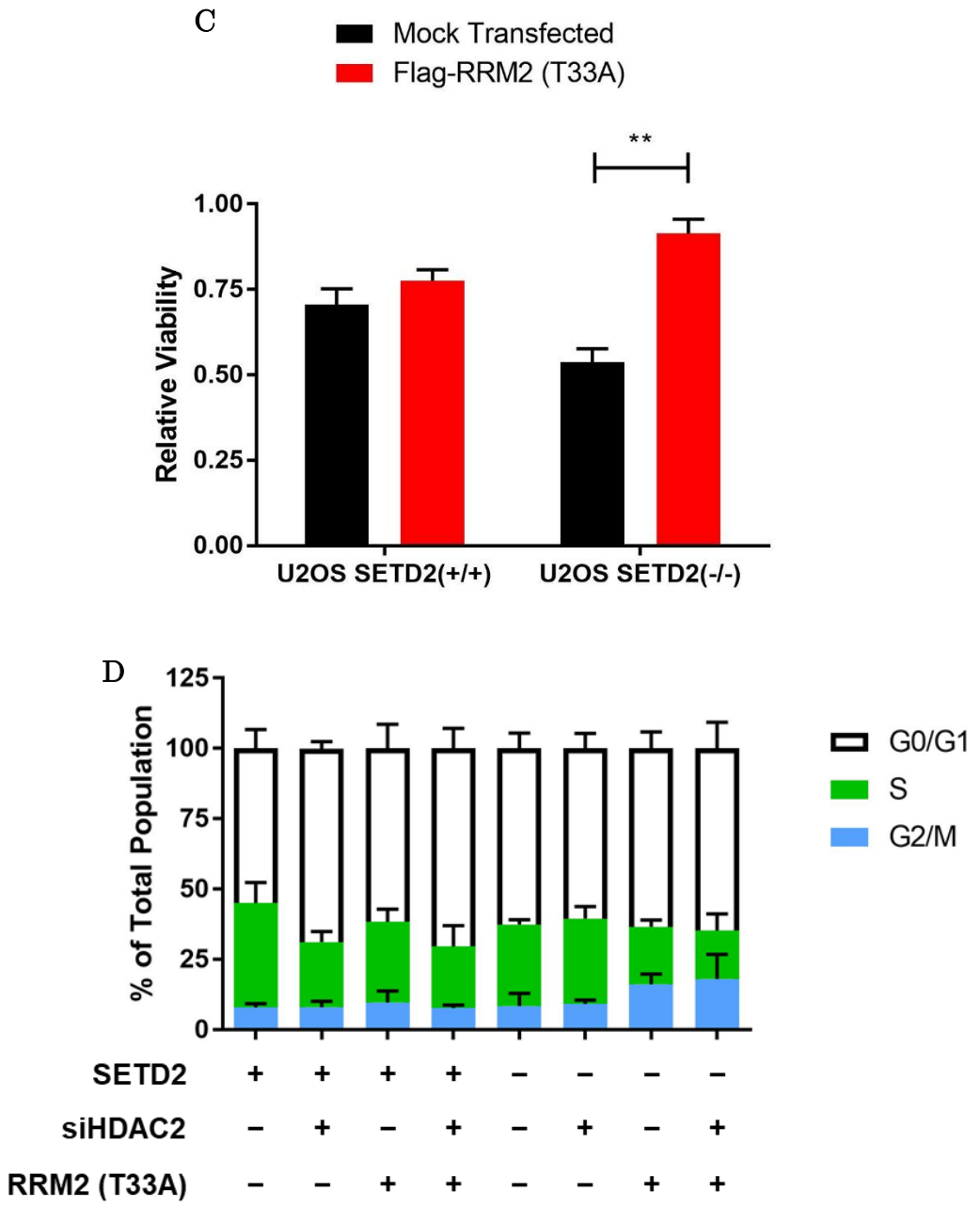



Figure 3.4. A. Cell viability assay after siRNA depletion of HDAC1, HDAC2, or both in parental and SETD2-CRISPR U2OS. Viability was calculated relative to cells incubated with non-targeting siRNA. Data are shown as mean ± SD (n = 3). P-values were calculated using the Student's two-tailed t-test. ** $p < 0.01$, *** $p < 0.001$. B. Western blot of HDAC2, RRM2, and Flag tag after siRNA depletion of HDAC2 and/or stable expression of Flag-RRM2 (T33A). C. Cell viability assay after siRNA depletion of HDAC2 with or without stable expression of RRM2 (T33A). Viability was calculated relative to cells incubated with non-targeting siRNA. Data are shown as mean ± SD (n = 3). P-values were calculated using the Student's two-tailed t-test. ** $p < 0.01$. D. Cell cycle distribution of U2OS cells with or without siRNA depletion of HDAC2 and/or stable expression of RRM2 (T33A). Data are shown as mean ± SD (n = 3).

expression (Fig. 3.3C-D). To confirm the involvement of RRM2 in this loss of viability after HDAC2 depletion, exogenous RRM2 protein was expressed in U2OS cells. In healthy wild-type cells, RRM2 expression is strictly regulated in a cell-cycle-dependent manner; its transcription is induced by the E2F family of transcription factors at the G1/S transition (Chabes et al., 2004; DeGregori et al., 1995). Furthermore, the RRM2 protein is degraded in G2 via the $SCF^{Cyclin\ F}$ ubiquitin ligase complex, which requires phosphorylation of RRM2 at Thr33 by CDK1-Cyclin B or CDK2-Cyclin A (D'Angiolella et al., 2012). Mutating the aforementioned phosphorylation site produces a non-degradable form of the RRM2 protein (RRM2 (T33A)) that persists throughout the cell cycle (D'Angiolella et al., 2012). After stable transfection of this mutant into U2OS cells, overexpression was demonstrated via Western blot (Fig. 3.4B). Unexpectedly, in the absence of HDAC2 siRNA, HDAC2 expression was greatly diminished in pooled SETD2-CRISPR cells stably overexpressing RRM2 (T33A), implying the existence of a reciprocal feedback mechanism. Viability experiments were conducted and RRM2 (T33A) expression was shown to be able to rescue the viability of U2OS SETD2-CRISPR after HDAC2 knockdown (Fig. 3.4C). These results suggest that the loss of viability induced by HDAC2 loss specifically in SETD2-deficient cells involves an RRM2-dependent mechanism.

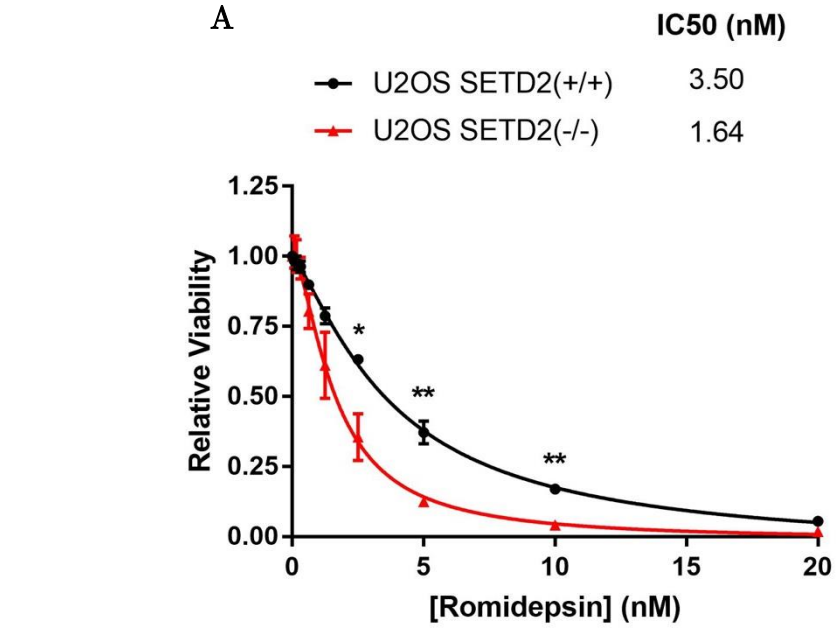
Cell cycle progression is a tightly regulated process that requires the induction and repression of specific genes at specific times, particularly at the transition points between two cell cycle phases. Alterations in gene expression can perturb the timely advance of the cell from one phase to the next; conversely, any cellular stresses that

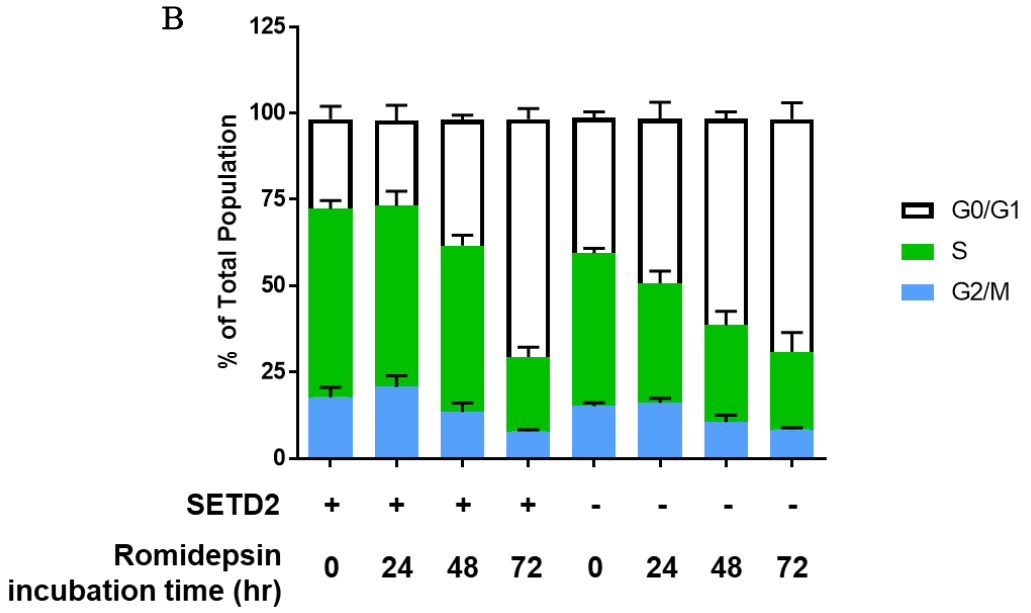
prevent the transition into the subsequent phase will consequently affect the expression of cell cycle-regulated genes. It has long been established that RRM2 expression is induced only at late G1 (Engstrom et al., 1985), and published reports have demonstrated that RRM2 downregulation in tumour cells leads to G1 arrest (Li et al., 2018; Wang et al., 2018; Zhang et al., 2013). Given these observations and RRM2's critical role in DNA synthesis and S-phase progression (Wright et al., 1990), cell cycle profiles were analysed via FACS after addition of HDAC2 siRNA and RRM2 (T33A). In parental U2OS cells, there was a significant increase ($p = 0.03$) in the G0/G1 population with a corresponding decrease ($p = 0.017$) in the S-phase population after HDAC2 knockdown (Fig. 3.4D). This may account for the approximately 20% reduction in viability observed in parental U2OS cells (Fig. 3.3A) and is consistent with published reports that HDAC inhibitors can induce cell cycle arrest, primarily at the G1/S transition via upregulation of CDK inhibitors such as p21 (Falkenberg and Johnstone, 2014; Newbold et al., 2014). In contrast, HDAC2 knockdown did not lead to major cell cycle defects in SETD2-CRISPR cells. This indicates that the observed reduction in RRM2 levels after HDAC2 depletion is not due to G1 arrest or a smaller S-phase population. Also, this suggests that the loss of viability induced by low HDAC2 expression is not a result of cell cycle arrest. Interestingly, despite observing reduced HDAC2 protein levels after RRM2 (T33A) expression in U2OS SETD2-CRISPR, HDAC2 depletion by itself did not lead to the same cell cycle profile as RRM2 (T33A) expression.

## 3.5 Dual HDAC1/2 inhibitor romidepsin selectively targets SETD2-deficient cells and induces more rapid G1 arrest in the absence of SETD2

In order to determine the clinical potential of the observed synthetic lethality between the combined loss of either HDAC1 or HDAC2 and SETD2, specific inhibitors of HDAC1 and HDAC2 would need to be tested. However, the development of HDAC1- or HDAC2-specific inhibitors is a challenging endeavour due to the high degree of sequence homology between the two genes, which is a result of their common origin as products of a gene duplication event (Brunmeir et al., 2009). In the absence of such a specific inhibitor, a dual HDAC1/HDAC2-specific drug was tested instead. Romidepsin is a bicyclic peptide that has been approved by the FDA for the treatment of cutaneous T-cell lymphoma (CTCL). It is highly specific against HDAC1 and HDAC2, with IC50s of 1.6 nM and 3.9 nM respectively after it is metabolised into its active, reduced form (Furumai et al., 2002).

Viability experiments revealed that, much like the pan-HDAC inhibitor panobinostat, romidepsin is highly potent against both parental and SETD2-CRISPR cells (Fig. 3.5A). In the absence of SETD2, there is a slight but significant increase in sensitivity, culminating in an approximately 2-fold reduction in cellular IC50 (Fig. 3.5A). To further investigate romidepsin's mechanism of action in these cells, cell cycle progression was monitored in the presence of romidepsin over several days. Both parental and SETD2-CRISPR cells displayed extraordinary levels of G1 arrest by 72 hours of romidepsin treatment (parental: $p = 0.0001$; SETD2-CRISPR: $p = 0.0006$),


A
IC50 (nM)
U2OS SETD2(+/+) 3.50
U2OS SETD2(-/-) 1.64
Relative Viability
1.25
1.00
0.75
0.50
0.25
0.00
0
5
10
15
20
[Romidepsin] (nM)
*
**
**


B
% of Total Population
125
100
75
50
25
0
G0/G1
S
G2/M
SETD2 + + + + - - - -
Romidepsin incubation time (hr) 0 24 48 72 0 24 48 72

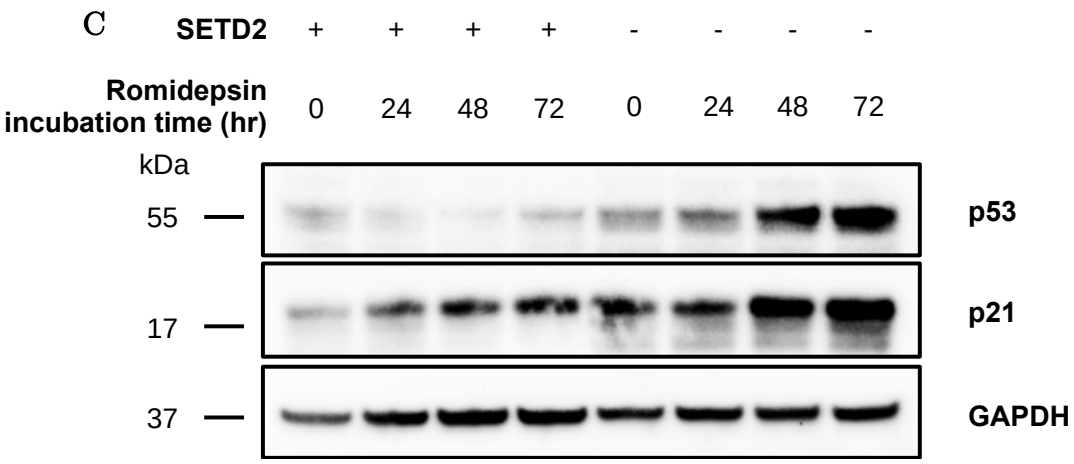



Figure 3.5. A. Dose-response viability curves for romidepsin in parental and SETD2-CRISPR U2OS cells. Data are shown as mean ± SD (n = 3). IC50 values were calculated via nonlinear regression (4-parameter curve fitting). P-values were calculated using the Student's two-tailed t-test. * $p < 0.05$, ** $p < 0.01$ B. Cell cycle distribution of U2OS cells in the presence or absence of romidepsin at the indicated time points. Data are shown as mean ± SD (n = 3). C. Western blot of p53 and p21 after romidepsin treatment of U2OS cells at the indicated time points.

with a corresponding significant reduction in S-phase cells (parental: $p = 0.0001$; SETD2-CRISPR: $p = 0.0029$). However, this accumulation began as early as 24 hours in cells lacking SETD2 (G1 population at 0 hr vs 24 hr: $p = 0.0467$; S-phase population at 0 hr vs 24 hr: $p = 0.0113$), while wild-type cells remained unperturbed until the 48-hour time point (Fig. 3.5B). These results suggest that SETD2 loss renders cells more vulnerable to phenomena that disrupt the G1/S transition, leading to a more rapid activation of this particular cell cycle checkpoint.

One of the most important regulators of the G1/S checkpoint is the p53 pathway. Induction of p53 expression exogenously or via DNA-damaging agents is sufficient to arrest cells in G1 (Kastan et al., 1991; Lin et al., 1992). The key p53 target that mediates its effects on the G1/S transition is the CDK inhibitor *CDKN1A* (p21); even in the absence of p53, p21 expression on its own is able to hinder G1/S progression (Rousseau et al., 1999). Moreover, as mentioned previously, HDAC inhibitors in general have been shown to induce G1 arrest via the upregulation of p21 (Falkenberg and Johnstone, 2014; Newbold et al., 2014). In light of these observations, the effect of romidepsin on p53 and p21 was determined by Western blot in parallel with the cell cycle measurements. Even in the absence of treatment, p53 and p21 are expressed at higher levels in SETD2-CRISPR cells compared to parental cells (Fig. 3.5C). However, while p21 levels increase over time in both cell lines, p53 accumulates only in cells lacking SETD2 and remains at relatively low levels in wild-type cells (Fig. 3.5C). Furthermore, the levels of p21 at the latest time point (72 hours) is notably higher in the absence of SETD2. These findings suggest a potential SETD2-dependent

mechanism that prevents p53 or p21 activation, the loss of which may lead to an increased sensitivity to G1/S perturbations that culminate in rapid G1 arrest and/or cell death. Published reports have claimed a physical interaction between SETD2 and p53 *in vivo*, although their results point towards a positive effect of SETD2 on p53 activation and stability (Xie et al., 2008).

## 3.6 Chapter Discussion

A key challenge in the treatment of cancer is achieving sufficient anti-tumour activity while limiting any negative impact on the patient. Maximising a drug's therapeutic index, defined as the ratio between the dose that induces toxicity and the dose needed for therapeutic efficacy (Kaelin, 2005), is a problem that still plagues researchers and clinicians alike. One strategy to achieve a high therapeutic index is to discover synergistic interactions between therapeutic agents. Although the exact criteria for defining synergy may vary considerably, the general concept requires that the combination of two or more treatments must be more potent than any individual treatment on its own. Effective drug combinations can potentially enable reduced drug doses, lowered toxicity, and delayed drug resistance (Chou, 2006). The aim of this chapter was to search for compounds that enhance the potency of the WEE1 inhibitor, thereby laying the groundwork for possible drug combinations in the clinic.

The appearance of several HDAC inhibitors in the top 20 hits of the combination screen was a strong indicator that combined loss of HDACs and WEE1 would have a clinical benefit. This was further encouraged by the fact that several pan-HDAC

inhibitors, such as panobinostat, are already approved by the FDA for clinical use in certain cancers. Validation of the screen results confirmed the enhancement of AZD1775 sensitivity when combined with panobinostat (Fig. 3.2B) and this phenomenon was independent of any further downregulation of RRM2 (Fig. 3.2C), which is consistent with a true synergistic interaction wherein HDAC inhibition affects downstream pathways independently of WEE1. One potential explanation for this effect is hinted at by a report that demonstrates the role of HDACs in maintaining checkpoint activation (Goder et al., 2018). Specifically, the authors observed that inhibition of Class I HDACs (HDAC1, 2, 3) allows cells to bypass the intra-S checkpoint during replicative stress, leading to increased entry into G2 and M phase. Although their findings are associated with a reduction in WEE1 expression and CDK1 phosphorylation, which would be the same as WEE1 inhibition, there was also a decrease in p53 levels and activation and upregulation of PR130, a subunit of the PP2A phosphatase that dephosphorylates checkpoint kinases (Goder et al., 2018). It is therefore possible that in the presence of replication stress induced by WEE1 inhibition, the addition of an HDAC inhibitor prematurely releases SETD2-deficient cells from the intra-S checkpoint, resulting in unrepaired DNA damage during G2 and mitosis. If p53 and PR130 play a role in this mechanism, the reported attenuation of the p53 pathway and enhanced dephosphorylation of checkpoint mediators after HDAC inhibition may also hinder the activation of the G2/M checkpoint, thereby preventing DNA repair prior to mitosis. Future experiments would need to determine whether ATR/CHK1 phosphorylation after WEE1 inhibition and cell cycle progression from S to G2/M are

affected by HDAC inhibitors.

At the time the screen was conducted, the combination of the WEE1 inhibitor AZD1775 and pan-HDAC inhibitors vorinostat and SBHA had already been investigated in acute myeloid leukaemia cell lines (Zhou et al., 2015) but had not been reported for any other tumour type. This changed in subsequent years with published data on the synergism between vorinostat and AZD1775 in p53-mutant head and neck squamous cell carcinoma cell lines (Tanaka et al., 2017). Furthermore, a phase I clinical trial using a combination of the pan-HDAC inhibitor belinostat and AZD1775 began in 2015 and was terminated in 2018 (ClinicalTrials.gov). In light of these findings, the focus of this chapter was shifted to the apparent synthetic lethality between SETD2 and HDAC1/2. The reduction in viability following HDAC1/2 depletion in cells that lack SETD2 (Fig. 3.4A), and the particular specificity of HDAC2 loss in targeting SETD2-deleted cells, prompted further investigation into a potential new therapeutic strategy that could complement or replace WEE1 inhibition. The observation that HDAC2 depletion leads to RRM2 downregulation, especially in the absence of SETD2 (Fig. 3.3B), draws immediate parallels to the published mechanism of the SETD2-WEE1 synthetic lethality (Pfister et al., 2015). However, the observed downregulation of HDAC2 protein in the presence of exogenous RRM2 was an unexpected development. The obvious next step would be to confirm these results with a chemical inhibitor; however, an HDAC2-specific inhibitor has yet to be developed, most likely because of the challenges inherent in creating a molecule that can distinguish between the highly homologous Class I HDACs in general, and HDAC1 and HDAC2 in particular.

In the absence of a specific HDAC2 inhibitor, the next best option is to target as few other HDACs as possible. The HDAC1/2-specific inhibitor romidepsin displays incredible potency in U2OS cells with some degree of specificity for SETD2 loss (Fig. 3.5A), which is a tantalising hint of what might be observed with HDAC2 inhibition alone. The observed G1 arrest (Fig. 3.5B) is consistent with published reports on other HDAC inhibitors (Falkenberg and Johnstone, 2014; Newbold et al., 2014); however, romidepsin itself has been shown to exert different cell cycle effects in different cell lines, with p21 upregulation (Fig. 3.5C) as a recurring phenotype (Sun et al., 2017; Vinodhkumar et al., 2008). The romidepsin-induced accumulation of p21 in parental U2OS cells, which appears to be unaccompanied by a corresponding increase in p53 (Fig. 3.5C), indicates a p53-independent method of p21 upregulation. Several such mechanisms have been described in published literature, some of which involve acetylation of the *CDKN1A* promoter (Gartel and Tyner, 1999; Li et al., 2005); thus, inhibition of histone deacetylases may enable this acetylation or prolong its effects, leading to increased p21 expression.

In summary, the key findings of this chapter are:

- Several of the top hits for compounds that enhance sensitivity to the WEE1 inhibitor AZD1775 are histone deacetylase (HDAC) inhibitors
- The pan-HDAC inhibitor panobinostat is able to increase sensitivity to AZD1775 regardless of SETD2 status
- Depletion of HDAC1, but not HDAC2, is able to sensitise SETD2-CRISPR cells to AZD1775

- Depletion of both HDAC1 and HDAC2 individually leads to a significant loss of viability specifically in SETD2-CRISPR cells
- Depletion of HDAC2, but not HDAC1, leads to a striking downregulation of the ribonucleotide reductase subunit RRM2 at both the mRNA and protein level
- Expression of a nondegradable variant of RRM2 rescues the viability of SETD2-CRISPR cells after HDAC2 knockdown
- The reduction in RRM2 expression after HDAC2 knockdown is not due to G1 arrest or a smaller S-phase population
- The dual HDAC1/2 inhibitor romidepsin shows a slight but significant selectivity against SETD2-CRISPR cells, associated with a more rapid G1 arrest and p21 induction after drug treatment

# 4. Therapeutic targeting of SETD2 loss with novel synthetic lethal interactions

The previous chapter explored the possibility of enhancing a known synthetic lethality and potentially widening its therapeutic window. In the process of this investigation, a putative novel synthetic lethal interaction between Class I histone deacetylases HDAC1/HDAC2 and SETD2 was discovered, which may have important therapeutic implications given the plethora of increasingly specific HDAC inhibitors currently under clinical development. The identification of synthetic lethal strategies to target H3K36me3 loss was the second aim of the compound screen discussed previously, and the validation and characterisation of the hits from that arm of the screen will be described in this chapter.

## 4.1. Identification and validation of putative synthetic lethal hits

Similar to the previously discussed synergy screen, hits for the synthetic lethality screen were ranked based on the difference between Z-scores of the parental and SETD2-CRISPR U2OS groups, which were treated with either the ODL or Selleck libraries alone without any other compounds. The list was further refined based on criteria such as their clinical development status (i.e. whether the compound is in clinical trials or has been approved) and their relevance to pathways of interest. Five putative synthetic lethal hits were selected for validation and dose-response viability curves were generated for each compound (Fig. 4.1). MK-8776, a highly selective CHK1 inhibitor, was able to serve as a positive control because our group has previously shown that H3K36me3-deficient cells are highly sensitive to CHK1 inhibition (Pfister et al., 2015) (Fig. 4.1, top-right).

Another compound that showed selective activity against SETD2-CRISPR cells is ABT-263, which targets BCL-2, BCL-xL, and BCL-w (Fig. 4.1, middle-left). The BCL-2 family is comprised of genes that are key regulators of apoptosis, a tightly controlled cell death pathway wherein internal or external stimuli trigger a cascade of enzymatic reactions mediated by cysteinyl aspartate proteinases known as caspases (Yuan et al., 1993). Specifically, the BCL-2 family is critical in the intrinsic or mitochondrial pathway of apoptosis, which involves the permeabilisation of the mitochondrial membrane, the release of cytochrome c, and the activation of effector caspases that mediate the disassembly of cellular organelles and degradation of DNA, RNA, and proteins (Tsujimoto, 2003). In unperturbed cells, the mitochondrial

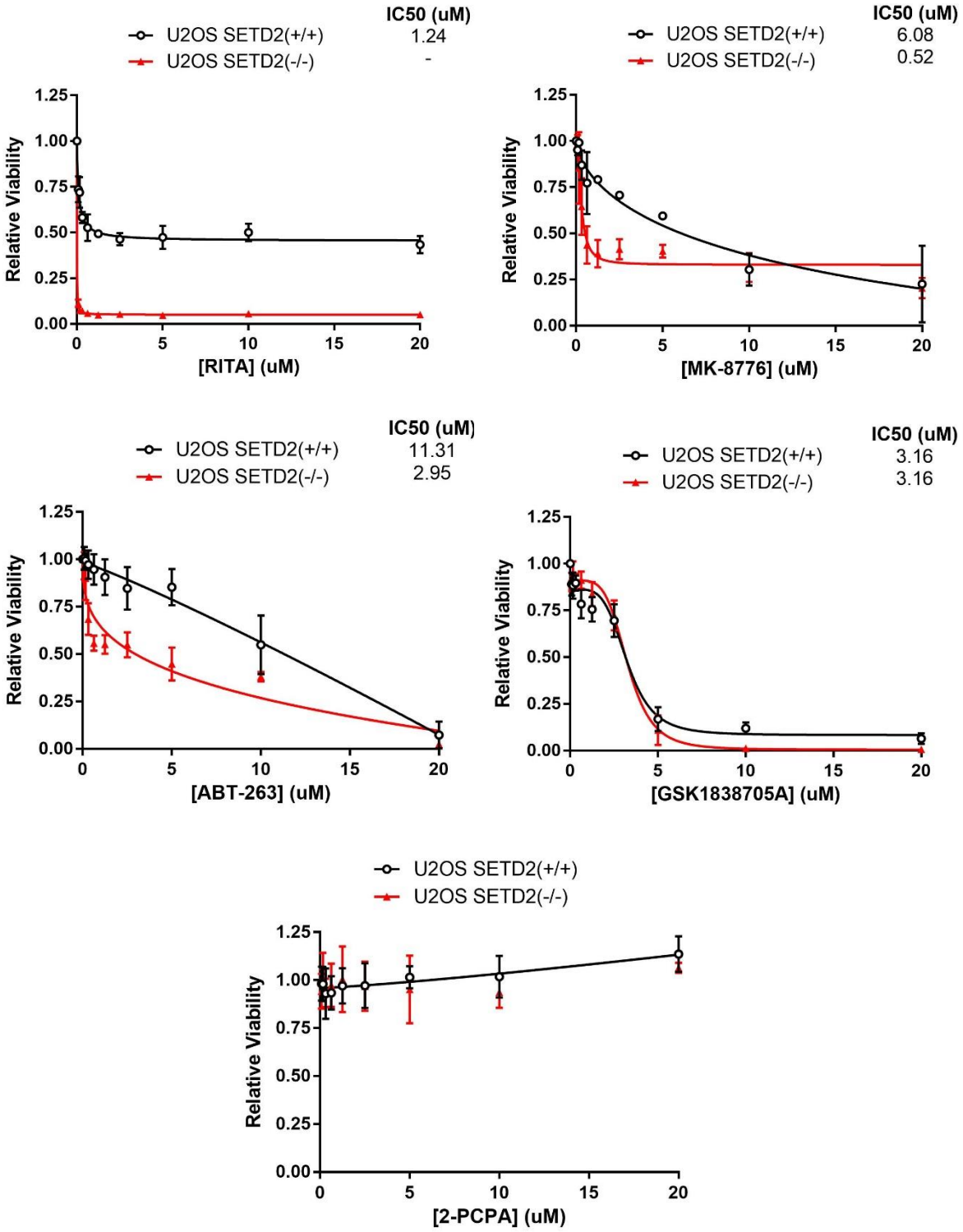



Figure 4.1. Dose-response viability curves for putative new synthetic lethal hits. Data are shown as mean ± SD (n ≥ 4). Results were independently confirmed by Dr. Sovan Sarkar and our data were combined for the statistical analysis. IC50 values were calculated via nonlinear regression (4-parameter curve fitting) when possible.

membrane remains intact through a carefully maintained balance between pro-apoptotic and anti-apoptotic BCL-2 proteins; cellular stresses can swing the balance towards apoptosis by transcriptional upregulation and/or post-translational modification and activation of the pro-apoptotic BCL-2 members (Gross et al., 1999). ABT-263 is a BH3 mimetic that binds to the anti-apoptotic proteins BCL-2, BCL-xL, and BCL-w and prevents them from sequestering their pro-apoptotic counterparts (Tse et al., 2008). To confirm its selectivity against SETD2-deficient cells, ABT-263 was tested in the SETD2-mutant renal cancer cell line A498. Unfortunately, A498 cells displayed minimal sensitivity to ABT-263 relative to the SETD2 wild-type 786-O cells (Fig. 4.2A).

Data from lymphoid cell lines indicate that BCL-2 is the main target of ABT-263 and its predecessor ABT-737; overexpression of BCL-2, which leads to accumulation of the pro-apoptotic protein Bim, sensitised both normal and transformed lymphoid cells to both drugs, whereas high levels of BCL-xL and BCL-w induced resistance (Merino et al., 2012). To further investigate the mechanism behind ABT-263's selective potency in our screen, U2OS cells and RCC cell lines were treated with a BCL-2-specific inhibitor, ABT-199. However, this compound did not demonstrate any degree of selectivity against SETD2-CRISPR cells compared to the parental cells (Fig. 4.2B), nor against A498 cells compared to 786-O cells (Fig. 4.2C). These results suggest that the observed synthetic lethal interaction between ABT-263 and SETD2 deletion is not mediated exclusively by BCL-2 and may necessitate inhibition of all three anti-apoptotic BCL-2 family proteins.

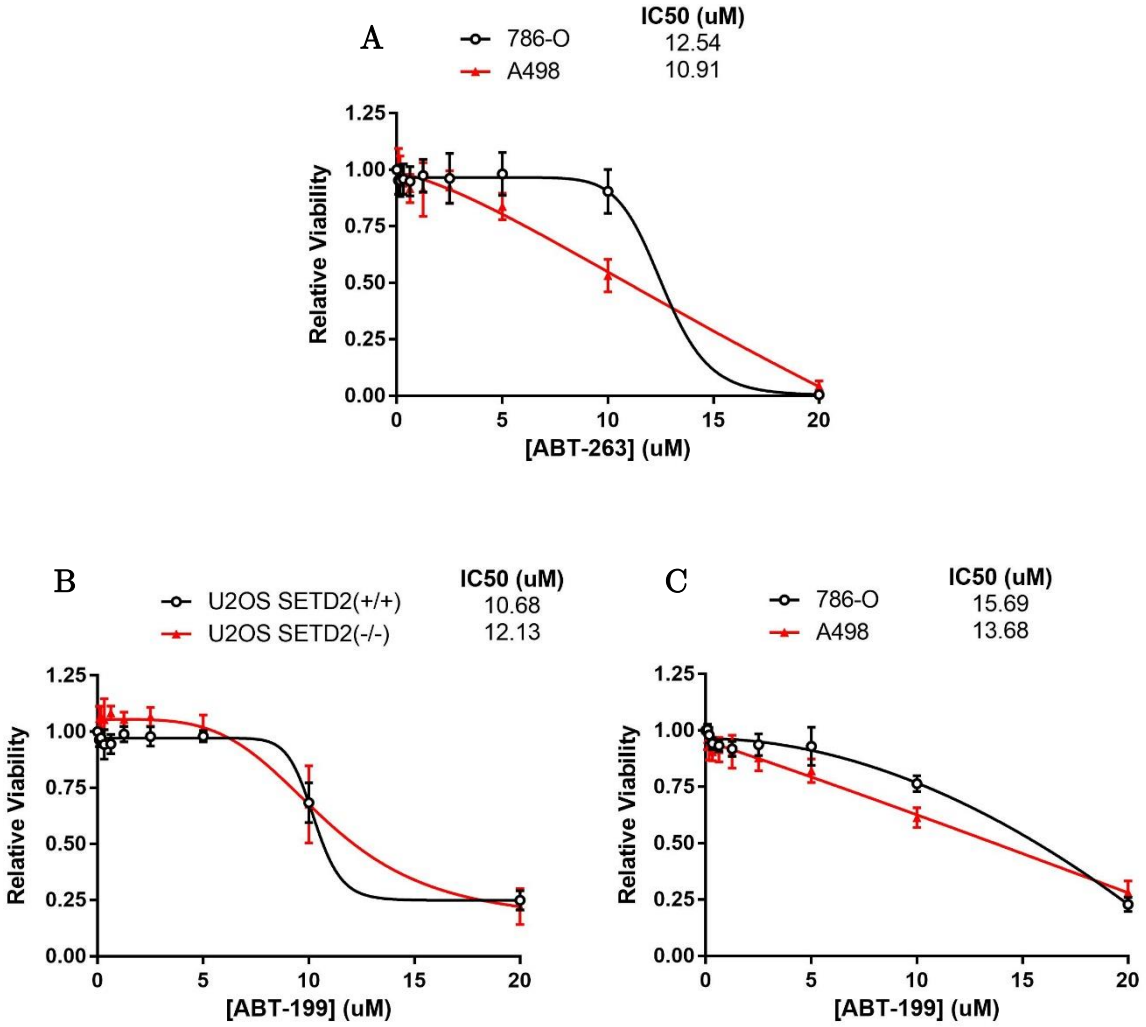



Figure 4.2. Dose-response viability curves for A. ABT-263 in RCC cell lines, B. ABT-199 in U2OS cells, and C. ABT-199 in RCC cell lines. Data are shown as mean ± SD (n = 4). Results were independently confirmed by Dr. Sovan Sarkar and our data were combined for the statistical analysis. IC50 values were calculated via nonlinear regression (4-parameter curve fitting).

The compound that showed the most drastic anti-tumour activity specifically against SETD2-CRISPR cells was RITA (Reactivation of p53 and Induction of Tumour cell Apoptosis) (Fig. 4.1, top-left). Because U2OS SETD2-CRISPR cells were only 24% viable at the lowest concentration used in the initial dose-response experiment, this was repeated at a lower dose range. Encouragingly, the striking difference in viability was maintained even at lower RITA concentrations (Fig. 4.3A). RITA was initially discovered due to its high potency and selectivity against a number of tumour types in the National Cancer Institute (NCI) Anticancer Drug Screen, which used a cell line panel comprised of 60 different human cancer cell lines (Rivera et al., 1999). This was particularly striking in several renal cell carcinoma (RCC) cell lines, including the SETD2-mutant A498 cell line. To confirm whether this result could be replicated in our system, dose-response curves for RITA were obtained in the RCC cell lines A498, LB996, and 786-O. Even at low concentrations of RITA, both SETD2-mutant cell lines (A498 and LB996) were markedly more sensitive compared to 786-O (Fig. 4.3B). RITA's potent selectivity for SETD2-deficient cells was further confirmed using a clonogenic survival assay (Fig. 4.3C), as well as siRNA-mediated depletion of SETD2 in wild-type U2OS cells (Fig. 4.3D).

## 4.2.RITA induces p53 upregulation and activation, as well as apoptotic cell death, specifically in SETD2-deficient cancer cells

One possible mechanism underlying RITA's remarkable potency may involve its ability to stabilise the p53 protein. p53 is the most frequently lost tumour suppressor in human cancers (Beroud and Soussi, 2003; Hussain and Harris, 1998) and coordinates

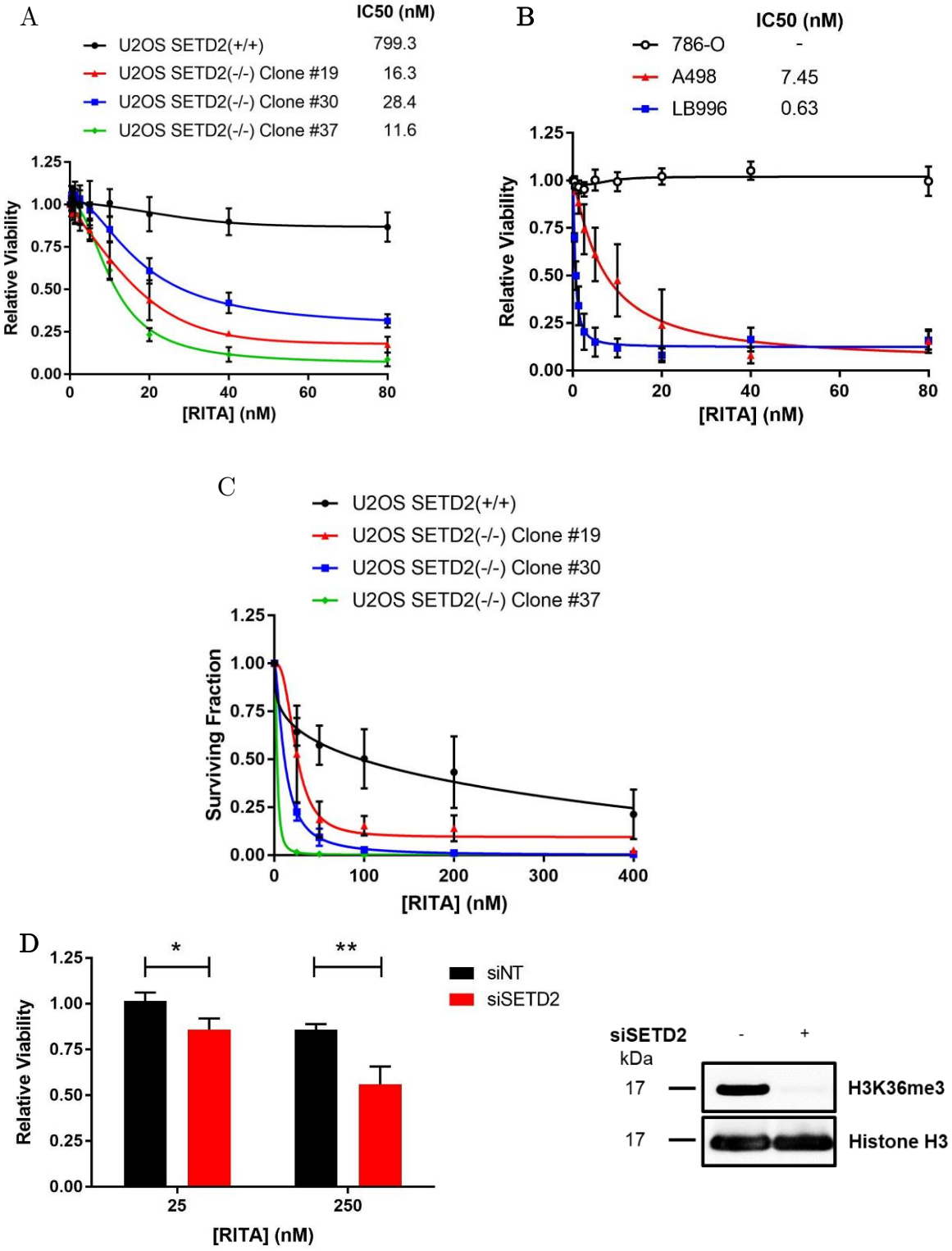
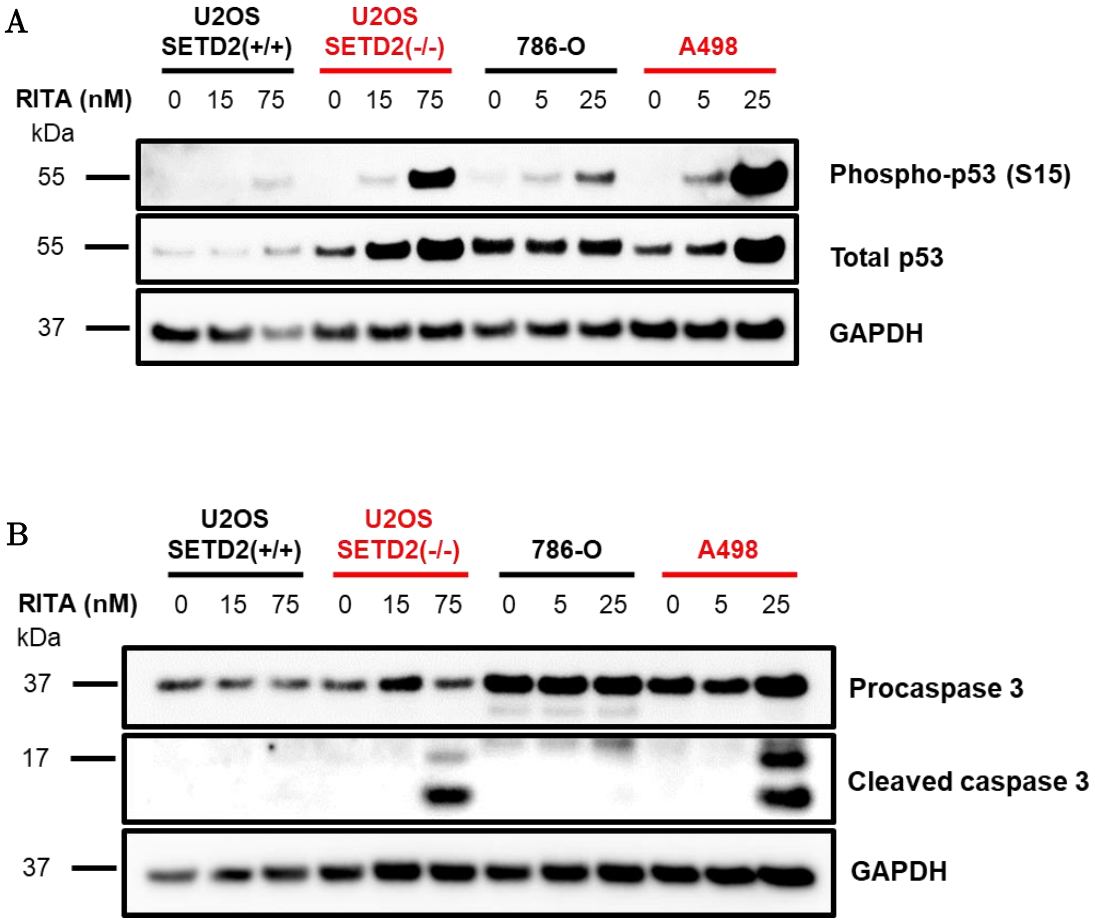



Figure 4.3. Dose-response viability curves for RITA in A. U2OS cells and B. RCC cell lines. Data are shown as mean ± SD (n ≥ 3). IC50 values were calculated via nonlinear regression (4-parameter curve fitting). C. Clonogenic survival assay after RITA treatment of parental and SETD2-CRISPR U2OS. Data are shown as mean ± SD (n = 3). D. Cell viability assay after RITA treatment of U2OS cells transfected with non-targeting (NT) or SETD2 siRNA. Data are shown as mean ± SD (n = 3). P-values were calculated using the two-tailed Student's t-test (*$p < 0.05$, **$p < 0.01$). SETD2 knockdown efficiency was confirmed by Western blotting for H3K36me3.

cellular responses to a wide variety of stresses, culminating in either cell cycle arrest, senescence, or apoptosis (Chen, 2016). p53 dynamics during the stress response occurs at a rapid pace and is thus generally accepted to occur via post-translational rather than transcriptional regulation (Oren, 1999). In unperturbed cells, p53 is continuously ubiquitinated and degraded via the proteasome (Maki et al., 1996), and its ubiquitination is primarily mediated by its own target gene MDM2 (Haupt et al., 1997; Kubbutat et al., 1997), leading to a negative feedback loop. RITA has been reported to bind p53, prevent its interaction with MDM2, and restore its functions in transactivation and apoptosis (Issaeva et al., 2004). Furthermore, p53 has been shown to interact with SETD2, which is capable of regulating certain p53 target genes, including MDM2 (Xie et al., 2008). Consistent with published reports in other cell lines, RITA treatment led to a striking increase in p53 protein levels in SETD2-CRISPR U2OS and A498 cells (Fig. 4.4A). In addition, RITA greatly induced the phosphorylation of p53 at Ser15 (Fig. 4.4A), which is known to be mediated directly by the DNA damage response kinases ATM and ATR (Banin et al., 1998; Lakin et al., 1999), specifically in SETD2-deficient cells. This phosphorylation site has been reported to amplify p53 activity in multiple ways, such as by enhancing its interaction with transcriptional machinery (Dornan and Hupp, 2001; Lambert et al., 1998), triggering a phosphorylation cascade that either stimulates or modulates further post-translational modifications (Saito et al., 2003; Sakaguchi et al., 1998), and promoting p53 protein stability by interfering with its interaction with MDM2 (Ito et al., 2002).


A
U2OS SETD2(+/+)
U2OS SETD2(-/-)
786-O
A498
RITA (nM)
0 15 75 0 15 75 0 5 25 0 5 25
kDa
55
55
37
Phospho-p53 (S15)
Total p53
GAPDH
B
U2OS SETD2(+/+)
U2OS SETD2(-/-)
786-O
A498
RITA (nM)
0 15 75 0 15 75 0 5 25 0 5 25
kDa
37
17
37
Procaspase 3
Cleaved caspase 3
GAPDH
C
SETD2(+/+)
SETD2(-/-)
Relative Luminescence
0
1
2
3
4
**
**
20
100
[RITA] (nM)

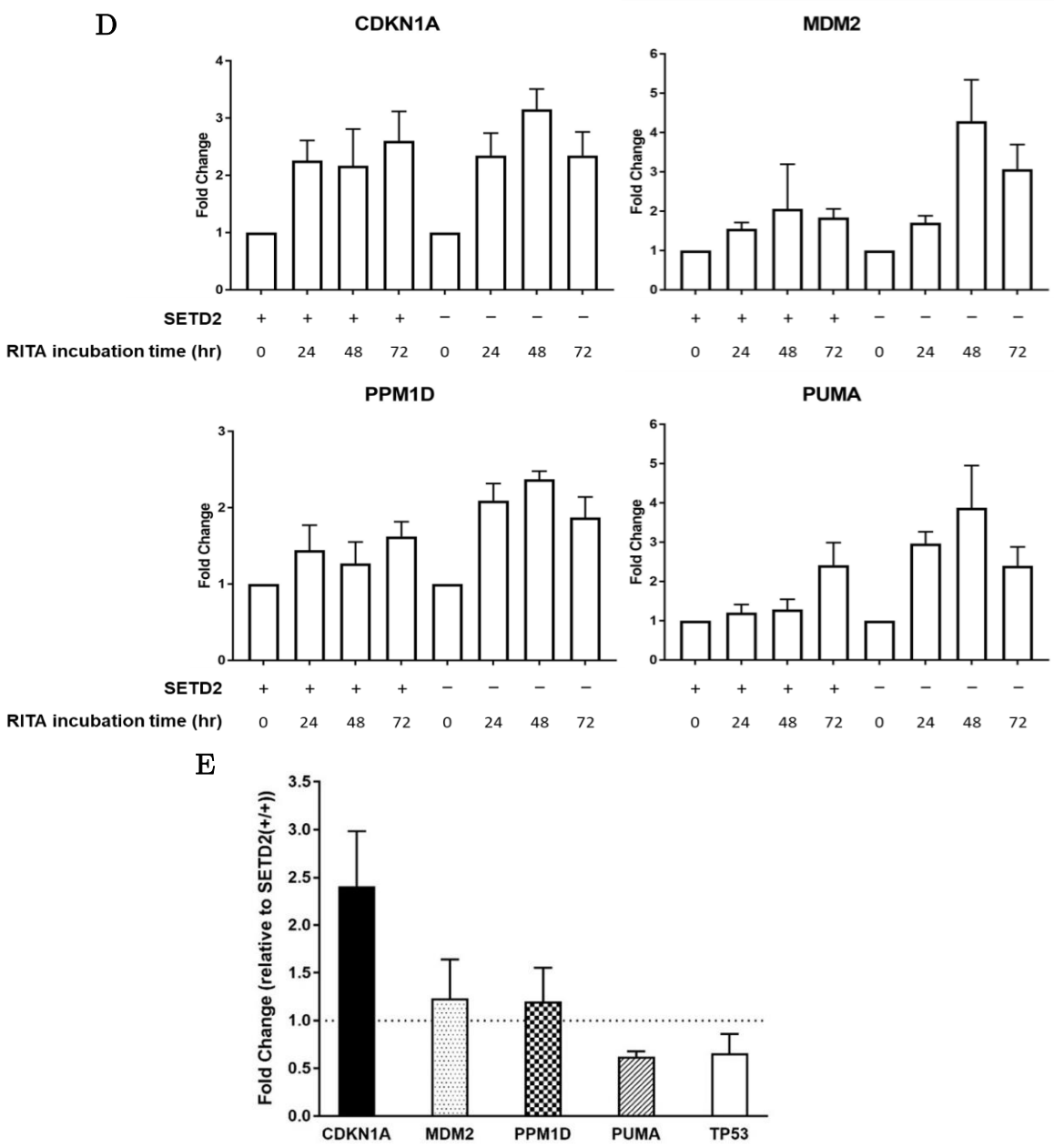



Figure 4.4. A. Western blot of total and phospho-p53 (Ser15) in parental and SETD2-CRISPR U2OS and RCC cell lines treated with the indicated doses of RITA for 48 hours. B. Western blot of procaspase 3 and cleaved caspase 3 in parental and SETD2-CRISPR U2OS and RCC cell lines after RITA treatment for 48 hours. C. Annexin V levels in SETD2-CRISPR and parental U2OS cells after RITA treatment for 30 hours. Luminescence readings were normalised to DMSO-treated controls. Data are shown as mean ± SD (n = 3). P-values were calculated using the two-tailed Student's t-test. **p < 0.01. D. Quantitative RT-PCR analysis of p53 target gene expression after RITA treatment. Samples were normalised to the housekeeping gene GAPDH. Fold change was calculated relative to untreated controls. Data are shown as mean ± SD (n = 3). E. Quantitative RT-PCR analysis of p53 and its target genes in untreated SETD2-CRISPR U2OS. Samples were normalised to the housekeeping gene GAPDH. Fold change was calculated relative to untreated parental U2OS. Data are shown as mean ± SD (n = 3).

Given p53's established role in promoting apoptotic cell death in response to radiation and chemotherapy (Lowe et al., 1993a; Lowe et al., 1993b), the induction of apoptosis was measured after exposure to RITA. The final step in the caspase cascade, regardless of stimulus, is the cleavage and activation of caspase-3, one of the executioner caspases whose cleavage of its many substrates leads to the downstream events of apoptosis (Schlegel et al., 1996). Western blot analysis of caspase-3 cleavage revealed elevated levels in SETD2-CRISPR U2OS and A498 cells, but not their SETD2-wildtype counterparts (Fig. 4.4B). Another hallmark of apoptosis is the disruption of plasma membrane symmetry, leading to the extracellular exposure of phosphatidylserine that is normally on the cytosolic side of the cell membrane in healthy cells (Devaux, 1991; Fadok et al., 1992); this can be detected by the addition of annexin V, a vascular anticoagulant that displays high affinity for negatively charged phospholipids (Andree et al., 1990). Using a luminescence-based assay, it was observed that annexin V binding was significantly elevated in SETD2-CRISPR U2OS cells after RITA treatment (Fig. 4.4C).

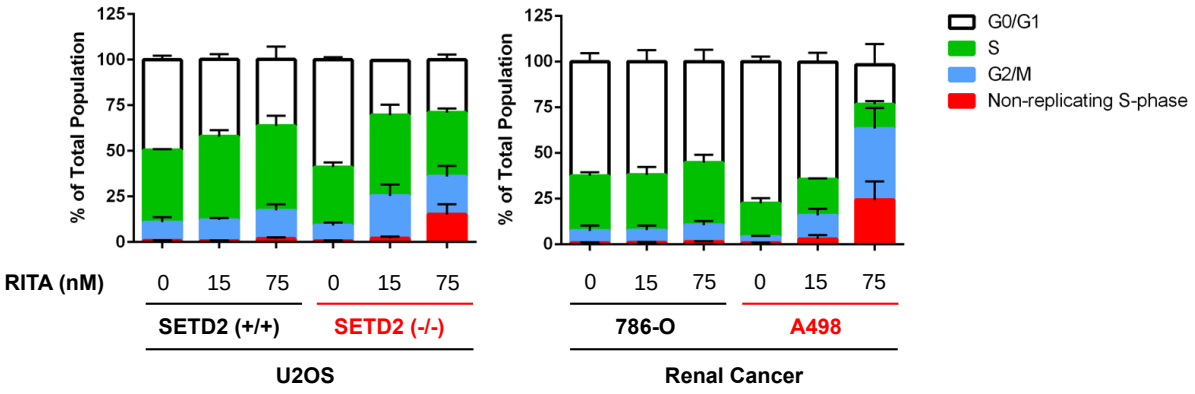
To verify whether the observed upregulation of p53 was leading to activation of its downstream targets, the expression levels of some canonical p53 target genes were analysed by quantitative RT-PCR. Indeed, mRNA levels of the genes *CDKN1A*, *MDM2*, *PPM1D*, and *PUMA* were increased after RITA treatment, and this effect was stronger in the absence of SETD2 (Fig. 4.4D). In the case of *CDKN1A*, RITA induced gene expression to a similar extent in both parental and SETD2-CRISPR cells, but it is worth noting that *CDKN1A* expression is already more than 2-fold higher after

SETD2 deletion in unperturbed conditions (Fig. 4.4D); thus, *CDKN1A* expression after RITA treatment is still 2-fold higher in SETD2-CRISPR cells relative to parental cells. Overall, these results demonstrate that RITA leads to the upregulation and activation of p53, associated with the induction of p53-mediated transcription and apoptosis, particularly in cells that lack functional SETD2.

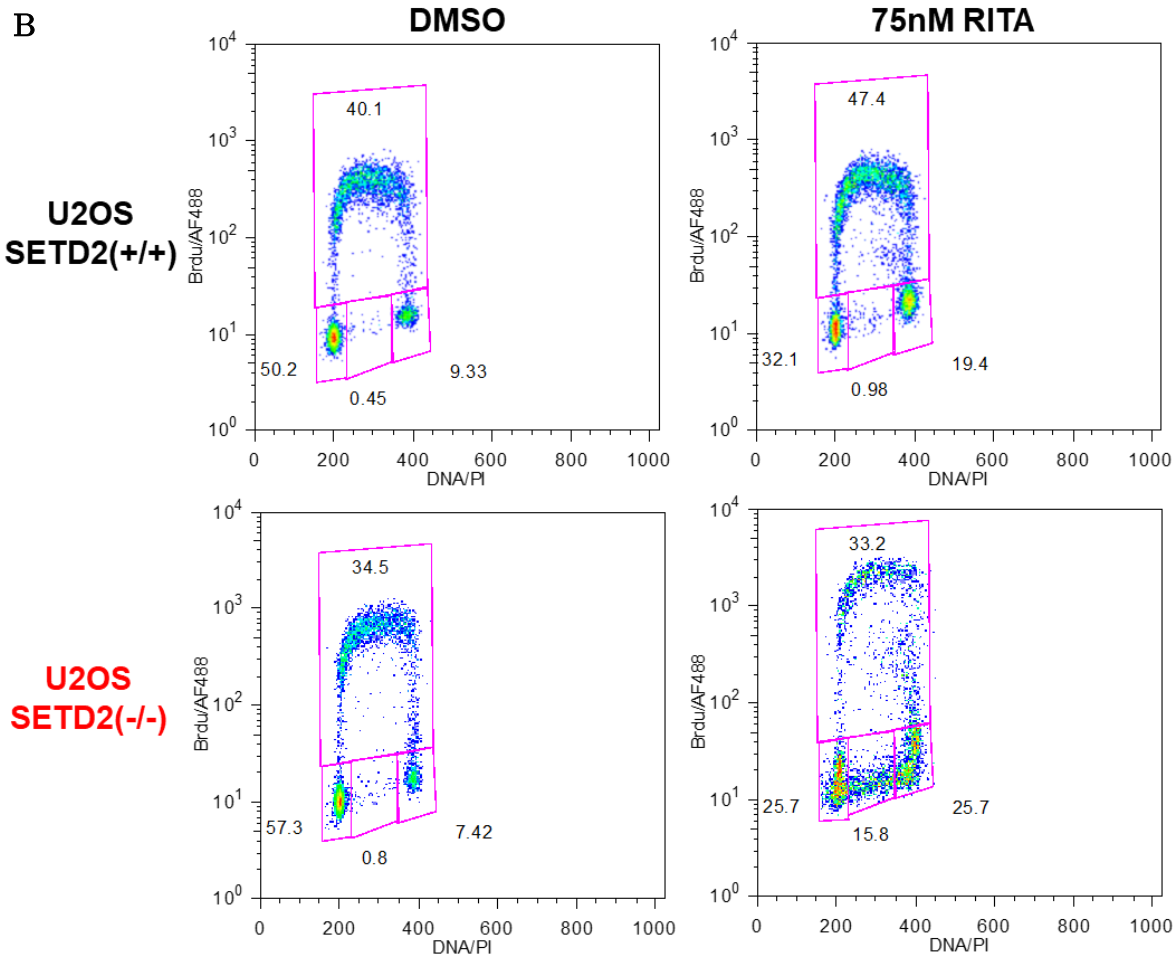
## 4.3. RITA induces cell cycle arrest and activates the DNA damage response specifically in SETD2-deficient cancer cells

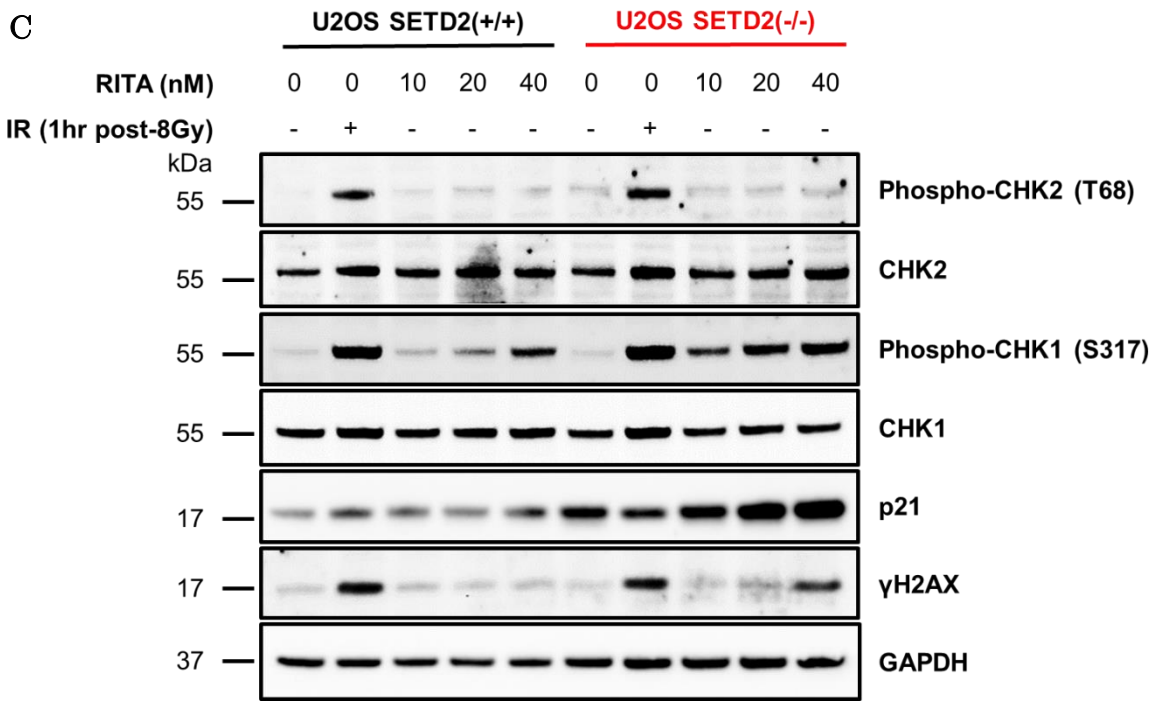
To investigate the mechanism through which RITA targets SETD2-deficient cells, cell cycle progression was compared between treated and untreated cells. The orderly advancement through the cell cycle can be interrupted by various stresses and stimuli, such as direct physical damage to DNA or disruption of the DNA replication machinery. In response to such events, signalling pathways are activated at the boundary between each cell cycle phase that prevent cells from proceeding into the subsequent phase until the source of cellular stress has been dealt with. These cell cycle checkpoints are critical for sensing damaged DNA and allowing cells sufficient time for DNA repair, thus preserving genomic stability; unsurprisingly, many checkpoint mediators have come to be revealed as tumour suppressors (Kastan and Bartek, 2004). In both SETD2-CRISPR U2OS and SETD2-mutant A498 cells, RITA induced a dose-dependent accumulation in non-replicating S-phase (defined as having a DNA content between 2N and 4N but no incorporation of the synthetic nucleoside BrdU) and G2/M (Fig. 4.5A-B). These results suggest a disruption in DNA replication and the activation of the DNA damage response, leading to the activation of cell cycle checkpoints.

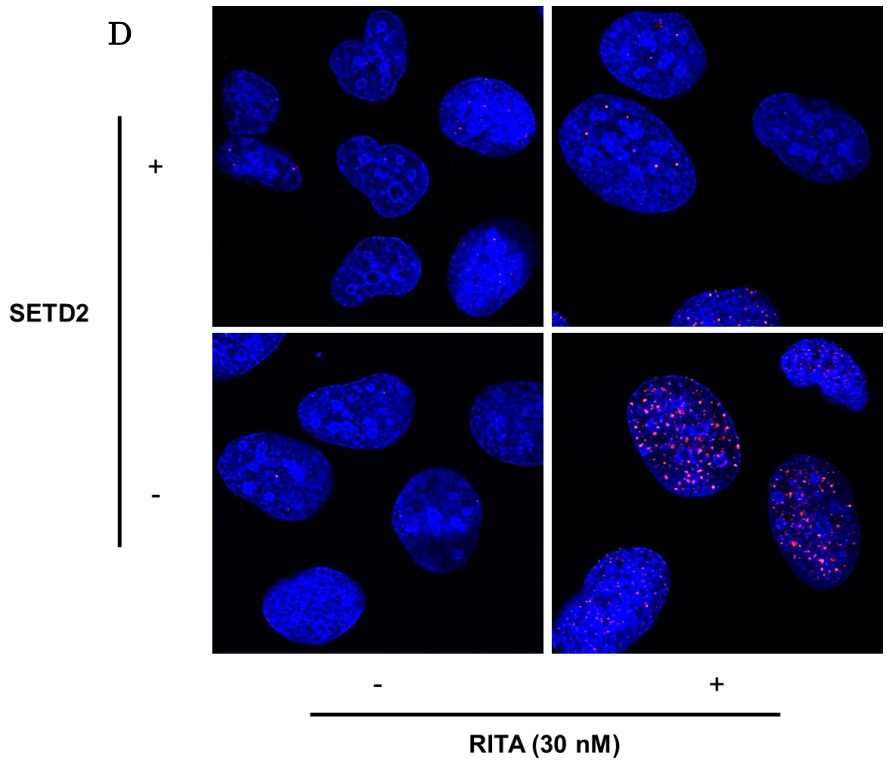
A


% of Total Population
125
100
75
50
25
0
G0/G1
S
G2/M
Non-replicating S-phase
RITA (nM)
0
15
75
0
15
75
SETD2 (+/+)
SETD2 (-/-)
U2OS
786-O
A498
Renal Cancer

B


DMSO
75nM RITA
U2OS
SETD2(+/+)
U2OS
SETD2(-/-)
Brdu/AF488
DNA/PI
40.1
50.2
9.33
0.45
47.4
32.1
19.4
0.98
34.5
57.3
7.42
0.8
33.2
25.7
25.7
15.8


C
U2OS SETD2(+/+)
U2OS SETD2(-/-)
RITA (nM)
0 0 10 20 40 0 0 10 20 40
IR (1hr post-8Gy)
- + - - - - + - - -
kDa
55
Phospho-CHK2 (T68)
55
CHK2
55
Phospho-CHK1 (S317)
55
CHK1
17
p21
17
γH2AX
37
GAPDH


D
SETD2
+
-
-
+
RITA (30 nM)

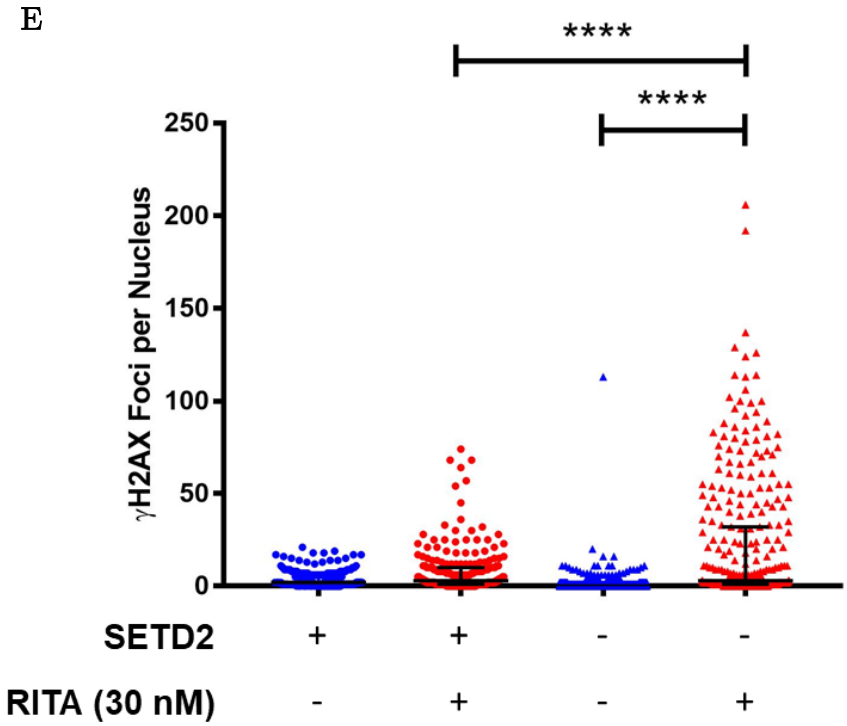
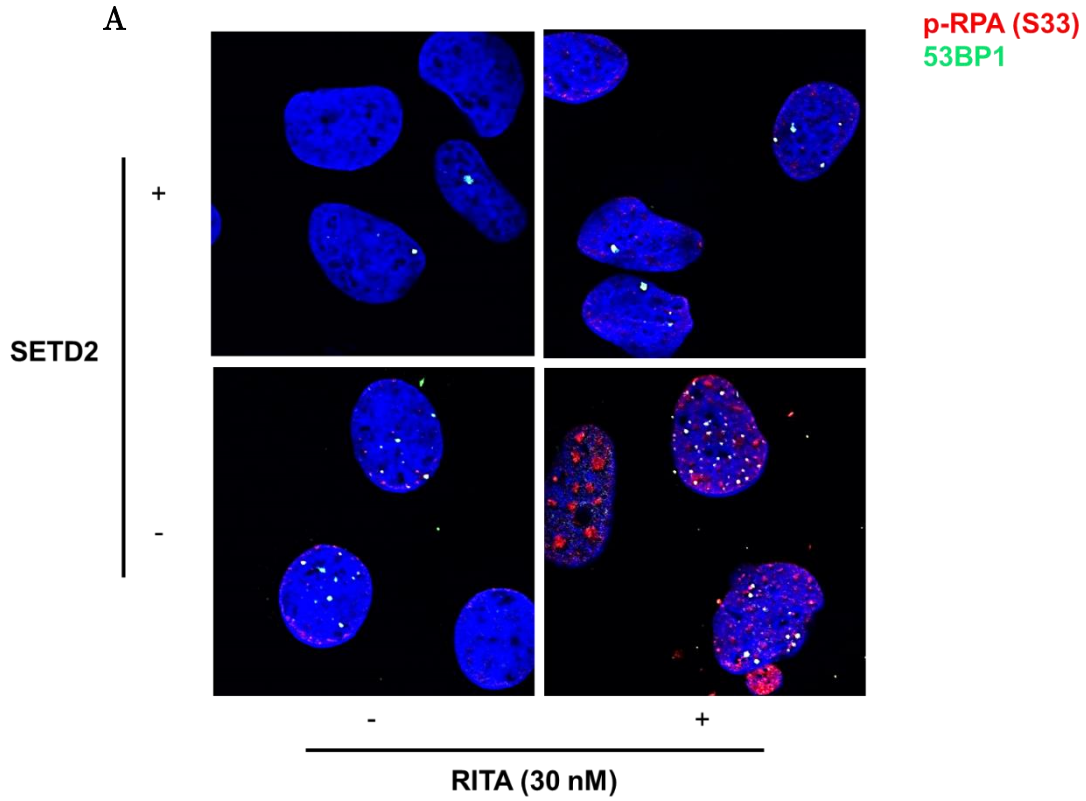


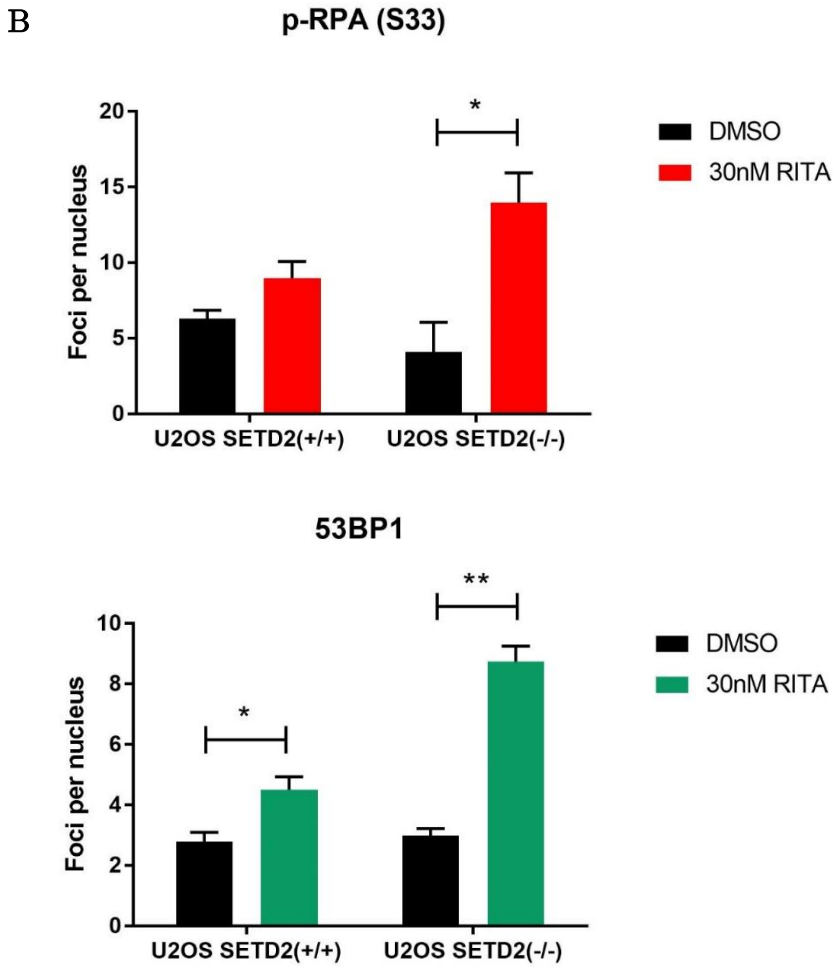

Figure 4.5. A. Cell cycle distribution of U2OS cells and RCC cell lines after treatment with increasing doses of RITA for 48 hours. Data shown as mean ± SD (n = 3). B. BrdU/PI cell cycle profiles of U2OS cells after DMSO or RITA treatment. Images are representative of 3 independent experiments. C. Western blot of total and phospho-CHK1 (Ser317), total and phospho-CHK2 (Thr68), p21, and γH2AX in U2OS cells after RITA treatment. Ionising radiation (IR) was used as a positive control. D. Confocal microscopy of γH2AX foci (red) in parental and SETD2-CRISPR U2OS cells after treatment with increasing doses of RITA. Representative images from 2 independent experiments are shown. E. Quantification of γH2AX foci per nucleus from C. At least 200 nuclei per sample were counted for statistical analysis. Data shown as median ± interquartile range. P-values obtained from two-tailed unpaired t-test. ****$p < 10^{-6}$

Different types of DNA damage, such as DNA double-strand breaks (DSBs) and replication stress, activate distinct signalling pathways, although they culminate in common outcomes such as cell cycle arrest or apoptosis. Generally, DSBs are the purview of the ATM/CHK2 pathway, whereas the presence of single-stranded DNA (ssDNA) from stalled replication forks stimulates the ATR/CHK1 pathway (Abraham, 2001). Consistent with the observed cell cycle defects, detection of key checkpoint mediators by Western blotting revealed the activation of CHK1, phosphorylation of histone H2AX (γH2AX), and upregulation of the CDK inhibitor p21 (CDKN1A) by RITA, which occurred to a markedly stronger degree in SETD2-CRISPR cells compared to their parental counterparts (Fig. 4.5C). Consistent with its mRNA expression levels (Fig. 4.4D), p21 is much more highly expressed in SETD2-CRISPR cells and is further upregulated upon RITA treatment. The absence of CHK2 phosphorylation implies that RITA is inducing replication stress and not DSBs. The presence of DNA damage after RITA treatment specifically in the absence of SETD2 was further verified by visualising γH2AX foci by immunofluorescence microscopy (Fig. 4.5D-E). Therefore, these findings indicate that, in the absence of functional SETD2, RITA treatment leads to some form of DNA damage or genotoxic stress that activates the DNA damage response via the ATR-CHK1 axis, and this is associated with impaired DNA synthesis and cell cycle arrest at the G2/M checkpoint.

## 4.4. RITA induces replication stress specifically in SETD2-deficient cancer cells

Replication stress is generally defined as any disruption to DNA replication fork progression, leading to decelerated or arrested DNA synthesis (Mazouzi et al., 2014; Zeman and Cimprich, 2014). At stalled replication forks, unreplicated ssDNA becomes a signalling hub for the replication stress response pathway; ssDNA is quickly sensed by and coated with Replication Protein A (RPA), which in turn is bound by ATR-Interacting Protein (ATRIP) and various other mediators with the ultimate goal of recruiting and activating ATR and its downstream targets (Osborn et al., 2002). To determine whether replication stress is present after RITA treatment, parental and SETD2-CRISPR U2OS cells were stained for markers of replication stress, namely phospho-RPA (Ser33) and 53BP1. RPA is one of the multitude of substrates phosphorylated by ATR at stalled replication forks (Olson et al., 2006), whereas 53BP1 has been shown to accumulate on chromosomal DNA after aphidicolin-induced replication stress (Lukas et al., 2011). RITA treatment led to significantly higher levels of both types of foci particularly in SETD2-CRISPR cells (Fig. 4.6A-B), indicating increased replication stress in the presence of RITA. Another method of detecting replication stress is the direct measurement of replication fork velocity using the DNA fibre assay. The incorporation of the synthetic nucleosides CldU and IdU, which can be detected by specific antibodies, can be used to visualise the extent of replication fork progression in response to various conditions and treatments (Nieminuszczy et al., 2016). Consistent with the increased number of replication stress foci, SETD2-CRISPR


A
p-RPA (S33)
53BP1
SETD2
+
-
-
+
RITA (30 nM)


B
p-RPA (S33)
Foci per nucleus
20
15
10
5
0
*
DMSO
30nM RITA
U2OS SETD2(+/+)
U2OS SETD2(-/-)
53BP1
Foci per nucleus
10
8
6
4
2
0
**
*
DMSO
30nM RITA
U2OS SETD2(+/+)
U2OS SETD2(-/-)

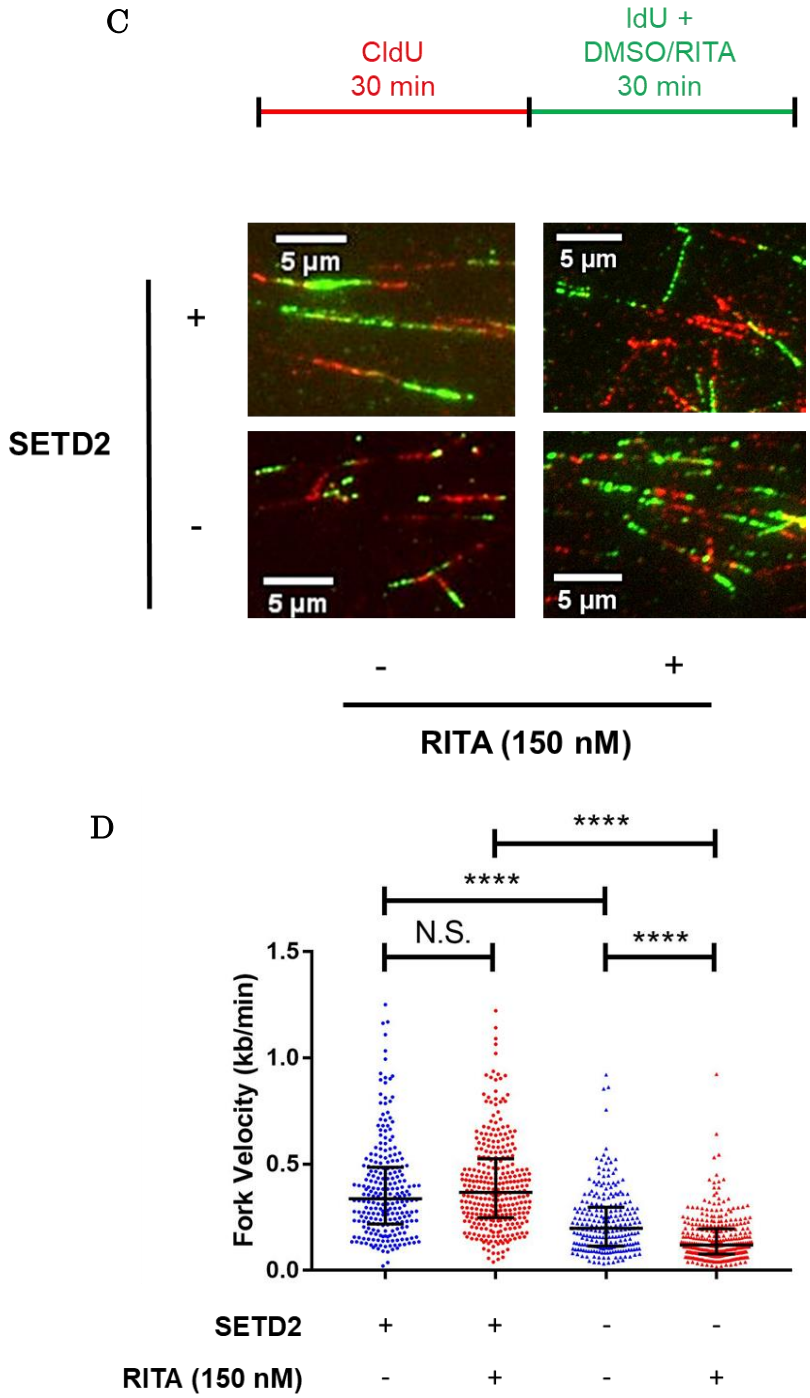



Fig. 4.6. A. Confocal microscopy of phospho-RPA Ser33 (red) and 53BP1 (green) foci in parental and SETD2-CRISPR U2OS in the presence or absence of RITA. Representative images from 3 independent experiments are shown. B. Quantification of the average number of foci per nucleus from A. At least 70 nuclei per sample were counted for statistical analysis. Data shown as mean ± SD. P-values were calculated using the two-tailed Student's t-test. *p $< 0.05$, **p $< 0.01$. C. DNA fibre assay of parental and SETD2-CRISPR U2OS. Cells were treated as indicated. Representative images from 2 independent experiments are shown. D. Quantification of replication fork velocity from C. At least 200 fibres per sample were measured for statistical analysis. Data shown as median ± interquartile range. P-values were calculated using the two-tailed Student's t-test. N.S. = non-significant, ****p $< 10^{-6}$

cells displayed a significant reduction in fork velocity after RITA treatment, whereas the parental cells remained unaffected (Fig. 4.6C-D). Moreover, this was observed within a short treatment window (30 minutes), indicating that RITA enters the cell and exerts its physiological effects very rapidly. Overall, these results demonstrate that RITA activates the DNA damage response by inducing replication stress, as demonstrated by increased phosphorylation of RPA and recruitment of 53BP1, and this is further associated with impaired DNA replication fork progression.

## 4.5.Chapter Discussion

Rapid and continuous improvements in biotechnology, especially in genome sequencing, have been accompanied by a rise in personalised medicine, where a patient's genotype informs his or her therapeutic options to maximise clinical benefits and minimise adverse effects. In oncology, personalised or precision medicine is enabled by the concept of synthetic lethality and has been demonstrated repeatedly over the years, most prominently in the case of BRCA mutations and PARP inhibition (Bryant et al., 2005; Farmer et al., 2005). The aim of this chapter was to apply this idea to SETD2-deficient cancers in order to provide new and complementary strategies in addition to WEE1 inhibition. In a large-scale screen comprised of thousands of compounds, the hit that displayed the highest potency against SETD2-deleted cells by a significant margin was RITA. In some ways, the phenotypes induced by RITA in SETD2-deficient cells harken back to the observations made with SETD2 and WEE1. The most obvious of these is the presence of replication stress, as denoted by the

increase in non-replicating S-phase (Fig. 4.5A-B), the activation of CHK1 (Fig. 4.5C), the accumulation of phospho-RPA and 53BP1 foci (Fig. 4.6A-B), and the decrease in replication fork velocity (Fig. 4.6C-D) after RITA treatment in the absence of SETD2. However, RITA is >10-fold more potent in reducing the viability of SETD2-deficient cells compared to the WEE1 inhibitor AZD1775, based on published data for the latter (11.6 nM vs. 151 nM for U2OS SETD2-CRISPR, 7.5 nM vs. 87 nM for A498, and 0.6 nM vs 68 nM for LB996) (Pfister et al., 2015). The mechanism through which RITA mediates its potent yet specific cytotoxicity will be explored in further detail in the succeeding chapter.

In the process of conducting this high-throughput compound screen, a number of issues and limitations became apparent. As with any screen of this magnitude, achieving sufficient reproducibility between replicates was a challenge that made the data analysis more complicated and forced a more stringent approach to limit false positive results, while potentially increasing the number of false negative hits. Furthermore, the use of only two doses for the compound libraries necessarily means reducing the pool of potential hits to those that are effective at either dose. One key drawback of using compounds and inhibitors is that the vast majority of them do not target a specific protein, as is the case with ABT-263; although synthetic lethality applies to pathway interactions as well as specific gene interactions, having multiple targets increases the complexity of the validation process, especially if the compound has different affinities for each target. An alternative method of identifying synthetic lethal interactions is via genetic screens. This has traditionally been done in yeast, with

some of the earliest examples of synthetic lethal genes and pathways being discovered in *Saccharomyces cerevisiae* (Bender and Pringle, 1991; Hennessy et al., 1991). This was eventually expanded to mammalian systems using RNA interference and, with recent developments in gene editing, CRISPR-Cas9 technology (Behan et al., 2019). Although genetic screens have their own drawbacks (Bhinder and Djaballah, 2013; Horlbeck et al., 2016; Kuscu et al., 2014; Munoz et al., 2016), not least of which is the reality that not all genes are druggable, they may prove useful as a complementary strategy for identifying novel targeted therapies against H3K36me3 loss.

In summary, the key findings of this chapter are:

- RITA potently and specifically targets SETD2-deficient cells
- RITA upregulates p53, leading to increased activation of downstream target genes and apoptotic cell death in SETD2-deficient cells
- RITA enhances non-replicating S-phase and G2/M arrest in SETD2-deficient cells and activates the DNA damage response, leading to increased levels of phospho-CHK1, p21, and γH2AX
- RITA increases the recruitment of replication stress markers phospho-RPA and 53BP1, which is associated with reduced replication fork velocity

# 5. Molecular mechanisms of the p53 reactivator RITA in the context of SETD2 loss

The previous chapter detailed the investigation into novel synthetic lethal interactions that can potentially be used therapeutically to target SETD2-deficient cancers. The most potent candidate, by a significant margin, is the p53-reactivating compound RITA; its remarkable ability to reduce cell viability and survival specifically in the absence of SETD2, which is associated with dysregulation of the cell cycle, activation of the DNA damage response, and increased replication stress, make it a promising therapeutic option in terms of both efficacy and specificity. However, its mechanism of action remains unclear, particularly in the context of its interaction with SETD2 and H3K36 trimethylation. This chapter aims to address this question via both a hypothesis-driven investigation based on the current body of knowledge available about SETD2 and RITA, as well as more exploratory approaches.

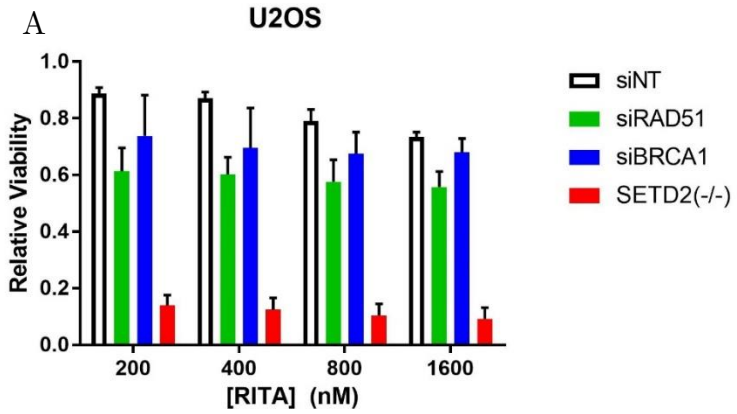
## 5.1. RITA sensitivity is not dependent on homologous recombination proficiency, dNTP supply, or CDK activation

One of the key questions in elucidating RITA's mechanism of action in the context of SETD2 deficiency is the importance of SETD2 and H3K36me3's myriad of cellular functions. Most pertinent of these to the phenotypes observed thus far is the published role of H3K36me3 in the repair of DNA double-strand breaks via homologous recombination (HR) (Pfister et al., 2014), which is consistent with the increased DDR activation, replication stress, and cell death induced by RITA in the absence of SETD2. To investigate this possibility, two crucial components of the HR pathway were depleted in SETD2-proficient cells: RAD51 and BRCA1. RAD51 is the eukaryotic homologue of the *Escherichia coli* protein RecA and mediates the strand invasion and homology search steps of HR by forming nucleoprotein filaments with single-stranded DNA (Baumann et al., 1996). BRCA1 is a commonly known tumour suppressor, particularly in breast and ovarian cancer, and interacts with a wide variety of other proteins to regulate multiple cellular processes (Huen et al., 2010). Its role in HR was established upon the discovery that this specific DSB repair pathway is impaired in BRCA1-deficient cells while nonhomologous end-joining (NHEJ) remains unaffected (Moynahan et al., 1999). Subsequent studies have shed further light on BRCA1's key functions in HR; it is required early on in the repair process to enable DNA end resection by removing 53BP1 (Bunting et al., 2010) and it facilitates the later stages of HR via its interaction with PALB2, which culminates in RAD51 nucleofilament formation (Sy et al., 2009; Zhang et al., 2009).

If HR plays a substantial role in the RITA sensitivity of SETD2-deficient cells, we can hypothesise that other HR factors would behave similarly in this context. However, siRNA-mediated knockdown of RAD51 and BRCA1 in SETD2-positive U2OS cells and 786-O cells did not sensitise them to RITA to the same extent as their SETD2-deficient counterparts, even at high drug concentrations above 1 µM (Fig. 5.1A-B). Furthermore, in the case of U2OS, no dose-dependent increase in RITA sensitivity was observed after depletion of RAD51 or BRCA1. One possible caveat for these results is that the importance of these two genes, especially RAD51, in essential cellular processes means that simply depleting them reduces cell viability, which may impact any further effects of RITA treatment. However, these findings still suggest that SETD2's function in the repair of DNA damage via homologous recombination is not the main mechanism through which RITA exerts its cytotoxicity.

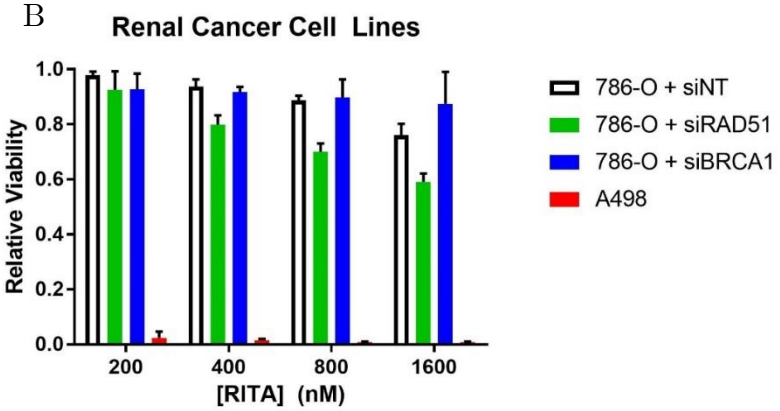
A crucial function of SETD2 and H3K36me3 that recently came to light is its role in the maintenance of the cellular deoxyribonucleoside triphosphate (dNTP) supply. dNTPs are substrates for DNA polymerases that are necessary for both DNA replication and repair; their overall levels, as well as the ratios of each type of dNTP, have a significant impact on normal cell division and the preservation of genome stability (Pai and Kearsey, 2017). In actively dividing cells, the *de novo* synthesis pathway is responsible for the bulk of cellular dNTPs required during S-phase and the rate-limiting step is catalysed by ribonucleotide reductase (RNR), which converts ribonucleoside diphosphates (NDPs) into their deoxyribonucleoside equivalents (dNDPs) (Reichard et al., 1961). RNR is a heterotetramer comprised of two subunits,

A




| U2OS Parental siRNA | Mean Viability | SD |
|---|---|---|
| siRAD51 | 0.656 | 0.236 |
| siBRCA1 | 0.897 | 0.221 |

B




| 786-O siRNA | Mean Viability | SD |
|---|---|---|
| siRAD51 | 0.756 | 0.088 |
| siBRCA1 | 0.856 | 0.245 |

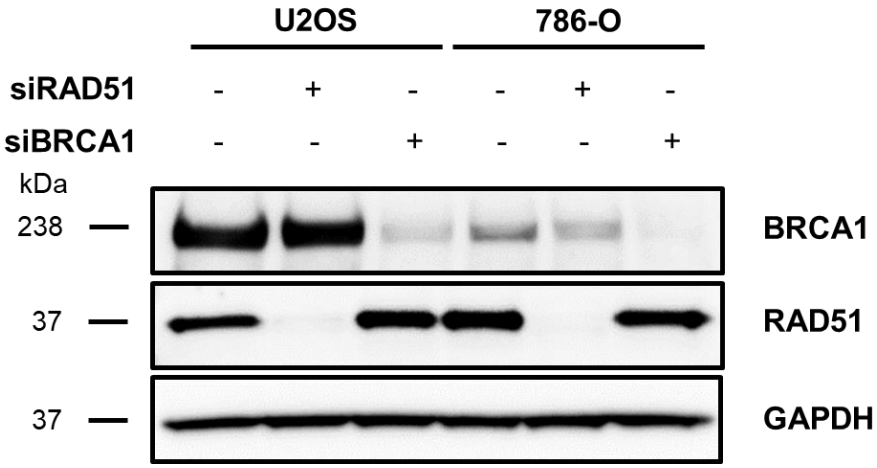
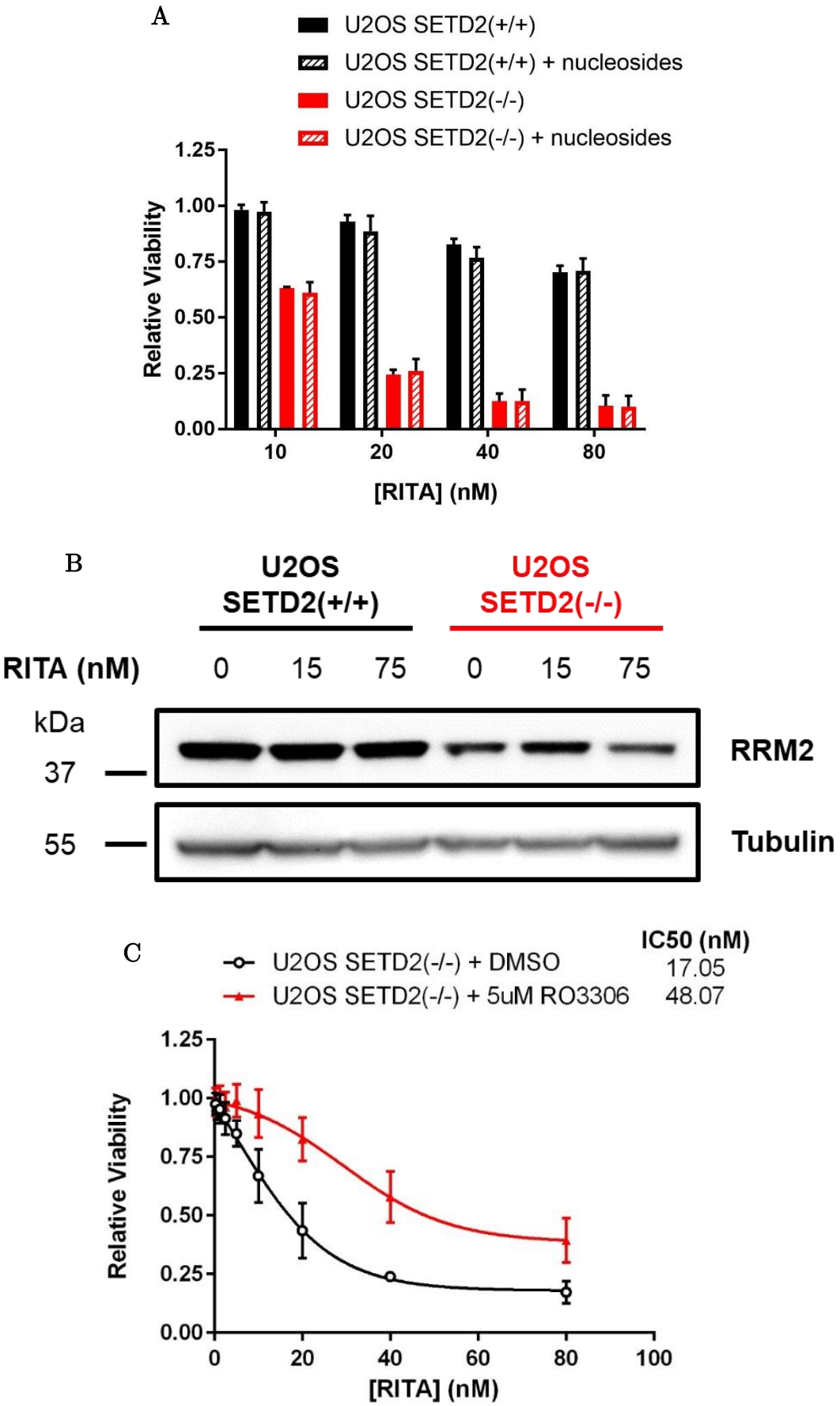



Figure 5.1. Cell viability assay after RITA treatment of A. U2OS cells or B. 786-O cells transfected with non-targeting (NT), RAD51, or BRCA1 siRNA. Data are shown as mean ± SD (n = 3). Viability of the knockdown samples relative to NT controls in the absence of drug treatment is denoted in the adjacent tables. siRNA knockdown efficiency in A. and B. was confirmed by Western blot.

RRM1 and RRM2, that are regulated by multiple mechanisms. RRM1 is the allosteric component that modulates enzymatic activity by inducing the formation of a hexamer, instead of a tetramer, when bound by dATP (Fairman et al., 2011). RRM2, on the Other hand, is the catalytic subunit and its expression is controlled both transcriptionally via E2F transcription factors (Chabes et al., 2004) and post-translationally via ubiquitin-dependent proteasomal degradation (D'Angiolella et al., 2012). The relationship between RRM2 and SETD2 was revealed during our group's investigation into the SETD2-WEE1 synthetic lethality, where it was discovered that both SETD2 and WEE1 independently regulate RRM2 expression – SETD2 via control of RRM2 transcription and WEE1 via CDK-dependent phosphorylation and degradation of the RRM2 protein (Pfister et al., 2015).

Since the mechanism of a previously established synthetic lethality with SETD2 involves dNTP pools, it seemed logical to ask whether RITA sensitivity was related to nucleotides or RRM2 in some way. To test this, cells were incubated with RITA in culture medium that was supplemented with exogenous nucleosides. It has been previously observed that SETD2 loss leads to reduced dNTP supply within the cell (Pfister et al., 2015) so the addition of nucleosides from an external source would help to determine whether increased dNTP levels in SETD2-deficient cells affects their response to RITA. However, there was no observable difference in RITA sensitivity between SETD2-CRISPR cells in normal and supplemented media (Fig. 5.2A), suggesting that dNTP supply does not play a role in the cytotoxicity of RITA in this context. These results were further corroborated by the finding that RRM2 protein


A
U2OS SETD2(+/+)
U2OS SETD2(+/+) + nucleosides
U2OS SETD2(-/-)
U2OS SETD2(-/-) + nucleosides
Relative Viability
1.25
1.00
0.75
0.50
0.25
0.00
10
20
40
80
[RITA] (nM)
B
U2OS SETD2(+/+)
U2OS SETD2(-/-)
RITA (nM)
0
15
75
0
15
75
kDa
37
55
RRM2
Tubulin
C
IC50 (nM)
U2OS SETD2(-/-) + DMSO
17.05
U2OS SETD2(-/-) + 5uM RO3306
48.07
Relative Viability
1.25
1.00
0.75
0.50
0.25
0.00
0
20
40
60
80
100
[RITA] (nM)

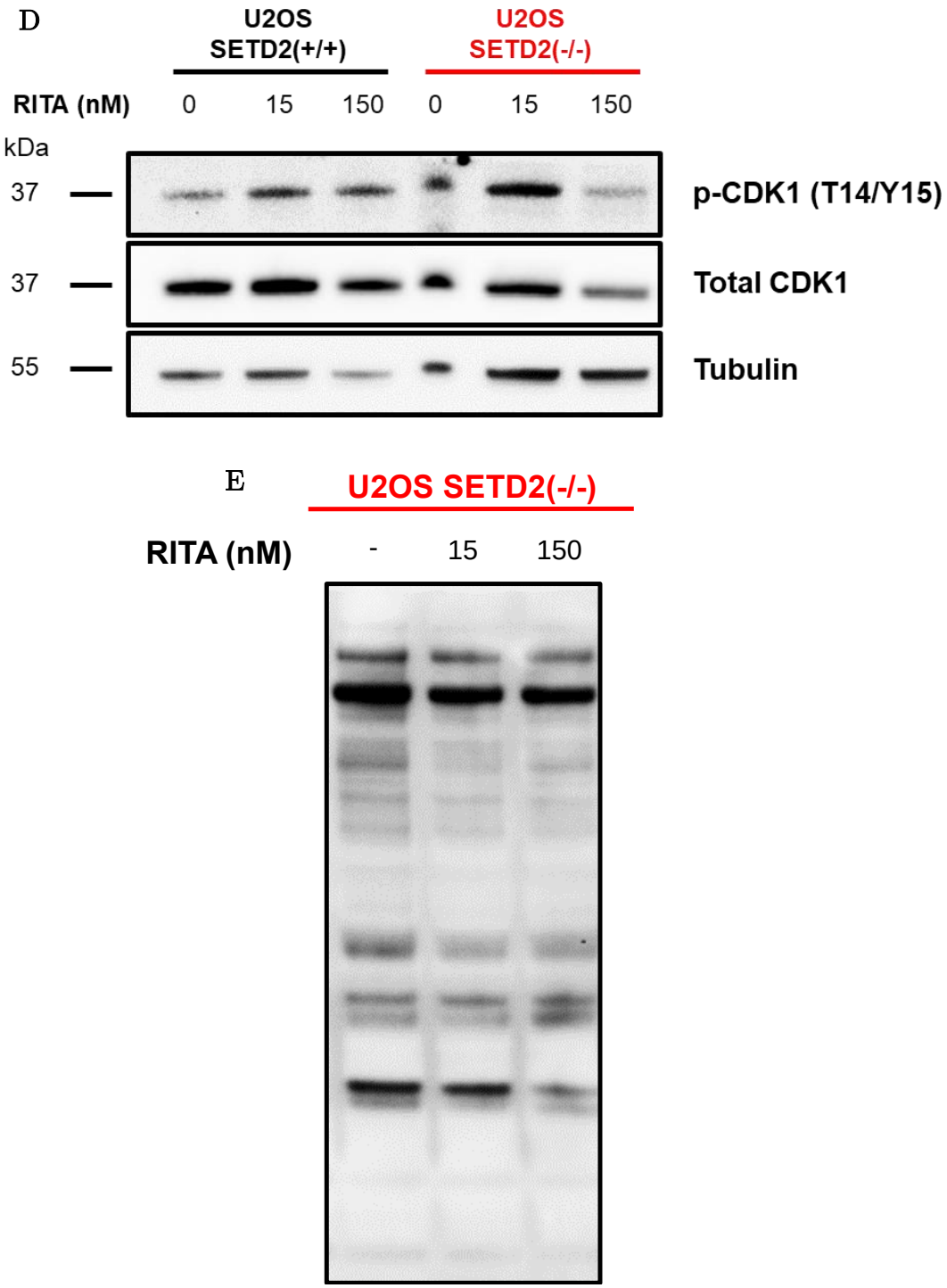



Figure 5.2. A. Cell viability assay after RITA treatment of U2OS cells in the presence or absence of exogenous nucleosides. Data are shown as mean ± SD (n = 3). B. Western blot of RRM2 protein in parental and SETD2-CRISPR U2OS cells treated with the indicated doses of RITA for 24 hours. C. Dose-response viability curves for RITA with or without the CDK inhibitor RO3306 in SETD2-CRISPR U2OS cells. Data are shown as mean ± SD (n = 3). IC50 values were calculated via nonlinear regression (4-parameter curve fitting). D. Western blot of total and phosphorylated CDK1 (Thr14/Tyr15) after RITA treatment of parental and SETD2-CRISPR U2OS cells. E. Western blot of phosphorylated CDK substrates after RITA treatment of SETD2-CRISPR U2OS cells.

levels, while reduced in the absence of SETD2 as previously reported (Pfister et al., 2015), do not change after RITA treatment. Thus, there is currently no evidence to support a role for dNTP maintenance in the RITA sensitivity of SETD2-deficient cells.

In addition to accelerating the degradation of RRM2, CDK hyperactivation via WEE1 inhibition further exacerbates dNTP starvation via the dysregulated firing of replication origins, which rapidly exhausts the cellular dNTP supply (Beck et al., 2012). This raises the question of whether CDK activity is involved in RITA's targeting of SETD2 deficiency. Combining RITA with the CDK1/2 inhibitor RO3306 led to reduced RITA sensitivity in SETD2-CRISPR cells, corresponding to a nearly 3-fold increase in cellular IC50 (Fig. 5.2C). This suggests that increased CDK activity is somehow contributing to RITA's cytotoxicity against SETD2-deficient cells. To investigate whether RITA treatment itself leads to changes in CDK activity, the levels of CDK1 phosphorylation were measured by Western blot. CDK1 is phosphorylated by WEE1 on two residues, Thr14 and Tyr15, which renders it inactive (Parker and Piwnica-Worms, 1992; Watanabe et al., 1995). Western blot analysis of phospho-CDK1 did not demonstrate any visible change in the levels of CDK1 phosphorylation at those residues after RITA treatment (Fig. 5.2D), which rules out a direct effect of RITA on inhibitory phosphorylation of CDK1. To confirm this, the phosphorylation state of CDK substrates was also measured. CDKs have a wide variety of substrates that can be phosphorylated on serine and/or threonine residues, with an S/T-P-X-R/K consensus sequence motif where X can be any amino acid (Songyang et al., 1994). Any alterations in CDK activity would naturally result in altered substrate phosphorylation. Consistent

with the lack of change in CDK1 phosphorylation, there was also no change in the levels of phospho-CDK substrates (Fig. 5.2E). These results demonstrate that the RITA compound has minimal impact on CDK activity, despite the reduction in RITA sensitivity in the presence of a CDK inhibitor. One possible explanation is that this resistance phenotype is a consequence of one or more of the many downstream effects of CDK inhibition; for example, dysregulated cell cycle progression may somehow impair RITA's ability to target SETD2-deficient cells through the downregulation of key mediators of its cytotoxicity or upregulation of factors that reduce its activity. Another possibility is that RITA impedes the phosphorylation of one or more specific CDK substrates, few enough that they would be barely noticeable using a global view of CDK substrate phosphorylation.

## 5.2. RITA sensitivity is enhanced by SETD2 loss in the presence or absence of p53

As mentioned in the previous chapter, RITA gained prominence because of its ability to inhibit the interaction between p53 and MDM2 (Issaeva et al., 2004), and this was further corroborated by our own data showing remarkable p53 upregulation in SETD2-deficient cells treated with RITA. An obvious question, therefore, is whether p53 stabilisation is the mechanism through which RITA is targeting cells that lack SETD2. First, to confirm that RITA is in fact inducing cytotoxicity in a p53-dependent manner, the compound was tested in p53-deleted cells and their isogenic counterparts to determine its effect on viability in the absence of p53. RITA was found to be more

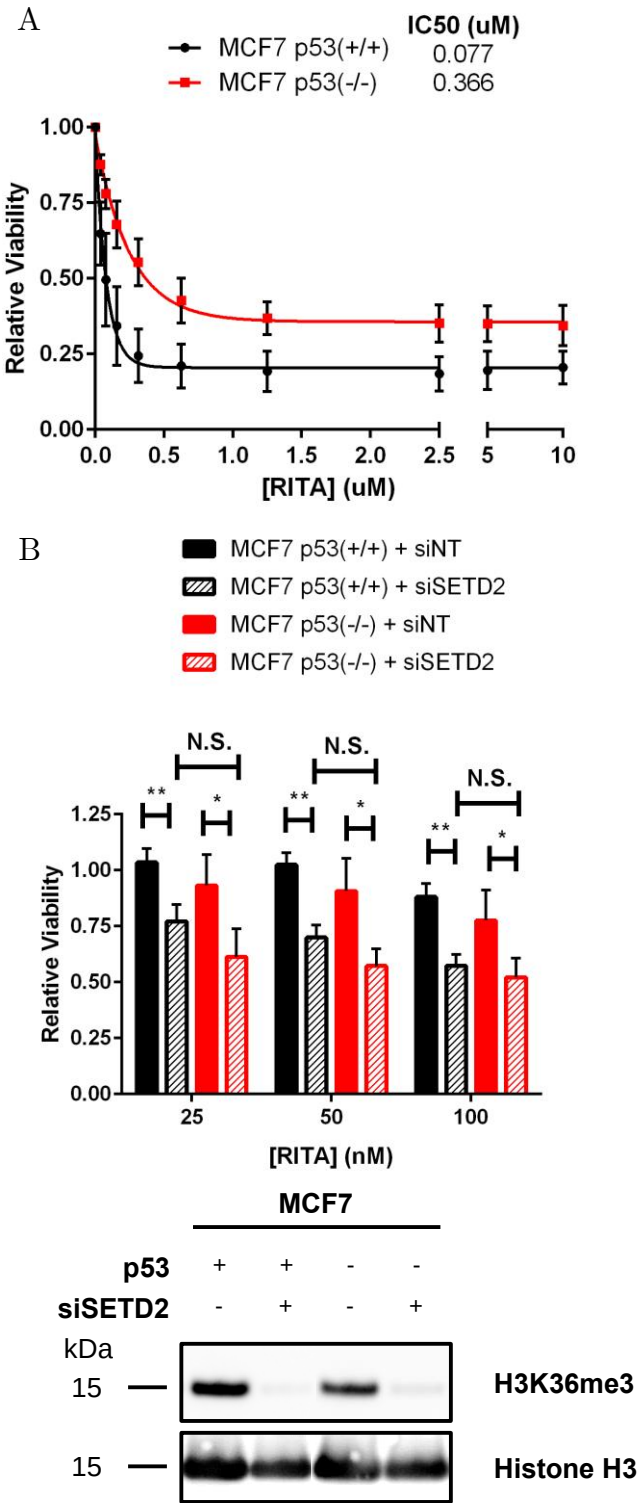



Figure 5.3. A. Dose-response viability curves for RITA in parental and p53-CRISPR MCF7 cells. Data are shown as mean ± SD (n = 3). IC50 values were calculated via nonlinear regression (4-parameter curve fitting). B. Cell viability assay after RITA treatment combined with siRNA depletion of SETD2 in parental and p53-CRISPR MCF7 cells. Viability was calculated relative to cells incubated with non-targeting siRNA. Data are shown as mean ± SD (n = 3). P-values were calculated using the Student's two-tailed t-test (* $p < 0.05$, ** $p < 0.01$, N.S. = non-significant). SETD2 knockdown efficiency was confirmed by Western blotting for H3K36me3.

potent in parental compared to p53-CRISPR MCF7 cells, displaying an approximately 5-fold difference in cellular IC50 (Fig. 5.3A). This indicates that RITA is less effective when p53 is lost, which is consistent with its purported p53-binding activity.

If RITA is indeed exerting its effects via the p53 pathway, the next step is to determine the relationship, if any, between SETD2 and p53. Very little has been published to date about molecular or genetic interactions between SETD2 and p53. One group has reported that SETD2 directly binds to p53 and augments the transcription of specific downstream targets while improving p53 stability via MDM2 downregulation (Xie et al., 2008). Similarly, another group has claimed that SETD2-deficient cells are unable to effectively activate the p53 pathway in response to DNA damage; treatment of SETD2-mutant renal cell carcinoma (RCC) cell lines with DNA-damaging agents failed to induce p53 phosphorylation and accumulation, as well as expression of classical p53 targets such as p21, culminating in the absence of G1/S checkpoint activation (Carvalho et al., 2014). This directly contradicts the results from the previous chapter, where RITA quite strikingly induced total and phospho-p53 in both SETD2-CRISPR U2OS cells and SETD2-mutant A498 cells. To determine whether SETD2 loss remains a determinant of RITA sensitivity even in the absence of p53, SETD2 was depleted in the isogenic MCF7 cell lines. As shown in Fig. 5.3B, siRNA-mediated knockdown of SETD2 was able to enhance RITA's detrimental effects on cell viability regardless of p53 status. These results indicate that SETD2 loss is able to exacerbate RITA's cytotoxicity whether or not p53 is present, although it does not

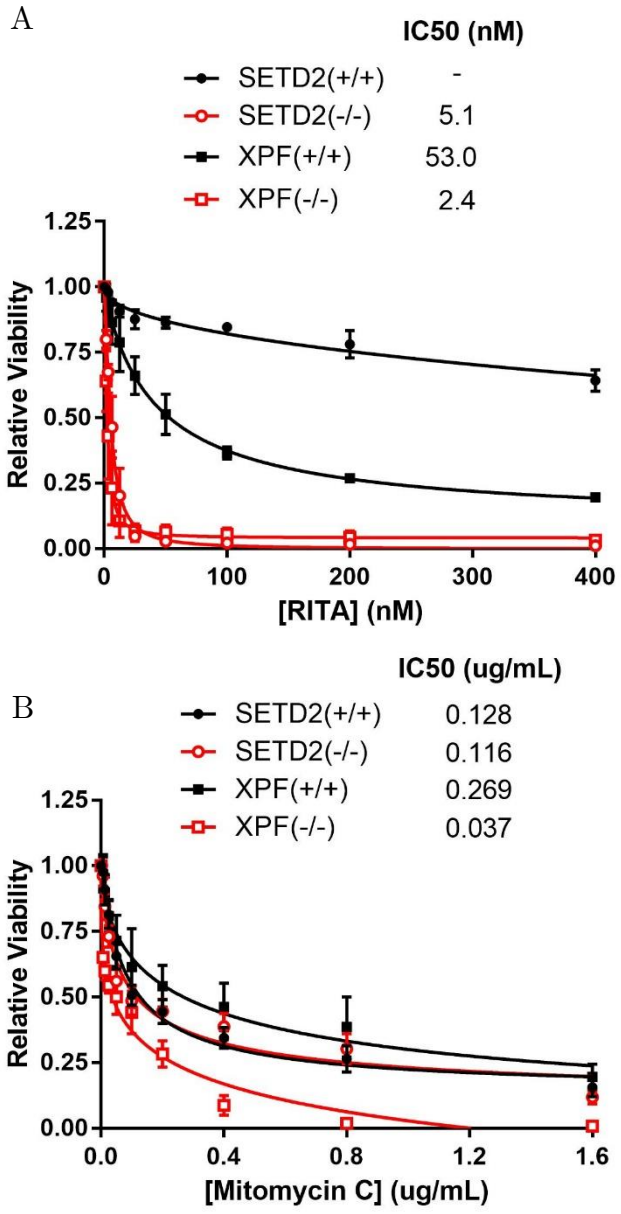
rule out the possibility that RITA has multiple mechanisms of action, some of which may be p53-independent.

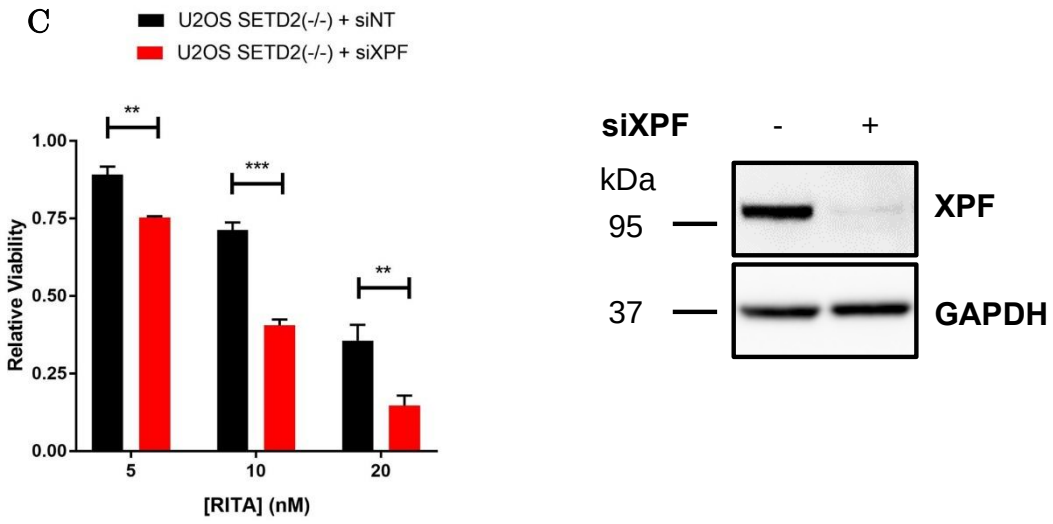
## 5.3. RITA is able to target cells deficient in the crosslink repair protein XPF but does not lead to increased DNA-DNA crosslink formation in the absence of SETD2

Soon after the discovery of RITA's potent anti-tumour effects in an NCI-60 cancer cell line screen (Rivera et al., 1999), it was reported to have the ability to induce DNA-DNA and DNA-protein crosslinks (Nieves-Neira et al., 1999). DNA inter-strand crosslinks (ICLs) are a particularly toxic type of lesion because of how they prevent the unwinding of the DNA double helix by forming an irreversible covalent bond between the two DNA strands, thereby interfering with normal DNA replication and transcription. There are several pathways to repair ICLs, and various sources of DNA damage (e.g. ultraviolet radiation, chemotherapy drugs, endogenous aldehydes) induce crosslink conformations that need to be dealt with in different ways. Some of the most important mediators of ICL repair belong to the Fanconi Anaemia (FA) pathway, named after a rare hereditary type of anaemia that results from the mutation of one or more genes in this pathway and is associated with increased risk of genomic aberrations and cancer (Fanconi, 1967; Niedernhofer et al., 2005). Over the years, more and more components have been added to the FA pathway, and the current model is that it mediates ICL repair by bringing together multiple repair mechanisms, including

nucleotide excision repair (NER), translesion synthesis (TLS), and homologous recombination (HR) (Niedzwiedz et al., 2004).

To confirm whether RITA cytotoxicity is related to the formation of crosslinks, the compound was tested in U2OS cells in which the repair protein XPF/ERCC4 has been deleted. XPF and its partner ERCC1 form a structure-specific endonuclease that mediates the initial "unhooking" step of ICL repair by creating an incision on the 5' side of the lesion (Niedernhofer et al., 2004). XPF is a recent addition to the FA pathway (Bogliolo et al., 2013; Kashiyama et al., 2013) and cells deficient in XPF have been reported to display a striking sensitivity to crosslinking agents (Andersson et al., 1996; Damia et al., 1996; Hoy et al., 1985). After RITA treatment, XPF-CRISPR cells had markedly reduced cell viability compared to parental cells, with an approximately 25-fold difference in cellular IC50 (Fig. 5.4A). Although there is still a greater discrepancy between SETD2-proficient and deficient cells in terms of RITA sensitivity, these results demonstrate that XPF loss greatly enhances RITA-mediated cytotoxicity. However, while XPF-CRISPR cells also exhibited hypersensitivity to the well-established crosslinking agent mitomycin C (MMC), SETD2-CRISPR cells did not (Fig. 5.4B). This suggests that crosslinking may not be the major mechanism through which RITA targets SETD2-deficient cells. To determine whether SETD2 and XPF are epistatic in the context of RITA sensitivity, XPF was depleted in SETD2-CRISPR cells prior to RITA treatment. Cell viability was further reduced after XPF knockdown in the presence of RITA (Fig. 5.4C), providing evidence that SETD2 and XPF operate via independent mechanisms to mediate the cellular response to RITA. Overall, these


A
IC50 (nM)
SETD2(+/+) -
SETD2(-/-) 5.1
XPF(+/+) 53.0
XPF(-/-) 2.4
Relative Viability
1.25
1.00
0.75
0.50
0.25
0.00
0
100
200
300
400
[RITA] (nM)
B
IC50 (ug/mL)
SETD2(+/+) 0.128
SETD2(-/-) 0.116
XPF(+/+) 0.269
XPF(-/-) 0.037
Relative Viability
1.25
1.00
0.75
0.50
0.25
0.00
0.0
0.4
0.8
1.2
1.6
[Mitomycin C] (ug/mL)


C
U2OS SETD2(-/-) + siNT
U2OS SETD2(-/-) + siXPF
**
***
**
1.00
0.75
0.50
0.25
0.00
Relative Viability
5
10
20
[RITA] (nM)
siXPF - +
kDa
95
37
XPF
GAPDH

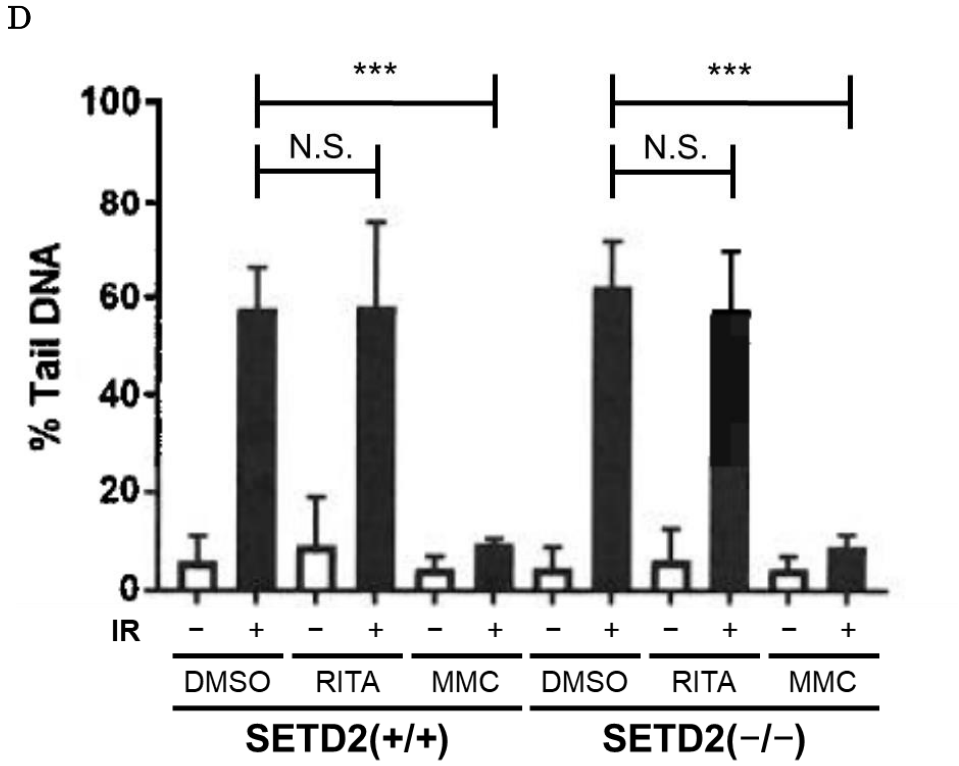



Figure 5.4. Dose-response viability curves for A. RITA and B. mitomycin C in parental XPF-CRISPR, and SETD2-CRISPR U2OS cells. Data are shown as mean ± SD (n = 3). IC50 values were calculated via nonlinear regression (4-parameter curve fitting). C. Cell viability assay after RITA treatment of SETD2-CRISPR U2OS cells transfected with non-targeting (NT) or XPF siRNA. Data are shown as mean ± SD (n = 3). P-values were calculated using the two-tailed Student's t-test (**$p < 0.01$, ***$p < 0.001$). XPF knockdown efficiency was confirmed by Western blotting. D. Amount of fragmented (tail) DNA after ionising radiation (IR) as measured by comet assay in parental and SETD2-CRISPR U2OS cells treated with RITA or mitomycin C (MMC). Data are shown as mean ± SEM of 3 independent replicates, each with 3 slides where 100 comets were counted per slide. The experiment and data analysis were performed by Mr. Christian Cooper and Mr. Michalis Challoumas from Prof. George D. Jones's group in the University of Leicester. P-values were calculated using the Student's two-tailed t-test (*** $p < 0.001$, N.S. = non-significant).

results indicate that while both XPF and SETD2 appear to be critical for cell survival after exposure to RITA, their roles are not necessarily related to crosslink repair.

To directly assess RITA's crosslinking capabilities, the compound was tested in a modified single-cell gel electrophoresis assay (a.k.a. comet assay) in collaboration with Prof. George Jones's laboratory. In the absence of ICLs, DNA is easily broken into small fragments after exposure to ionising radiation (IR) and their smaller size means faster migration through an agarose gel relative to intact DNA, thereby forming something similar to a comet's tail when visualised. When ICLs are present, however, DNA forms larger fragments after IR due to the covalent linkage of DNA strands, resulting in a smaller DNA tail (Spanswick et al., 2010). Using MMC as a positive control, the effect of each compound on the amount of tail DNA in individual cells after IR was measured. Although MMC (50 μM) was able to induce a significant reduction in IR-induced tail DNA, RITA (500 nM) had little to no effect even in SETD2-CRISPR cells (Fig. 5.4D), strongly suggesting that RITA has minimal crosslinking activity at this dose. Given that, as described in the previous chapter, a much lower dose (150 nM) was sufficient to impair replication fork progression within a similar time frame (30 min to 1 hour), these results provide a strong basis for concluding that the exquisite sensitivity of SETD2-deficient cells to RITA is not mediated by increased formation or persistence of DNA crosslinks.

## 5.4. RITA sensitivity in the absence of SETD2 is associated with altered expression of genes involved in DNA replication and the G1/S transition

In order to enhance our understanding of RITA's cellular effects, RNA-sequencing was performed on parental and SETD2-CRISPR cells after exposure to RITA. The fold change in transcript level was calculated relative to DMSO-treated samples for each cell line and plotted against the statistical significance of the expression change (Fig. 5.5A-B). It was immediately apparent that RITA induces more drastic alterations in gene expression in the absence of SETD2; while parental U2OS cells had <400 significantly altered genes in response to RITA, SETD2-CRISPR cells had >2000 genes whose expression changed significantly in either direction. Interestingly, there was a 3:1 ratio of downregulated versus upregulated genes in SETD2-CRISPR cells, suggesting that RITA's transcriptional impact is mainly inhibitory. To further understand the types of pathways perturbed by RITA, bioinformatics analysis was done on the genes that show a statistically significant difference in expression specifically in SETD2-CRISPR cells. Many of the gene ontology (GO) terms that were significantly enriched in this gene set are related to cell cycle and DNA replication (Table 5.1). This is consistent with the phenotypes described in the previous chapter – activation of the p53 pathway, increased non-replicating S-phase, accumulation in G2/M phase, and replication stress.

To further elaborate on the molecular pathways involved in RITA-mediated cytotoxicity, an RNAi sensitisation screen was conducted to identify other genes that enhance RITA sensitivity when lost. Based on our findings from the RNA-seq

experiment, as well as the phenotypes described in the previous chapter, the screen utilised siRNA libraries comprised of genes that regulate cell cycle progression (169 genes) and the DNA damage response (160 genes). After normalising each siRNA-treated well to the negative control (non-targeting siRNA), Z-scores were calculated for each gene and those with a more negative score (i.e. induced a greater reduction in cell viability) than SETD2 were selected as hits. This list of hits was then analysed bioinformatically to gain further understanding of the cellular pathways affected by these genes. Similar to the RNA-seq results, the GO terms significantly enriched in the hits from the screen include DNA replication and the G1/S transition (Table 5.2). Notably, several essential components of the DNA replication machinery were identified, including two of the single-stranded DNA-binding RPA proteins (*RPA2* and *RPA3*), the replication licensing factor *CDC6*, the DNA polymerase cofactor *PCNA*, and the pre-replication complex helicase component *MCM4*. Among the G1/S regulators that came out of the screen are the replication stress sensor and ATR substrate *CHEK1*, several G1/S cyclin-CDK inhibitors (*CDKN1B*, *CDKN1C*, *CDKN2D*), and the well-known tumour suppressor and transcriptional repressor *RB1*.

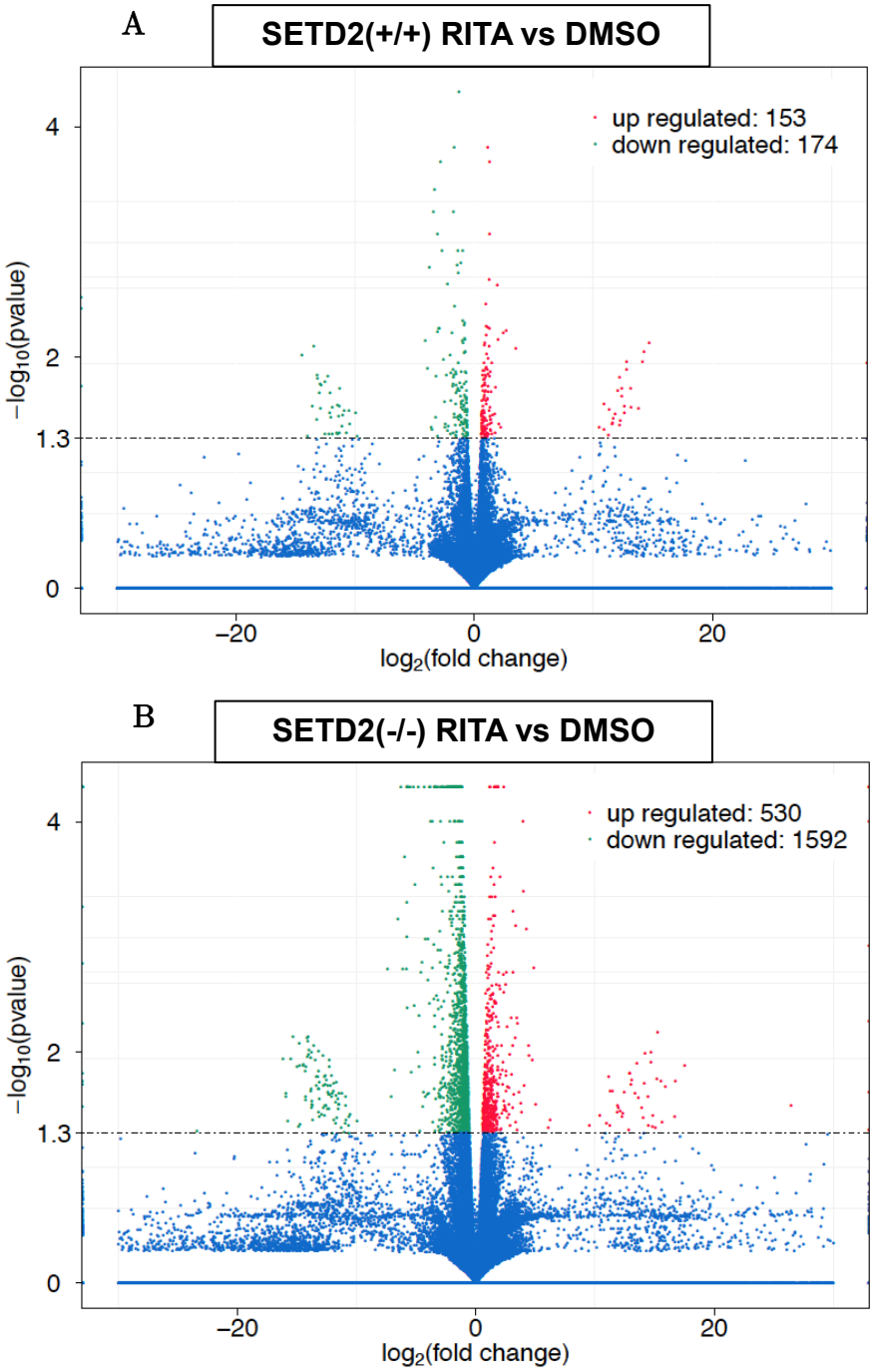



Figure 5.5. Volcano plots of gene transcripts differentially expressed in A. parental U2OS and B. SETD2-CRISPR U2OS cells after RITA treatment. Transcripts that underwent a significant ($p < 0.05$) change in expression are highlighted (red for upregulated genes, green for downregulated genes). The total number of significantly up/downregulated genes is indicated on the top-right of each plot.

Table 5.1. Notable gene ontology (GO) terms enriched among genes differentially expressed specifically in SETD2-CRISPR cells after RITA treatment

| GO Term | p-value | Up/Down |
|---|---|---|
| Negative regulation of cell proliferation | 0.00265718 | Up |
| DNA damage response, signal transduction by p53 class mediator resulting in cell cycle arrest | 0.00461277 | Up |
| Negative regulation of G1/S transition of mitotic cell cycle | 0.02420431 | Up |
| Anaphase-promoting complex-dependent catabolic process | 1.19E-15 | Down |
| G1/S transition of mitotic cell cycle | 1.19E-05 | Down |
| G2/M transition of mitotic cell cycle | 0.00105977 | Down |
| DNA replication | 0.00241917 | Down |
| Cell proliferation | 0.00334084 | Down |
| DNA replication initiation | 0.01095523 | Down |
| G2 DNA damage checkpoint | 0.01730346 | Down |
| Mitotic cell cycle checkpoint | 0.03669344 | Down |

The gene selected for initial validation of the siRNA screen was *RB1*, the first tumour suppressor ever identified. It was proposed to be involved in the carcinogenesis of retinoblastoma, a malignancy that affects retinal cells (Knudson, 1971), and this was eventually expanded to include multiple types of cancer (Dunn et al., 1988). The retinoblastoma (RB) protein has been shown to be a critical regulator of the G1/S transition via its inhibitory interaction with transcription factors such as the E2F family (Flemington et al., 1993) and is mainly regulated via CDK-mediated phosphorylation (Lees et al., 1991); it remains in a hypophosphorylated state in non-cycling cells and becomes progressively more phosphorylated throughout G1, which

abrogates its binding to E2Fs (Knudsen and Wang, 1997) and enables the transcription of genes necessary for normal S-phase entry (Sellers and Kaelin, 1996).

Given its prominent role in G1/S progression and the well-studied consequences of its loss on tumour development, it was of particular interest to confirm whether RB depletion could indeed enhance sensitivity to RITA. Consistent with the screen results, siRNA-mediated knockdown in U2OS cells demonstrated that reduced levels of RB significantly increased their sensitivity to RITA, with a 36% decrease in viability at the relatively low dose of 100 nM (Fig. 5.6). These findings support the reliability of the siRNA screen and provide evidence that further implicates the dysregulation of the G1/S transition and impairment of DNA replication as key processes in the mechanism of RITA's cytotoxicity against SETD2-deficient cells. Validation of the other G1/S regulatory genes that were identified as hits may lend additional credence to this hypothesis, although the possibility remains that these genes may generate similar phenotypes via completely independent pathways unrelated to SETD2.

Table 5.2. Notable gene ontology (GO) terms enriched among the hits from the RITA siRNA sensitisation screen

| GO Term | p-value | Genes |
|---|---|---|
| DNA replication | 1.56E-09 | RPA2, CDC6, HMGB2, CDKN2D, PCNA, CHEK1, CDC34, CHAF1A, MCM4, RPA3 |
| Regulation of cyclin-dependent protein kinase activity | 6.42E-09 | CDKN1C, ANAPC2, CDC6, CDK5R1, CDKN1B, CDKN2D, CHEK1 |
| G1/S transition of mitotic cell cycle | 1.57E-05 | CDKN1B, CDKN2D, CDC34, RB1, RBBP8 |
| DNA-dependent DNA replication | 5.24E-04 | RPA2, HMGB2, CDC34, MCM4 |
| Regulation of DNA replication | 6.37E-04 | CDC6, GMNN, PCNA, TGFB1 |
| G1 phase | 0.001479 | CDKN1C, CDC6, RB1 |
| Negative regulation of DNA replication | 0.002631 | CDC6, GMNN, TGFB1 |

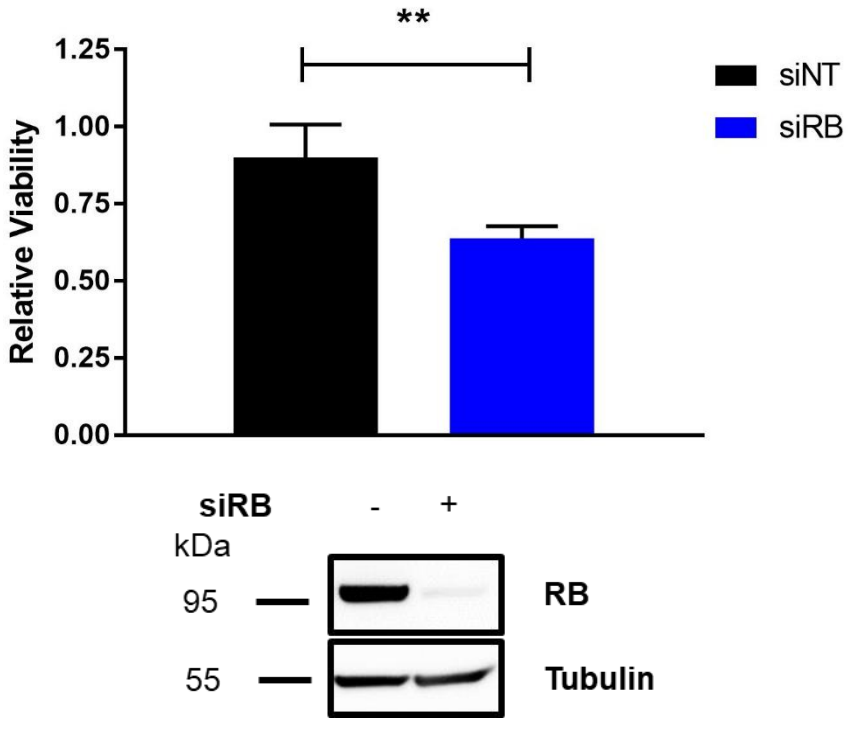



Fig. 5.6 Cell viability assay after RITA treatment (100 nM) combined with siRNA depletion of RB in U2OS cells. Viability was calculated relative to cells incubated with non-targeting siRNA. Data are shown as mean ± SD (n = 3). P-values were calculated using the Student's two-tailed t-test (** $p < 0.01$). RB knockdown efficiency was confirmed by Western blotting.

## 5.5. Modification of RITA's terminal hydroxyls and ring groups modulates its potency against SETD2-deficient cells

Another approach to unravelling RITA's mechanism of action is to learn from its chemistry. RITA has a perfectly symmetrical structure with three five-sided carbon ring groups (a thiophene, a furan, and another thiophene) in the middle and a hydroxyl group at each end (Fig. 5.7). In order to obtain information about the importance of each of RITA's chemical components, we collaborated with chemists in Dr. Bart Cornelissen's and Prof. Stuart Conway's groups to create RITA variants in which different parts of the molecule were modified. These variants were then tested for their effects on cell viability and their potency was evaluated relative to the original RITA compound. The structures of these variants are shown in Fig. 5.5. The vast majority of the modified versions were largely ineffective in terms of cytotoxicity, with most of them displaying little to no reduction in cell viability at concentrations of up to 1 µM. The most notable exceptions to this are DSCH04023 (#4023) and DSCH04033 (#4033). Variant #4023 is a dialdehyde version of the original dihydroxyl compound, whereas #4033 is a version with the middle furan ring removed. Both of these compounds were able to selectively target SETD2-CRISPR cells (Fig. 5.8A-B), albeit with a higher cellular IC50 than the original RITA (RITA IC50 for SETD2-CRISPR U2OS = 11.6 nM).

The rationale for the modifications made to Variant #4023 is related to our investigation into RITA's potential crosslinking activity; aldehydes react readily with DNA and proteins to form crosslinks, as evidenced by studies on both endogenous and

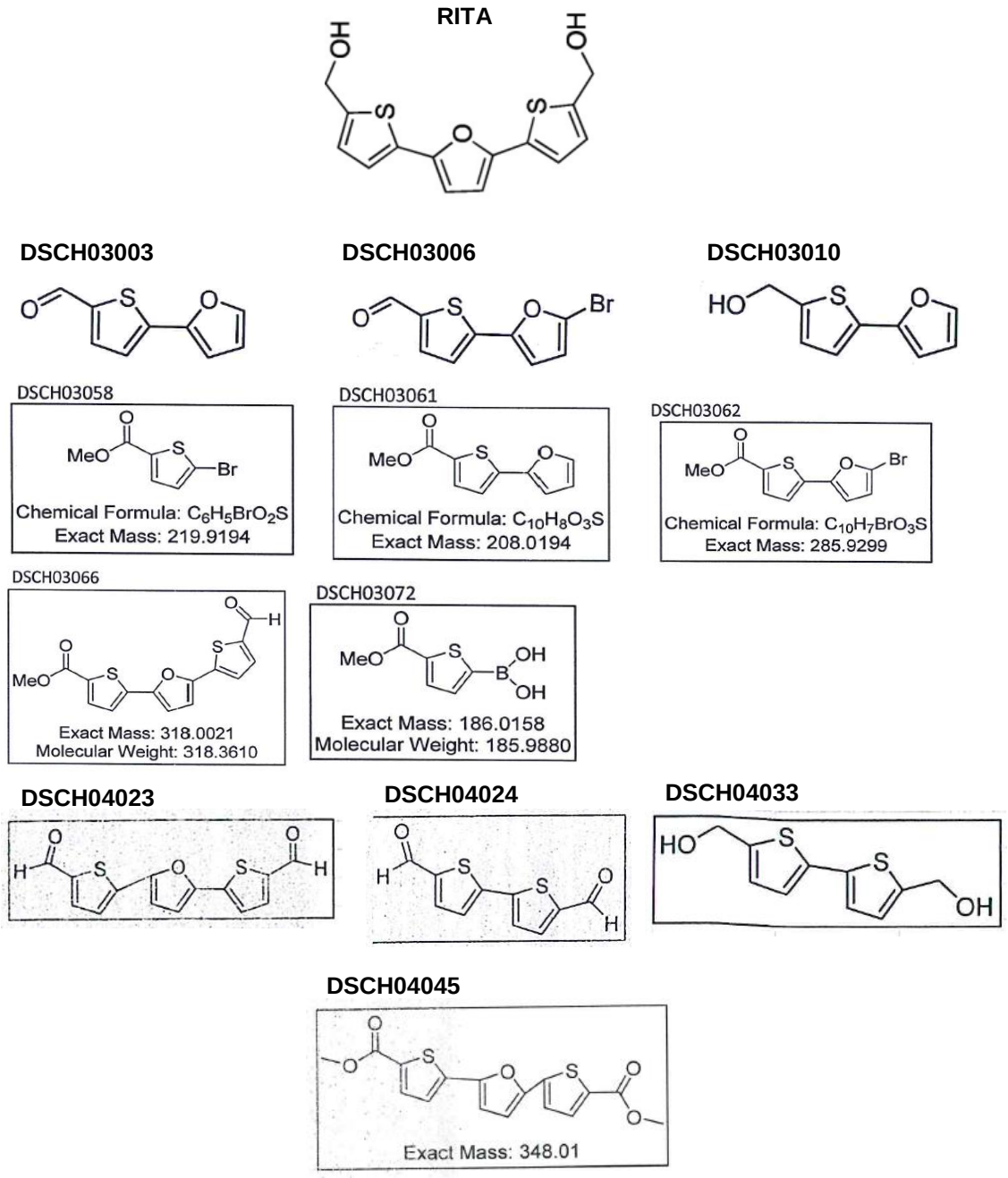
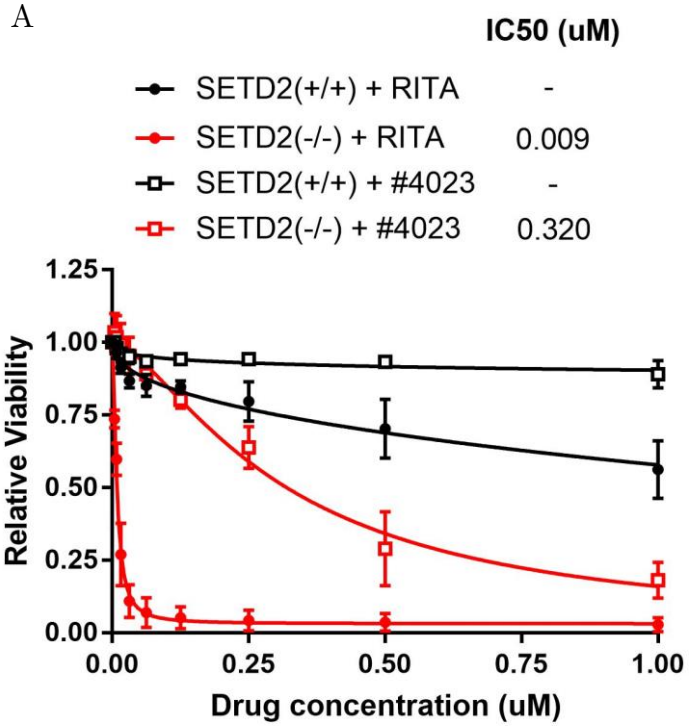


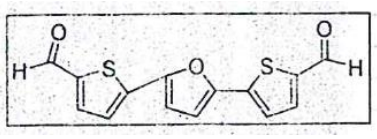

Figure 5.7. Chemical structures of the original RITA compound and various chemically modified versions. The RITA variants were synthesised by Dr. Deborah Sneddon from Dr. Bart Cornelissen's group, with assistance from the lab of Prof. Stuart Conway at the Department of Chemistry.

synthetic aldehydes (Cheng et al., 2003; Murata-Kamiya and Kamiya, 2001; Stein et al., 2006; Wang et al., 2000). We therefore hypothesised that an aldehyde version of RITA would be a more efficient crosslinking agent and would display toxicity in parental as well as SETD2-CRISPR cells. However, as seen in Fig. 5.8A, the aldehyde variant was less potent than RITA in SETD2-deficient cells and completely ineffective in the parental cells, which supports the findings of the comet assay (Fig. 5.4C) and is consistent with the notion that DNA crosslinking is not RITA's primary mode of action in the absence of SETD2.

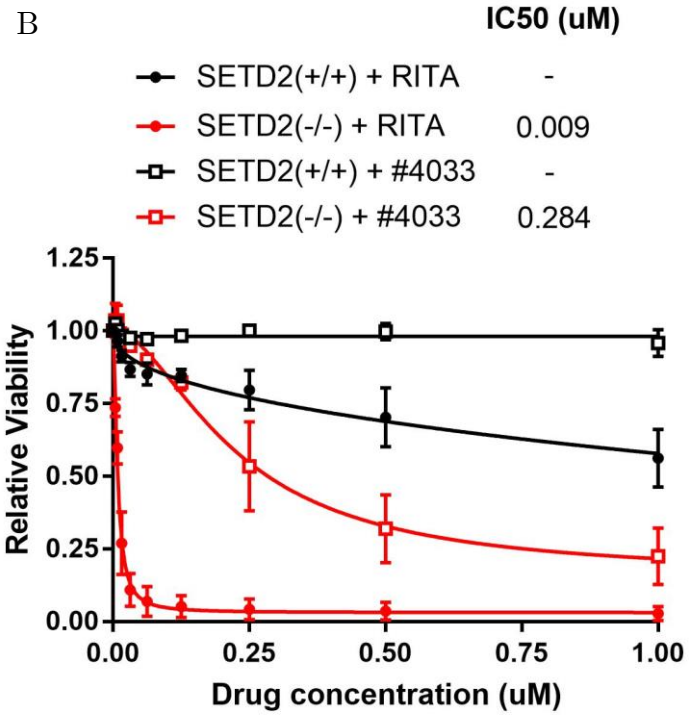
Variant #4033 was designed on the basis of RITA's reported p53-binding ability. The interaction between RITA and p53's N-terminus was demonstrated more than a decade ago (Issaeva et al., 2004), with further details on the residues involved in this interaction made available recently in an as-yet unpublished report (Zawacka-Pankau et al., 2018). Computational modelling of the RITA-p53 structure predicts that two serines (Ser33 and Ser37) on the p53 protein form hydrogen bonds with RITA's hydroxyl groups while two prolines (Pro34 and Pro36) are part of a hydrophobic interface with RITA's thiophene and furan rings (Zawacka-Pankau et al., 2018). If this model is accurate, the length of the RITA molecule should have a significant impact on its activity, given that both its hydroxyl ends and carbon rings are involved in its interaction with p53. As shown in Fig. 5.8B, the shortened variant is indeed less potent than the original RITA, indicating that all three of the rings play a role in RITA's interaction with its target(s) in the absence of SETD2, although whether p53 is one of those targets remains inconclusive.

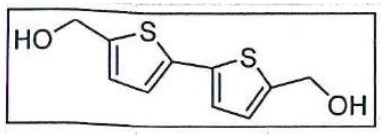
A


IC50 (uM)
SETD2(+/+) + RITA -
SETD2(-/-) + RITA 0.009
SETD2(+/+) + #4023 -
SETD2(-/-) + #4023 0.320
Relative Viability
1.25
1.00
0.75
0.50
0.25
0.00
0.00
0.25
0.50
0.75
1.00
Drug concentration (uM)


O
H
S
O
S
O
H

B


IC50 (uM)
SETD2(+/+) + RITA -
SETD2(-/-) + RITA 0.009
SETD2(+/+) + #4033 -
SETD2(-/-) + #4033 0.284
Relative Viability
1.25
1.00
0.75
0.50
0.25
0.00
0.00
0.25
0.50
0.75
1.00
Drug concentration (uM)


HO
S
S
OH

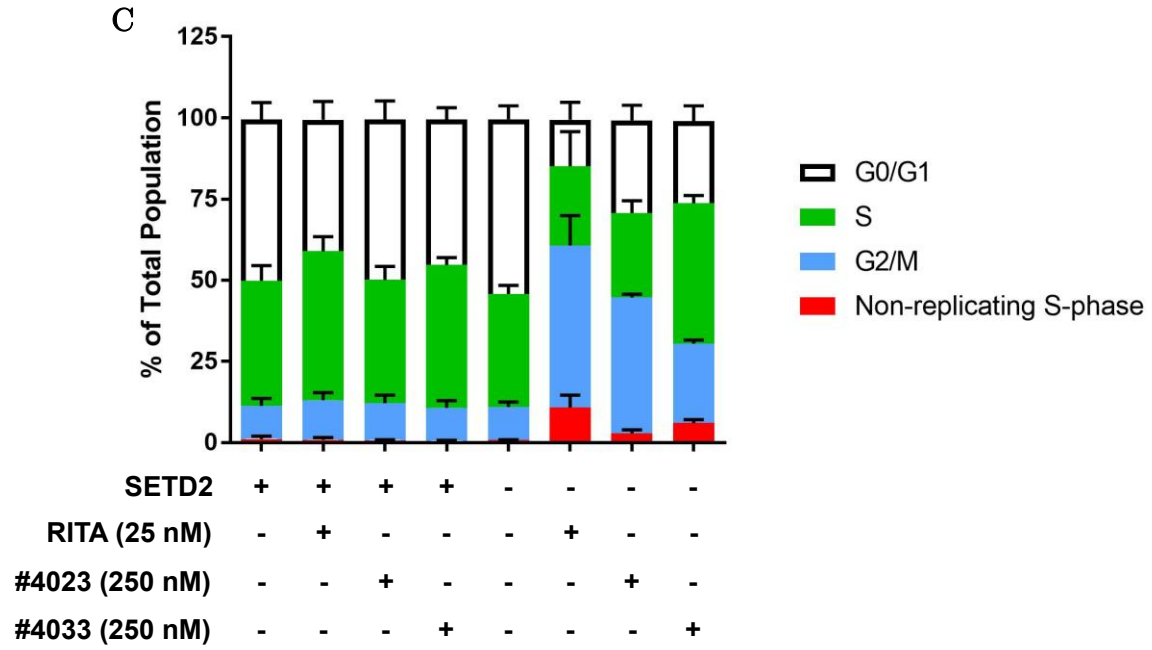



Figure 5.8. Dose-response viability curves for RITA and its variants A. DSCH04023 (#4023) and B. DSCH04033 (#4033) in parental and SETD2-CRISPR U2OS cells. Data are shown as mean ± SD (n = 3). IC50 values were calculated via nonlinear regression (4-parameter curve fitting). The structures of each variant are displayed to the right of each graph. C. Cell cycle distribution of U2OS cells after treatment with the indicated doses of RITA, DSCH04023 (#4023), and DSCH04033 (#4033) for 48 hours. Data shown as mean ± SD (n = 3).

The similarities and differences between RITA and Variants #4023 and #4033 were further investigated by measuring cell cycle progression after treatment with each compound. Consistent with the viability data, #4023 induced a weaker phenotype compared to RITA in SETD2-CRISPR cells, with a smaller non-replicating S-phase population (2.8% vs. 10.8%) and less severe G2/M arrest (41.9% vs. 49.9%) even at a 10-fold higher dose (Fig. 5.8C). Interestingly, #4033 displayed a markedly different phenotype; compared to the RITA group, its S-phase levels were markedly higher and more similar to the DMSO control (43.3% vs. 24.4%), its G2/M population was notably smaller (24.4% vs. 49.9%), and it had an intermediate amount of non-replicating S-phase (6.1% vs. 10.8%). Preliminary Western blot data suggest that exposure to both variants leads to increased total p53 and phospho-p53 (Ser15) specifically in SETD2-CRISPR cells, although to a lesser extent than the original RITA compound. These results reinforce the conclusions alluded to by the data accumulated thus far, namely that RITA's main mechanism of action in SETD2-deficient cells is unrelated to any purported crosslinking activity and appears to involve molecular interactions that require all three of its ring groups as well as its terminal hydroxyls.

## 5.6.Chapter Discussion

The discovery of the SETD2-WEE1 synthetic lethality (Pai et al., 2019; Pfister et al., 2015) brought new insights into the diverse biological roles of SETD2 and H3K36 trimethylation. This finding, along with the extant literature on SETD2/H3K36me3, provided a wealth of knowledge that informed the current investigation into this

putative novel synthetic lethal interaction. The observation that homologous recombination, despite being one of the key functions of this histone mark (Pfister et al., 2014) is not a major factor in RITA's cytotoxicity against SETD2-deficient cells (Fig. 5.1A-B) is consistent with the absence of a DSB response via ATM/CHK2, as discussed in the previous chapter. Furthermore, despite the critical role of RRM2 and dNTP homeostasis in the SETD2-WEE1 synthetic lethality, there is no indication that bolstering the dNTP supply of SETD2-deficient cells has any significant effect on RITA sensitivity (Fig. 5.2A). The importance of CDK activity, however, appears to be a more complex question. The reduction in RITA sensitivity in the presence of RO3306 points towards CDK hyperactivation being involved, but the absence of any obvious changes in the phosphorylation of CDK1 and its targets does not support a direct effect of RITA on CDK activity. As mentioned previously, these results do not exclude the possibility of an indirect relationship between RITA and CDKs. For example, the timely activation of CDK1 in mid to late S-phase is necessary for the firing of late replication origins (Katsuno et al., 2009); given that one of RITA's most striking phenotypes is the induction of replication stress, the inability to activate CDK1 during S-phase may attenuate any replication-induced DNA damage that arises after RITA treatment by blocking further replication. In addition, the consequences of CDK inhibition on cell cycle progression may also be relevant and future experiments should look into whether RITA-dependent cell cycle dysregulation in the absence of SETD2 still occurs when combined with RO3306.

The molecular mechanisms that RITA employs against a variety of tumours and cell lines have been the subject of many studies. Although most frequently associated with its inhibition of the p53-MDM2 interaction (Issaeva et al., 2004), a number of groups have reported RITA cytotoxicity in p53-independent settings. Unlike the MDM2 inhibitor nutlin-3, RITA has a demonstrable ability to target tumour cells of varying p53 states, with its activity against p53-mutant and null cell lines being linked to the mitogen-activated protein kinases (MAPK) p38 and JNK (Weilbacher et al., 2014). More recently, RITA's ability to activate JNK independently of p53 was linked to the inhibition of the Hedgehog pathway, which regulates stem cell differentiation and is overexpressed in certain cancers (Azatyan et al., 2019). RITA was also shown to be effective against p53-null leukaemia cells via the attenuation of pro-survival and anti-apoptotic pathways distinct from those regulated by p53 (Mobaraki et al., 2018). Perhaps most contradictory to the notion of RITA's dependence on p53 is a CRISPR screen conducted to shed light on this issue; whereas nutlin-3 treatment led to a significant enrichment in cells with CRISPR-induced insertion/deletion (indel) mutations or truncations in the *TP53* locus, RITA treatment did not (Wanzel et al., 2016). The data presented in this chapter demonstrate that p53-wild type MCF7 cells are more sensitive than their p53-deleted counterparts (Fig. 5.3A), which is consistent with RITA's initial description as a p53 reactivator. However, the enhanced sensitivity imparted by SETD2 depletion even in p53-CRISPR cells (Fig. 5.3B) is in agreement with subsequent studies. One possibility, which is supported by published literature (Weilbacher et al., 2014), is that in sensitive cell lines, RITA can affect p53 target

genes without the involvement of p53 itself, leading to the activation of cell cycle arrest and apoptosis pathways without requiring p53 function. Therefore, while RITA may indeed stabilise p53 when the protein is present in its wild-type conformation, the compound may not require it to mediate its anti-tumour effects.

In addition to its multifaceted effects on cell signalling, RITA has been reported to act directly on DNA via crosslinking (Nieves-Neira et al., 1999). The presence of RITA-induced replication stress in SETD2-deficient cells supports this notion, as crosslinking agents have been shown to mediate cellular cytotoxicity in a replication-dependent manner (Akkari et al., 2000). RITA's potency against XPF-deficient cells (Fig. 5.4A), with their well-established sensitivity to a variety of crosslinking agents (Andersson et al., 1996; Damia et al., 1996; Hoy et al., 1985), provided initial evidence that crosslinks may indeed be involved. However, the lack of sensitivity of SETD2-CRISPR cells to the more traditional crosslinker mitomycin C (Fig. 5.4B), combined with the observation that SETD2 and XPF are epistatic in the context of RITA sensitivity (Fig. 5.4C), indicate instead that RITA's targeting of both SETD2- and XPF-deficient cells is unrelated to any reported crosslinking activity. This was further corroborated by a direct measurement of crosslink formation, which failed to show any significant increase after RITA treatment (Fig. 5.4D). Given the key role played by the HR pathway in ICL repair (Niedzwiedz et al., 2004), the absence of crosslinks in this case is consistent with the minimal effects of HR deficiency on RITA sensitivity (Fig. 5.1A-B).

A recurring theme linking RITA's phenotypes in SETD2-deficient cells is DNA replication. This was further emphasised by the results of both the RNA-seq and the cell cycle/DDR siRNA screen, with the G1/S transition and DNA replication featuring prominently among the enriched GO terms (Table 5.1 and 5.2). As exemplified by depletion of the tumour suppressor and E2F inhibitor RB (Fig. 5.6), perturbations in G1/S progression that could potentially lead to dysregulated DNA replication appear to play an important role in determining RITA sensitivity. Unpublished data from our group suggest that, like RB, SETD2 may be a critical regulator of E2F transcription during G1; SETD2-deficient cells progress more slowly from G1 to S, which is associated with impaired activation of E2F target genes necessary for the initiation of S phase. In contrast, RB loss would be predicted to accelerate S-phase entry through the inappropriate activation of those same targets, which has been shown to lead to replication stress (Tort et al., 2006). Further investigation into the commonalities between SETD2 and known G1/S regulators should be undertaken by validating other relevant hits from the siRNA screen and determining whether they produce similar phenotypes as SETD2 loss in the presence of RITA.

RITA's relatively simple molecular structure has provided the opportunity to probe its mechanism of action via chemical modifications. Replacing its terminal hydroxyls or changing its ring groups has led to distinct changes in its activity against SETD2-deficient cells, indicating that the specific combination of its functional groups is vital for its potency. Modifications of RITA's structure and their effects on its cytotoxicity have been reported before (Lin et al., 2012); in particular, the dialdehyde

version of RITA (#4023) was also synthesised and tested in viability assays and was significantly less effective than the original molecule, consistent with the data from SETD2-CRISPR cells (Fig. 5.8A). The most potent variant generated by this group had three thiophene rings (S-S-S) rather than two thiophenes and a furan (S-O-S), and was similar to RITA in terms of cellular IC50, induction of apoptosis, and upregulation of p53 protein levels (Lin et al., 2012). This may be in accordance with the proposed molecular interactions between p53 and RITA, which asserts that the terminal hydroxyls are necessary for interaction with specific serines while the ring groups act as a hydrophobic interface for two specific prolines in p53's N-terminus (Zawacka-Pankau et al., 2018). Therefore, changing the hydroxyl groups is likely to have a drastic impact on RITA's chemistry, while altering the ring groups may be not be meaningful as long as the hydrophobicity of the moieties is retained.

In summary, the key findings of this chapter are:

- RITA sensitivity is not mediated by deficiencies in homologous recombination repair or nucleotide pools
- RITA sensitivity can be partially modulated by CDK1/2 inhibition but is not associated with direct activation of CDK1 by RITA
- RITA targets cells deficient in the crosslink repair protein XPF but does not lead to increased crosslink formation
- RITA alters the transcriptome more severely in the absence of SETD2, particularly with respect to genes involved in DNA replication and the G1/S transition

- RITA sensitivity is enhanced by the depletion of certain cell cycle regulators, particularly those involved in G1/S progression such as the tumour suppressor RB
- Modifying RITA's chemical groups, specifically its terminal hydroxyls and thiophene/furan rings, modulates its cytotoxic activity against SETD2-deficient cells

# 6. Discussion

## 6.1 Epigenetic modifiers as targets in cancer therapy

Dysregulation of epigenetic marks has been established alongside genome instability as a key mechanism through which tumour cells aberrantly activate oncogenes and inactivate tumour suppressors. DNA hypomethylation has been observed both globally (Bedford and van Helden, 1987; Lin et al., 2001) and at specific locations in the genome, such as in the gene body of insulin growth factor 2 (IGF2) (Cui et al., 2002). At the other end of the spectrum, DNA hypermethylation has been associated with the silencing of tumour suppressor genes such as *TP53*, *RB1*, and *BRCA1* (Baldwin et al., 2000; Rideout et al., 1991; Sakai et al., 1991). The plethora of histone modifications provides even more examples of how carcinogenesis can be driven by epigenetic abnormalities. Histone hypoacetylation has been established as one of the earliest steps in gene silencing (Mutskov and Felsenfeld, 2004) and increasing the acetylation status of tumour suppressor genes has been shown to restore their expression (Pruitt et al., 2006). In addition, the dysregulation of multiple histone marks, such as histone acetylation and methylation, have been observed to work

together to create an epigenetic landscape that is favourable for tumour growth (Fraga et al., 2005). The status of histone modifying enzymes such as SETD2 (Duns et al., 2012) as either tumour suppressors or oncogenes emphasises the importance of these genes in the development of cancer.

It is thus unsurprising that epigenetic modifiers have been extensively studied as potential therapeutic targets. Among the first epigenetic inhibitors to be developed were aimed at histone deacetylases (HDACs), with the first compound discovered even before the biology of histones and nucleosomes was established (Riggs et al., 1977). Several HDAC inhibitors have been approved for clinical use as monotherapies mainly against haematological malignancies (Bertino and Otterson, 2011; Lee et al., 2015; Mann et al., 2007). The pan-HDAC inhibitor used in this study, panobinostat, is approved in combination with the proteasome inhibitor bortezomib and the corticosteroid dexamethasone for the treatment of multiple myeloma (San-Miguel et al., 2014). Interestingly, this inhibitor was tested up to a Phase II trial as a monotherapy in advanced clear cell renal cell carcinoma (ccRCC), which has been shown to have frequent mutations in SETD2 (Dalgliesh et al., 2010) and low levels of H3K36me3 (Ho et al., 2016), but was discontinued due to a lack of clinical response (Hainsworth et al., 2011). Given that SETD2-deleted U2OS cells were no more sensitive to panobinostat than their parental counterparts, both the clinical results and the *in vitro* data presented in Chapter 3 may indicate that SETD2 loss does not predict the efficacy of pan-HDAC inhibitors.

HDAC inhibitors are being investigated in combination with a wide variety of other therapeutic agents, encompassing both traditional chemotherapy and radiotherapy as well as targeted drugs such as kinase inhibitors (Suraweera et al., 2018). A combined regimen of the WEE1 inhibitor AZD1775 and the pan-HDAC inhibitor belinostat was being tested in a Phase I trial for use against acute myeloid leukaemia, but was subsequently terminated in May 2018 (ClinicalTrials.gov). The synergy between HDAC and WEE1 inhibition in AML was demonstrated both *in vitro* and in mouse xenografts and the combination was effective in cell lines with mutations in p53 and/or the leukaemia-associated fusion protein FLT3-ITD (Zhou et al., 2015). Importantly, this study did not explicitly establish that the combined regimen was more potent in the presence of a specific mutation or genotype, although the high frequency of p53 (Ferrari et al., 2014) and FLT3-ITD (Daver et al., 2019) mutations in AML could be a positive indicator of this combination's potential clinical utility against an aggressive subtype of this disease with limited therapeutic options. Chapter 3's findings that panobinostat potentiates the anti-tumour effects of AZD1775 specifically in SETD2-deficient cells provide a similar hope for tumours such as advanced or metastatic ccRCC, adding to the small number of available regimens for this subset of RCC (Atkins and Tannir, 2018). In addition, if the ongoing clinical trial succeeds (ClinicalTrials.gov) and the SETD2-WEE1 synthetic lethality is eventually approved for clinical use, combining WEE1 and HDAC inhibition may be one strategy for addressing the inevitable evolution of drug resistance. Similar tactics have already proven their worth clinically, such as with combined chemotherapies in metastatic

breast cancer (Albain et al., 2008) and the combination of a targeted drug with chemotherapy in the standard regimen for B-cell lymphoma (Mounier et al., 2003).

## 6.2 Targeting the loss of epigenetic regulators via synthetic lethality

In addition to SETD2 and WEE1, other synthetic lethal interactions that involve epigenetic pathways have been described in published literature. Mutations in the SWI/SNF family of chromatin remodellers, which form large multi-subunit complexes that mediate the movement of nucleosomes (Phelan et al., 1999), are present in approximately 20% of all human cancers (Kadoch et al., 2013). Multiple synthetic lethal interactions between SWI/SNF genes and other epigenetic regulators have been identified. Inhibitors of EZH2, a histone methyltransferase and the catalytic subunit of the Polycomb Repressive Complex 2 (PRC2) that mediates the silencing of many tumour suppressor genes via histone H3K27 di- and trimethylation (Cao et al., 2002; Kuzmichev et al., 2002), have been shown to target tumours with inactivating mutations in SWI/SNF family members *SNF5* (Knutson et al., 2013), *ARID1A*, *PBRM1*, and *SMARCA4* (Bitler et al., 2015; Kim et al., 2015).

Many examples of the interplay between histone acetylation and methylation have been reported. The SAGA histone acetyltransferase (HAT) complex component SGF29 is a reader of H3K4me3 and is necessary for SAGA recruitment to its target sites on histone H3 (Bian et al., 2011). Similarly, the yeast HDAC complex Rpd3S requires the H3K36me2/3 reader Eaf3 to be recruited onto chromatin (Carrozza et al., 2005; Joshi and Struhl, 2005). The observed loss of viability in SETD2-deficient cells after the depletion of HDAC1/2, as described in Chapter 3, hints at a genetic

relationship that is distinct from what is seen in yeast. If the requirement for H3K36me3 to mediate HDAC1/2 recruitment also applies in humans, SETD2-deficient cells would already have inadequate histone deacetylation and further HDAC depletion would not be expected to cause further physiological deficits. A synthetic lethal interaction between them would necessitate the independent regulation of one or more common processes; therefore, the viability data suggest that HDAC1/2 and SETD2 have at least some functions that are not in the same pathway but converge on the same outcome. Unpublished results from other members of our group show that depletion of SETD2 and HDAC2 both lead to significantly impaired transcription of E2F target genes, including a number of critical regulators of DNA replication such as RRM2. This is associated with decelerated progression from G1 to S phase and increased levels of endogenous replication stress and mitotic defects such as anaphase bridges. These findings suggest that, in the absence of SETD2, cells rely on HDAC2-mediated mechanisms of promoting the expression of E2F target genes necessary for S-phase entry. This would provide a rationale for targeting SETD2/H3K36me3-deficient cancers with HDAC2-specific inhibitors; in the absence of such compounds, the HDAC1/2 inhibitor romidepsin was able to provide some evidence to support this hypothesis in the form of a slightly but significantly higher potency in cells that lack SETD2. The observation that SETD2-deleted cells display more rapid G1 arrest and p53/p21 induction implies that SETD2-deleted cells are more sensitive to perturbations in the G1/S transition, further corroborating the aforementioned explanation of the SETD2-HDAC2 synthetic lethality.

## 6.3 Past and current attempts to target p53 in human cancers

p53's status as the most commonly mutated gene in human cancers (Beroud and Soussi, 2003; Hussain and Harris, 1998) has made it one of the most attractive targets for cancer therapy. The most well-known attempt is the synthesis of the nutlin family of compounds, which bind to MDM2 and inhibit its interaction with and degradation of p53 (Vassilev et al., 2004). Further optimisation of nutlin lead compounds eventually led to the development of RG7112 (Roche), the first MDM2 inhibitor to be evaluated in clinical trials. Unfortunately, the dose required to elicit significant clinical responses also led to marked haematological and gastrointestinal toxicities (Patnaik et al., 2015). This has spurred the development of a second-generation nutlin, RG7388/idasanutlin (Roche), that has superior potency and selectivity compared to its predecessor (Ding et al., 2013). According to ClinicalTrials.gov, idasanutlin is currently in 11 active clinical trials, either as monotherapy, combined with chemotherapeutic agents such as cytarabine (a nucleoside analog), or combined with targeted agents such as venetoclax (a BCL-2 inhibitor).

In contrast to the striking loss of viability observed in SETD2-deficient cells after RITA treatment as described in Chapter 4, nutlin-3a (the compound from which RG7112 was derived) failed to show any enhanced cytotoxicity against SETD2-CRISPR versus parental cells. This finding, together with the observed sensitisation of p53-negative cells to RITA after SETD2 depletion in Chapter 5, is consistent with published reports of RITA's p53-independent activities. It is also possible that SETD2 loss compromises MDM2 function in some way, although one previous report has

described the complete opposite, namely that SETD2 deficiency leads to increased MDM2 expression at both the mRNA and protein levels (Xie et al., 2008). However, preliminary data from our group has suggested the existence of a truncated form of MDM2 specifically in SETD2-CRISPR cells. This approximately 60-kilodalton peptide (compared to the 90 kDa full-length MDM2) has also been observed in other cancer cell lines either in the presence (Chen et al., 1997; Erhardt et al., 1997) or absence (Pochampally et al., 1998) of apoptosis. In specific contexts, such as after caspase 2-mediated cleavage of MDM2 during the process of apoptotic cell death, this p60 fragment retains the ability to bind to p53 but lacks the MDM2 RING domain and therefore its ubiquitin ligase activity; thus, cleaved MDM2 is able to compete with full-length MDM2 for p53 binding but is unable to induce p53 degradation, leading to the stabilisation and upregulation of p53 (Oliver et al., 2011). If this type of MDM2 cleavage is occurring at a higher rate in the absence of SETD2, it may explain why SETD2-CRISPR cells have a higher baseline level of p53 protein and are not sensitive to nutlins. Its implications for RITA sensitivity are more complex in light of RITA's multi-faceted cellular effects and its cytotoxicity even in the absence of p53. Further experiments are necessary to elucidate any potential link between SETD2 and MDM2 stability, as well as whether such a relationship has any bearing on the exquisite sensitivity of SETD2-deficient cells to RITA.

The RITA compound belongs to a small group of p53-targeting compounds that are reported to act on p53 directly, instead of on MDM2. Since many of the most common p53 mutations in human cancers affect p53's ability to bind to DNA

(Friedlander et al., 1996), one of the earliest therapeutic strategies was to use small molecules to restore the functionality of mutant p53 (Foster et al., 1999). RITA has been shown to reduce viability, induce apoptosis, and activate downstream p53 targets in both p53 wild-type and mutant cell lines (Burmakin et al., 2013; Zhao et al., 2010), suggesting that the presence of the p53 protein is sufficient for RITA to exert its cytotoxic effects. However, findings like these are contradicted by a CRISPR screen demonstrating that p53 deletion confers no survival advantage in response to RITA treatment, whereas nutlin-3a is significantly less effective in the absence of p53 (Wanzel et al., 2016). Instead, this report proposes that sensitivity to RITA is associated with defects in DNA damage signalling and repair, based on the observation that RITA-resistant cell lines have noticeably less γH2AX compared to their RITA-sensitive counterparts. Furthermore, cross-resistance between RITA and the platinum agents cisplatin and oxaliplatin was shown; consistent with this, depletion of the Fanconi anaemia pathway component FANCD2 was able to resensitise resistant cell lines to RITA (Wanzel et al., 2016). However, although the current study observed FANCD2 ubiquitination in response to RITA, there was no measurable difference between SETD2-CRISPR and parental cells.

Regardless, the published link between RITA and the DDR provides some useful clues for constructing a model pathway for RITA in the context of SETD2 deficiency (Fig. 6.1). Although the p53 pathway is a key component of the DDR and a direct substrate of ATR (Lakin et al., 1999), the replication stress response can trigger S-phase or G2 arrest independently of p53 via CHK1-mediated degradation of CDC25A,

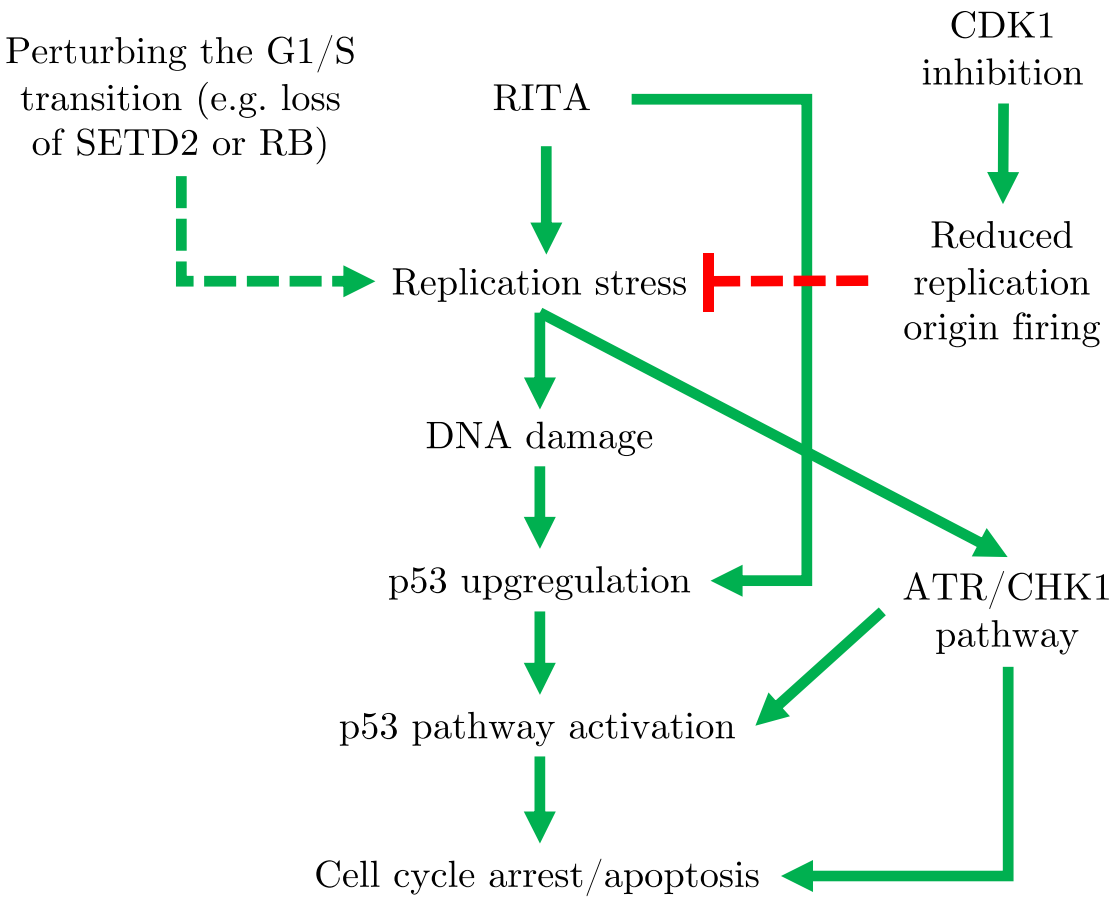



Figure 6.1. Proposed model of RITA's mechanism of action in the context of SETD2 loss and other disruptions to the G1/S transition. Dashed lines indicate partial or tolerable effects that lead to incomplete activation/inactivation of subsequent pathways.

thus preventing the dephosphorylation and activation of CDK2 (Mailand et al., 2000). In the case of replication stress induced by oncogene activation or tumour suppressor loss, as would be the case in SETD2-deficient cells, there is evidence of tolerance mechanisms through which cancer cells are able to grow and survive in the presence of replication defects. The detrimental effects of replication stress associated with CDK2 hyperactivation (via cyclin E overexpression, oncogenic RAS mutations, or WEE1 inhibition) are mitigated by the error-prone DNA polymerase Polκ (kappa), whose expression is negatively regulated by p53 in normal cells (Yang et al., 2017). Similarly, the translesion polymerase Polη (eta) protects against replication fork collapse caused by MYC-induced replication stress (Kurashima et al., 2018). Therefore, it is possible that replication stress induced by SETD2 loss is tolerated by the cell in the absence of any other insults, being insufficient for the complete activation of the replication stress response and the p53 pathway. The addition of RITA to these cells then tips the balance and pushes them over their threshold of damage tolerance, culminating in loss of viability and cell death. Furthermore, CDK hyperactivation via WEE1 inhibition has been shown to induce aberrantly high levels of replication origin firing, leading to replication stress that can be suppressed by the CDK1 inhibitor RO3306 or CDK1 depletion (Beck et al., 2012). This may explain the reduction in RITA potency observed when combined with RO3306 in SETD2-deficient cells, although the toxic effects of CDK1 inhibition would most likely prevent a complete rescue as the cells would be unable to replicate their DNA or continue cycling under these conditions. Conversely, in the context of low or no replication stress, such as in normal cells (Shin et al., 2017)

or SETD2-proficient cancer cells, RITA on its own is insufficient for a significant impact on cell survival. It would be interesting to test these hypotheses by observing RITA's potency in cancer cell lines that display oncogene-induced replication stress and CDK hyperactivation, such as in the case of cyclin E overexpression.

## 6.4 Future work

A key question regarding the putative SETD2-HDAC2 synthetic lethality is whether it has any clinical potential. A significant hurdle in the investigation of this issue is the lack of HDAC2-specific inhibitors. A collaboration with chemists in the field of epigenetic modulators could attempt to screen for lead compounds of sufficient specificity against HDAC2. If such compounds ever became available, they would enable *in vitro* and *in vivo* validation of the genetic interaction between SETD2 and HDAC2 and may help elucidate the molecular mechanisms underlying their synthetic lethality.

Much of the uncertainty regarding RITA's biological effects stems from conflicting evidence about its molecular target. To determine which protein(s) RITA is interacting with in the absence of SETD2, a collaboration with Dr. Kilian Huber at the Target Discovery Institute is planning to utilise the cellular thermal shift assay in combination with quantitative mass spectrometry (CETSA-MS) to identify proteins that have an altered thermal stability profile in the presence of RITA. This approach has previously been established as a tool for characterising a drug's cellular target, and was successfully used with the compounds methotrexate and crizotinib (Huber et al., 2015). One potential candidate was described in a study that used transcriptomic profiling to

predict sensitivity to almost 500 compounds, which calculated a significant correlation between RITA sensitivity and SULT1A1 mRNA and protein expression (Rees et al., 2016). SULT1A1 is a member of the cytosolic sulphotransferase family that catalyses the sulphonation of hormones, neurotransmitters, and xenobiotics (Falany, 1997). Preliminary data using SULT1A1 siRNA suggest that depleting this enzyme reduces the RITA sensitivity of SETD2-CRISPR cells, although SULT1A1 knockdown by itself leads to a striking loss of viability particularly in SETD2-negative cells. Dr. Huber's lab is currently performing a proof-of-concept experiment using CETSA with Western blot instead of mass spectrometry to determine whether SULT1A1 is stabilised by RITA, as well as to ascertain the best conditions for performing CETSA-MS. If this experiment is successful, it is to be hoped that the CETSA-MS will provide a list of candidates whose relevance to RITA's mechanism of action will be tested by siRNA-mediated gene knockdowns.

# 7. Bibliography


Abraham, R.T. 2001. Cell cycle checkpoint signaling through the ATM and ATR kinases. *Genes & development*. 15:2177-2196.

Akkari, Y.M., R.L. Bateman, C.A. Reifsteck, S.B. Olson, and M. Grompe. 2000. DNA replication is required To elicit cellular responses to psoralen-induced DNA interstrand cross-links. *Molecular and cellular biology*. 20:8283-8289.

Albain, K.S., S.M. Nag, G. Calderillo-Ruiz, J.P. Jordaan, A.C. Llombart, A. Pluzanska, J. Rolski, A.S. Melemed, J.M. Reyes-Vidal, J.S. Sekhon, L. Simms, and J. O'Shaughnessy. 2008. Gemcitabine plus Paclitaxel versus Paclitaxel monotherapy in patients with metastatic breast cancer and prior anthracycline treatment. *Journal of clinical oncology : official journal of the American Society of Clinical Oncology*. 26:3950-3957.

Allfrey, V.G., R. Faulkner, and A.E. Mirsky. 1964. Acetylation and Methylation of Histones and Their Possible Role in the Regulation of Rna Synthesis. *Proceedings of the National Academy of Sciences of the United States of America*. 51:786-794.

Andersson, B.S., T. Sadeghi, M.J. Siciliano, R. Legerski, and D. Murray. 1996. Nucleotide excision repair genes as determinants of cellular sensitivity to cyclophosphamide analogs. *Cancer chemotherapy and pharmacology*. 38:406-416.

Andree, H.A., C.P. Reutelingsperger, R. Hauptmann, H.C. Hemker, W.T. Hermens, and G.M. Willems. 1990. Binding of vascular anticoagulant alpha (VAC alpha) to planar phospholipid bilayers. *The Journal of biological chemistry*. 265:4923-4928.

Atkins, M.B., and N.M. Tannir. 2018. Current and emerging therapies for first-line treatment of metastatic clear cell renal cell carcinoma. *Cancer Treat Rev*. 70:127-137.

Azatyan, A., G. Gallo-Oller, Y. Diao, G. Selivanova, J.I. Johnsen, and P.G. Zaphiropoulos. 2019. RITA downregulates Hedgehog-GLI in medulloblastoma and rhabdomyosarcoma via JNK-dependent but p53-independent mechanism. *Cancer letters*. 442:341-350.

Bailey, M.L., N.J. O'Neil, D.M. van Pel, D.A. Solomon, T. Waldman, and P. Hieter. 2014. Glioblastoma cells containing mutations in the cohesin component STAG2 are sensitive to PARP inhibition. *Molecular cancer therapeutics*. 13:724-732.

Baldwin, R.L., E. Nemeth, H. Tran, H. Shvartsman, I. Cass, S. Narod, and B.Y. Karlan. 2000. BRCA1 promoter region hypermethylation in ovarian carcinoma: a population-based study. *Cancer research*. 60:5329-5333.

Banin, S., L. Moyal, S. Shieh, Y. Taya, C.W. Anderson, L. Chessa, N.I. Smorodinsky, C. Prives, Y. Reiss, Y. Shiloh, and Y. Ziv. 1998. Enhanced phosphorylation of p53 by ATM in response to DNA damage. *Science*. 281:1674-1677.

Baumann, P., F.E. Benson, and S.C. West. 1996. Human Rad51 protein promotes ATP-dependent homologous pairing and strand transfer reactions in vitro. *Cell*. 87:757-766.

Beck, H., V. Nahse-Kumpf, M.S. Larsen, K.A. O'Hanlon, S. Patzke, C. Holmberg, J. Mejlvang, A. Groth, O. Nielsen, R.G. Syljuasen, and C.S. Sorensen. 2012. Cyclin-dependent kinase suppression by WEE1 kinase protects the genome through control of replication initiation and nucleotide consumption. *Molecular and cellular biology*. 32:4226-4236.

Bedford, M.T., and P.D. van Helden. 1987. Hypomethylation of DNA in pathological conditions of the human prostate. *Cancer research*. 47:5274-5276.

Behan, F.M., F. Iorio, G. Picco, E. Goncalves, C.M. Beaver, G. Migliardi, R. Santos, Y. Rao, F. Sassi, M. Pinnelli, R. Ansari, S. Harper, D.A. Jackson, R. McRae, R. Pooley, P. Wilkinson, D. van der Meer, D. Dow, C. Buser-Doepner, A. Bertotti, L. Trusolino, E.A. Stronach, J. Saez-Rodriguez, K. Yusa, and M.J. Garnett. 2019. Prioritization of cancer therapeutic targets using CRISPR-Cas9 screens. *Nature*. 568:511-516.

Bender, A., and J.R. Pringle. 1991. Use of a screen for synthetic lethal and multicopy suppressee mutants to identify two new genes involved in morphogenesis in Saccharomyces cerevisiae. *Molecular and cellular biology*. 11:1295-1305.

Beroud, C., and T. Soussi. 2003. The UMD-p53 database: new mutations and analysis tools. *Hum Mutat*. 21:176-181.

Bertino, E.M., and G.A. Otterson. 2011. Romidepsin: a novel histone deacetylase inhibitor for cancer. *Expert Opin Investig Drugs*. 20:1151-1158.

Bessho, T. 2003. Induction of DNA replication-mediated double strand breaks by psoralen DNA interstrand cross-links. *The Journal of biological chemistry*. 278:5250-5254.

Beucher, A., J. Birraux, L. Tchouandong, O. Barton, A. Shibata, S. Conrad, A.A. Goodarzi, A. Krempler, P.A. Jeggo, and M. Löbrich. 2009. ATM and Artemis promote homologous recombination of radiation-induced DNA double-strand breaks in G2. *The EMBO journal*. 28:3413-3427.

Bhalla, K., R. Nayak, and S. Grant. 1984. Isolation and characterization of a deoxycytidine kinase-deficient human promyelocytic leukemic cell line highly resistant to 1-beta-D- arabinofuranosylcytosine. *Cancer research*. 44:5029-5037.

Bhinder, B., and H. Djaballah. 2013. Systematic analysis of RNAi reports identifies dismal commonality at gene-level and reveals an unprecedented enrichment in pooled shRNA screens. *Comb Chem High Throughput Screen*. 16:665-681.

Bian, C., C. Xu, J. Ruan, K.K. Lee, T.L. Burke, W. Tempel, D. Barsyte, J. Li, M. Wu, B.O. Zhou, B.E. Fleharty, A. Paulson, A. Allali-Hassani, J.Q. Zhou, G. Mer, P.A. Grant, J.L. Workman, J. Zang, and J. Min. 2011. Sgf29 binds histone H3K4me2/3 and is required for SAGA complex recruitment and histone H3 acetylation. *The EMBO journal*. 30:2829-2842.

Bicaku, E., D.C. Marchion, M.L. Schmitt, and P.N. Munster. 2008. Selective inhibition of histone deacetylase 2 silences progesterone receptor-mediated signaling. *Cancer research*. 68:1513-1519.

Bitler, B.G., K.M. Aird, A. Garipov, H. Li, M. Amatangelo, A.V. Kossenkov, D.C. Schultz, Q. Liu, M. Shih Ie, J.R. Conejo-Garcia, D.W. Speicher, and R. Zhang.

2015. Synthetic lethality by targeting EZH2 methyltransferase activity in ARID1A-mutated cancers. *Nature medicine*. 21:231-238.

Blomberg, I., and I. Hoffmann. 1999. Ectopic expression of Cdc25A accelerates the G(1)/S transition and leads to premature activation of cyclin E- and cyclin A-dependent kinases. *Molecular and cellular biology*. 19:6183-6194.

Bogliolo, M., B. Schuster, C. Stoepker, B. Derkunt, Y. Su, A. Raams, J.P. Trujillo, J. Minguillon, M.J. Ramirez, R. Pujol, J.A. Casado, R. Banos, P. Rio, K. Knies, S. Zuniga, J. Benitez, J.A. Bueren, N.G. Jaspers, O.D. Scharer, J.P. de Winter, D. Schindler, and J. Surralles. 2013. Mutations in ERCC4, encoding the DNA-repair endonuclease XPF, cause Fanconi anemia. *Am J Hum Genet*. 92:800-806.

Brandsma, I., E.D.G. Fleuren, C.T. Williamson, and C.J. Lord. 2017. Directing the use of DDR kinase inhibitors in cancer treatment. *Expert Opin Investig Drugs*. 26:1341-1355.

Brenner, J.C., B. Ateeq, Y. Li, A.K. Yocum, Q. Cao, I.A. Asangani, S. Patel, X. Wang, H. Liang, J. Yu, N. Palanisamy, J. Siddiqui, W. Yan, X. Cao, R. Mehra, A. Sabolch, V. Basrur, R.J. Lonigro, J. Yang, S.A. Tomlins, C.A. Maher, K.S. Elenitoba-Johnson, M. Hussain, N.M. Navone, K.J. Pienta, S. Varambally, F.Y. Feng, and A.M. Chinnaiyan. 2011. Mechanistic rationale for inhibition of poly(ADP-ribose) polymerase in ETS gene fusion-positive prostate cancer. *Cancer cell*. 19:664-678.

Brenner, J.C., F.Y. Feng, S. Han, S. Patel, S.V. Goyal, L.M. Bou-Maroun, M. Liu, R. Lonigro, J.R. Prensner, S.A. Tomlins, and A.M. Chinnaiyan. 2012. PARP-1 inhibition as a targeted strategy to treat Ewing's sarcoma. *Cancer research*. 72:1608-1613.

Brookes, P., and P.D. Lawley. 1961. The reaction of mono- and di-functional alkylating agents with nucleic acids. *Biochem J*. 80:496-503.

Brunmeir, R., S. Lagger, and C. Seiser. 2009. Histone deacetylase HDAC1/HDAC2-controlled embryonic development and cell differentiation. *Int J Dev Biol*. 53:275-289.

Bryant, H.E., N. Schultz, H.D. Thomas, K.M. Parker, D. Flower, E. Lopez, S. Kyle, M. Meuth, N.J. Curtin, and T. Helleday. 2005. Specific killing of BRCA2-deficient tumours with inhibitors of poly(ADP-ribose) polymerase. *Nature*. 434:913-917.

Bunting, S.F., E. Callen, N. Wong, H.T. Chen, F. Polato, A. Gunn, A. Bothmer, N. Feldhahn, O. Fernandez-Capetillo, L. Cao, X. Xu, C.X. Deng, T. Finkel, M. Nussenzweig, J.M. Stark, and A. Nussenzweig. 2010. 53BP1 inhibits homologous recombination in Brca1-deficient cells by blocking resection of DNA breaks. *Cell*. 141:243-254.

Bunz, F., A. Dutriaux, C. Lengauer, T. Waldman, S. Zhou, J.P. Brown, J.M. Sedivy, K.W. Kinzler, and B. Vogelstein. 1998. Requirement for p53 and p21 to sustain G2 arrest after DNA damage. *Science*. 282:1497-1501.

Burmakin, M., Y. Shi, E. Hedstrom, P. Kogner, and G. Selivanova. 2013. Dual targeting of wild-type and mutant p53 by small molecule RITA results in the inhibition of N-Myc and key survival oncogenes and kills neuroblastoma cells in

vivo and in vitro. *Clinical cancer research : an official journal of the American Association for Cancer Research*. 19:5092-5103.

Caldecott, K.W. 2008. Single-strand break repair and genetic disease. *Nat Rev Genet*. 9:619-631.

Cao, R., L. Wang, H. Wang, L. Xia, H. Erdjument-Bromage, P. Tempst, R.S. Jones, and Y. Zhang. 2002. Role of histone H3 lysine 27 methylation in Polycomb-group silencing. *Science*. 298:1039-1043.

Carrassa, L., R. Chila, M. Lupi, F. Ricci, C. Celenza, M. Mazzoletti, M. Broggini, and G. Damia. 2012. Combined inhibition of Chk1 and Wee1: in vitro synergistic effect translates to tumor growth inhibition in vivo. *Cell Cycle*. 11:2507-2517.

Carrozza, M.J., B. Li, L. Florens, T. Suganuma, S.K. Swanson, K.K. Lee, W.J. Shia, S. Anderson, J. Yates, M.P. Washburn, and J.L. Workman. 2005. Histone H3 methylation by Set2 directs deacetylation of coding regions by Rpd3S to suppress spurious intragenic transcription. *Cell*. 123:581-592.

Carvalho, S., A.C. Raposo, F.B. Martins, A.R. Grosso, S.C. Sridhara, J. Rino, M. Carmo-Fonseca, and S.F. de Almeida. 2013. Histone methyltransferase SETD2 coordinates FACT recruitment with nucleosome dynamics during transcription. *Nucleic acids research*. 41:2881-2893.

Carvalho, S., A.C. Vitor, S.C. Sridhara, F.B. Martins, A.C. Raposo, J.M. Desterro, J. Ferreira, and S.F. de Almeida. 2014. SETD2 is required for DNA double-strand break repair and activation of the p53-mediated checkpoint. *Elife*. 3:e02482.

Chabes, A.L., S. Bjorklund, and L. Thelander. 2004. S Phase-specific transcription of the mouse ribonucleotide reductase R2 gene requires both a proximal repressive E2F-binding site and an upstream promoter activating region. *The Journal of biological chemistry*. 279:10796-10807.

Chan, D.A., and A.J. Giaccia. 2011. Harnessing synthetic lethal interactions in anticancer drug discovery. *Nature reviews. Drug discovery*. 10:351-364.

Chen, J. 2016. The Cell-Cycle Arrest and Apoptotic Functions of p53 in Tumor Initiation and Progression. *Cold Spring Harb Perspect Med*. 6:a026104.

Chen, L., V. Marechal, J. Moreau, A.J. Levine, and J. Chen. 1997. Proteolytic cleavage of the mdm2 oncoprotein during apoptosis. *The Journal of biological chemistry*. 272:22966-22973.

Cheng, G., Y. Shi, S.J. Sturla, J.R. Jalas, E.J. McIntee, P.W. Villalta, M. Wang, and S.S. Hecht. 2003. Reactions of formaldehyde plus acetaldehyde with deoxyguanosine and DNA: formation of cyclic deoxyguanosine adducts and formaldehyde cross-links. *Chem Res Toxicol*. 16:145-152.

Cheung, H.W., G.S. Cowley, B.A. Weir, J.S. Boehm, S. Rusin, J.A. Scott, A. East, L.D. Ali, P.H. Lizotte, T.C. Wong, G. Jiang, J. Hsiao, C.H. Mermel, G. Getz, J. Barretina, S. Gopal, P. Tamayo, J. Gould, A. Tsherniak, N. Stransky, B. Luo, Y. Ren, R. Drapkin, S.N. Bhatia, J.P. Mesirov, L.A. Garraway, M. Meyerson, E.S. Lander, D.E. Root, and W.C. Hahn. 2011. Systematic investigation of genetic vulnerabilities across cancer cell lines reveals lineage-specific dependencies in ovarian cancer. *Proceedings of the National Academy of Sciences of the United States of America*. 108:12372-12377.

Chila, R., A. Basana, M. Lupi, F. Guffanti, E. Gaudio, A. Rinaldi, L. Cascione, V. Restelli, C. Tarantelli, F. Bertoni, G. Damia, and L. Carrassa. 2015. Combined inhibition of Chk1 and Wee1 as a new therapeutic strategy for mantle cell lymphoma. *Oncotarget*. 6:3394-3408.

Chou, T.C. 2006. Theoretical basis, experimental design, and computerized simulation of synergism and antagonism in drug combination studies. *Pharmacol Rev*. 58:621-681.

Cleaver, J.E. 1968. Defective repair replication of DNA in xeroderma pigmentosum. *Nature*. 218:652-656.

ClinicalTrials.gov. Vol. 2019. Bethesda (MD): National Library of Medicine (US).

ClinicalTrials.gov. Vol. 2019. Bethesda (MD): National Library of Medicine (US).

Coiffier, B., E. Lepage, J. Briere, R. Herbrecht, H. Tilly, R. Bouabdallah, P. Morel, E. Van Den Neste, G. Salles, P. Gaulard, F. Reyes, P. Lederlin, and C. Gisselbrecht. 2002. CHOP chemotherapy plus rituximab compared with CHOP alone in elderly patients with diffuse large-B-cell lymphoma. *The New England journal of medicine*. 346:235-242.

Coller, H.A., L. Sang, and J.M. Roberts. 2006. A new description of cellular quiescence. *PLoS Biol*. 4:e83.

Cui, H., P. Onyango, S. Brandenburg, Y. Wu, C.L. Hsieh, and A.P. Feinberg. 2002. Loss of imprinting in colorectal cancer linked to hypomethylation of H19 and IGF2. *Cancer research*. 62:6442-6446.

D'Angiolella, V., V. Donato, F.M. Forrester, Y.T. Jeong, C. Pellacani, Y. Kudo, A. Saraf, L. Florens, M.P. Washburn, and M. Pagano. 2012. Cyclin F-mediated degradation of ribonucleotide reductase M2 controls genome integrity and DNA repair. *Cell*. 149:1023-1034.

Dalgliesh, G.L., K. Furge, C. Greenman, L. Chen, G. Bignell, A. Butler, H. Davies, S. Edkins, C. Hardy, C. Latimer, J. Teague, J. Andrews, S. Barthorpe, D. Beare, G. Buck, P.J. Campbell, S. Forbes, M. Jia, D. Jones, H. Knott, C.Y. Kok, K.W. Lau, C. Leroy, M.L. Lin, D.J. McBride, M. Maddison, S. Maguire, K. McLay, A. Menzies, T. Mironenko, L. Mulderrig, L. Mudie, S. O'Meara, E. Pleasance, A. Rajasingham, R. Shepherd, R. Smith, L. Stebbings, P. Stephens, G. Tang, P.S. Tarpey, K. Turrell, K.J. Dykema, S.K. Khoo, D. Petillo, B. Wondergem, J. Anema, R.J. Kahnoski, B.T. Teh, M.R. Stratton, and P.A. Futreal. 2010. Systematic sequencing of renal carcinoma reveals inactivation of histone modifying genes. *Nature*. 463:360-363.

Damia, G., L. Imperatori, M. Stefanini, and M. D'Incalci. 1996. Sensitivity of CHO mutant cell lines with specific defects in nucleotide excision repair to different anti-cancer agents. *Int J Cancer*. 66:779-783.

Daver, N., R.F. Schlenk, N.H. Russell, and M.J. Levis. 2019. Targeting FLT3 mutations in AML: review of current knowledge and evidence. *Leukemia*. 33:299-312.

Deans, A.J., and S.C. West. 2011. DNA interstrand crosslink repair and cancer. *Nature reviews. Cancer*. 11:467-480.

DeGregori, J., T. Kowalik, and J.R. Nevins. 1995. Cellular targets for activation by the E2F1 transcription factor include DNA synthesis- and G1/S-regulatory genes. *Molecular and cellular biology*. 15:4215-4224.

Devaux, P.F. 1991. Static and dynamic lipid asymmetry in cell membranes. *Biochemistry*. 30:1163-1173.

Devita, V.T., Jr., A.A. Serpick, and P.P. Carbone. 1970. Combination chemotherapy in the treatment of advanced Hodgkin's disease. *Ann Intern Med*. 73:881-895.

Dillon, S.C., X. Zhang, R.C. Trievel, and X. Cheng. 2005. The SET-domain protein superfamily: protein lysine methyltransferases. *Genome Biol*. 6:227.

Ding, Q., Z. Zhang, J.J. Liu, N. Jiang, J. Zhang, T.M. Ross, X.J. Chu, D. Bartkovitz, F. Podlaski, C. Janson, C. Tovar, Z.M. Filipovic, B. Higgins, K. Glenn, K. Packman, L.T. Vassilev, and B. Graves. 2013. Discovery of RG7388, a potent and selective p53-MDM2 inhibitor in clinical development. *J Med Chem*. 56:5979-5983.

Dixon, S.J., B.J. Andrews, and C. Boone. 2009. Exploring the conservation of synthetic lethal genetic interaction networks. *Commun Integr Biol*. 2:78-81.

Dolma, S., S.L. Lessnick, W.C. Hahn, and B.R. Stockwell. 2003. Identification of genotype-selective antitumor agents using synthetic lethal chemical screening in engineered human tumor cells. *Cancer cell*. 3:285-296.

Dornan, D., and T.R. Hupp. 2001. Inhibition of p53-dependent transcription by BOX-I phospho-peptide mimetics that bind to p300. *EMBO Rep*. 2:139-144.

Drake, J.W., B. Charlesworth, D. Charlesworth, and J.F. Crow. 1998. Rates of spontaneous mutation. *Genetics*. 148:1667-1686.

Druker, B.J. 2002. Perspectives on the development of a molecularly targeted agent. *Cancer cell*. 1:31-36.

Druker, B.J., M. Talpaz, D.J. Resta, B. Peng, E. Buchdunger, J.M. Ford, N.B. Lydon, H. Kantarjian, R. Capdeville, S. Ohno-Jones, and C.L. Sawyers. 2001. Efficacy and safety of a specific inhibitor of the BCR-ABL tyrosine kinase in chronic myeloid leukemia. *The New England journal of medicine*. 344:1031-1037.

Dunn, J.M., R.A. Phillips, A.J. Becker, and B.L. Gallie. 1988. Identification of germline and somatic mutations affecting the retinoblastoma gene. *Science*. 241:1797-1800.

Duns, G., R.M. Hofstra, J.G. Sietzema, H. Hollema, I. van Duivenbode, A. Kuik, C. Giezen, O. Jan, J.J. Bergsma, H. Bijnen, P. van der Vlies, E. van den Berg, and K. Kok. 2012. Targeted exome sequencing in clear cell renal cell carcinoma tumors suggests aberrant chromatin regulation as a crucial step in ccRCC development. *Hum Mutat*. 33:1059-1062.

Edmunds, J.W., L.C. Mahadevan, and A.L. Clayton. 2008. Dynamic histone H3 methylation during gene induction: HYPB/Setd2 mediates all H3K36 trimethylation. *The EMBO journal*. 27:406-420.

Engstrom, Y., S. Eriksson, I. Jildevik, S. Skog, L. Thelander, and B. Tribukait. 1985. Cell cycle-dependent expression of mammalian ribonucleotide reductase. Differential regulation of the two subunits. *The Journal of biological chemistry*. 260:9114-9116.

Erhardt, P., K.J. Tomaselli, and G.M. Cooper. 1997. Identification of the MDM2 oncoprotein as a substrate for CPP32-like apoptotic proteases. *The Journal of biological chemistry*. 272:15049-15052.

Evans, T., E.T. Rosenthal, J. Youngblom, D. Distel, and T. Hunt. 1983. Cyclin: a protein specified by maternal mRNA in sea urchin eggs that is destroyed at each cleavage division. *Cell*. 33:389-396.

Faber, P.W., G.T. Barnes, J. Srinidhi, J. Chen, J.F. Gusella, and M.E. MacDonald. 1998. Huntingtin interacts with a family of WW domain proteins. *Hum Mol Genet*. 7:1463-1474.

Fadok, V.A., D.R. Voelker, P.A. Campbell, J.J. Cohen, D.L. Bratton, and P.M. Henson. 1992. Exposure of phosphatidylserine on the surface of apoptotic lymphocytes triggers specific recognition and removal by macrophages. *J Immunol*. 148:2207-2216.

Fairman, J.W., S.R. Wijerathna, M.F. Ahmad, H. Xu, R. Nakano, S. Jha, J. Prendergast, R.M. Welin, S. Flodin, A. Roos, P. Nordlund, Z. Li, T. Walz, and C.G. Dealwis. 2011. Structural basis for allosteric regulation of human ribonucleotide reductase by nucleotide-induced oligomerization. *Nature structural & molecular biology*. 18:316-322.

Falany, C.N. 1997. Sulfation and sulfotransferases. Introduction: changing view of sulfation and the cytosolic sulfotransferases. *FASEB J*. 11:1-2.

Falkenberg, K.J., and R.W. Johnstone. 2014. Histone deacetylases and their inhibitors in cancer, neurological diseases and immune disorders. *Nature reviews. Drug discovery*. 13:673-691.

Fanconi, G. 1967. Familial constitutional panmyelocytopathy, Fanconi's anemia (F.A.). I. Clinical aspects. *Semin Hematol*. 4:233-240.

Farber, S., and L.K. Diamond. 1948. Temporary remissions in acute leukemia in children produced by folic acid antagonist, 4-aminopteroyl-glutamic acid. *The New England journal of medicine*. 238:787-793.

Farmer, H., N. McCabe, C.J. Lord, A.N. Tutt, D.A. Johnson, T.B. Richardson, M. Santarosa, K.J. Dillon, I. Hickson, C. Knights, N.M. Martin, S.P. Jackson, G.C. Smith, and A. Ashworth. 2005. Targeting the DNA repair defect in BRCA mutant cells as a therapeutic strategy. *Nature*. 434:917-921.

Ferrari, A., C. Papayannidis, C. Baldazzi, I. Iacobucci, S. Paolini, A. Padella, V. Guadagnuolo, M. Perricone, V. Robustelli, C. Venturi, M.C. Abbenante, S. Parisi, C. Sartor, F. Volpato, N. Testoni, G. Simonetti, E. Ottaviani, and G. Martinelli. 2014. Leukemia Associated TP53 Mutations in AML Patients ARE Strongly Associated with Complex Karyotype and Poor Outcome. *Blood*. 124:2379-2379.

Fisher, B., R.G. Ravdin, R.K. Ausman, N.H. Slack, G.E. Moore, and R.J. Noer. 1968. Surgical adjuvant chemotherapy in cancer of the breast: results of a decade of cooperative investigation. *Ann Surg*. 168:337-356.

Flemington, E.K., S.H. Speck, and W.G. Kaelin, Jr. 1993. E2F-1-mediated transactivation is inhibited by complex formation with the retinoblastoma

susceptibility gene product. *Proceedings of the National Academy of Sciences of the United States of America*. 90:6914-6918.

Fong, P.C., D.S. Boss, T.A. Yap, A. Tutt, P. Wu, M. Mergui-Roelvink, P. Mortimer, H. Swaisland, A. Lau, M.J. O'Connor, A. Ashworth, J. Carmichael, S.B. Kaye, J.H. Schellens, and J.S. de Bono. 2009. Inhibition of poly(ADP-ribose) polymerase in tumors from BRCA mutation carriers. *The New England journal of medicine*. 361:123-134.

Fontebasso, A.M., J. Schwartzentruber, D.A. Khuong-Quang, X.Y. Liu, D. Sturm, A. Korshunov, D.T. Jones, H. Witt, M. Kool, S. Albrecht, A. Fleming, D. Hadjadj, S. Busche, P. Lepage, A. Montpetit, A. Staffa, N. Gerges, M. Zakrzewska, K. Zakrzewski, P.P. Liberski, P. Hauser, M. Garami, A. Klekner, L. Bognar, G. Zadeh, D. Faury, S.M. Pfister, N. Jabado, and J. Majewski. 2013. Mutations in SETD2 and genes affecting histone H3K36 methylation target hemispheric high-grade gliomas. *Acta neuropathologica*. 125:659-669.

Foster, B.A., H.A. Coffey, M.J. Morin, and F. Rastinejad. 1999. Pharmacological rescue of mutant p53 conformation and function. *Science*. 286:2507-2510.

Fraga, M.F., E. Ballestar, A. Villar-Garea, M. Boix-Chornet, J. Espada, G. Schotta, T. Bonaldi, C. Haydon, S. Ropero, K. Petrie, N.G. Iyer, A. Perez-Rosado, E. Calvo, J.A. Lopez, A. Cano, M.J. Calasanz, D. Colomer, M.A. Piris, N. Ahn, A. Imhof, C. Caldas, T. Jenuwein, and M. Esteller. 2005. Loss of acetylation at Lys16 and trimethylation at Lys20 of histone H4 is a common hallmark of human cancer. *Nature genetics*. 37:391-400.

Franken, N.A., H.M. Rodermond, J. Stap, J. Haveman, and C. van Bree. 2006. Clonogenic assay of cells in vitro. *Nat Protoc*. 1:2315-2319.

Friedlander, P., Y. Legros, T. Soussi, and C. Prives. 1996. Regulation of mutant p53 temperature-sensitive DNA binding. *The Journal of biological chemistry*. 271:25468-25478.

Fritsche, P., B. Seidler, S. Schuler, A. Schnieke, M. Gottlicher, R.M. Schmid, D. Saur, and G. Schneider. 2009. HDAC2 mediates therapeutic resistance of pancreatic cancer cells via the BH3-only protein NOXA. *Gut*. 58:1399-1409.

Furumai, R., A. Matsuyama, N. Kobashi, K.H. Lee, M. Nishiyama, H. Nakajima, A. Tanaka, Y. Komatsu, N. Nishino, M. Yoshida, and S. Horinouchi. 2002. FK228 (depsipeptide) as a natural prodrug that inhibits class I histone deacetylases. *Cancer research*. 62:4916-4921.

Gartel, A.L., and A.L. Tyner. 1999. Transcriptional regulation of the p21((WAF1/CIP1)) gene. *Exp Cell Res*. 246:280-289.

Gerber, M., and A. Shilatifard. 2003. Transcriptional elongation by RNA polymerase II and histone methylation. *The Journal of biological chemistry*. 278:26303-26306.

Gilman, A., and F.S. Philips. 1946. The biological actions and therapeutic applications of the B-chloroethyl amines and sulfides. *Science*. 103:409-415.

Giunta, S., R. Belotserkovskaya, and S.P. Jackson. 2010. DNA damage signaling in response to double-strand breaks during mitosis. *The Journal of cell biology*. 190:197-207.

Goder, A., C. Emmerich, T. Nikolova, N. Kiweler, M. Schreiber, T. Kuhl, D. Imhof, M. Christmann, T. Heinzel, G. Schneider, and O.H. Kramer. 2018. HDAC1 and HDAC2 integrate checkpoint kinase phosphorylation and cell fate through the phosphatase-2A subunit PR130. *Nat Commun*. 9:764.

Goodman, L.S., M.M. Wintrobe, and et al. 1946. Nitrogen mustard therapy; use of methyl-bis (beta-chloroethyl) amine hydrochloride and tris (beta-chloroethyl) amine hydrochloride for Hodgkin's disease, lymphosarcoma, leukemia and certain allied and miscellaneous disorders. *J Am Med Assoc*. 132:126-132.

Gorre, M.E., M. Mohammed, K. Ellwood, N. Hsu, R. Paquette, P.N. Rao, and C.L. Sawyers. 2001. Clinical resistance to STI-571 cancer therapy caused by BCR-ABL gene mutation or amplification. *Science*. 293:876-880.

Green, C.L., E.L. Loechler, K.W. Fowler, and J.M. Essigmann. 1984. Construction and characterization of extrachromosomal probes for mutagenesis by carcinogens: site-specific incorporation of O6-methylguanine into viral and plasmid genomes. *Proceedings of the National Academy of Sciences of the United States of America*. 81:13-17.

Gross, A., J.M. McDonnell, and S.J. Korsmeyer. 1999. BCL-2 family members and the mitochondria in apoptosis. *Genes & development*. 13:1899-1911.

Hainsworth, J.D., J.R. Infante, D.R. Spigel, E.R. Arrowsmith, R.V. Boccia, and H.A. Burris. 2011. A phase II trial of panobinostat, a histone deacetylase inhibitor, in the treatment of patients with refractory metastatic renal cell carcinoma. *Cancer Invest*. 29:451-455.

Hakimi, A.A., I. Ostrovnaya, B. Reva, N. Schultz, Y.B. Chen, M. Gonen, H. Liu, S. Takeda, M.H. Voss, S.K. Tickoo, V.E. Reuter, P. Russo, E.H. Cheng, C. Sander, R.J. Motzer, and J.J. Hsieh. 2013. Adverse outcomes in clear cell renal cell carcinoma with mutations of 3p21 epigenetic regulators BAP1 and SETD2: a report by MSKCC and the KIRC TCGA research network. *Clinical cancer research : an official journal of the American Association for Cancer Research*. 19:3259-3267.

Hanahan, D., and R.A. Weinberg. 2000. The hallmarks of cancer. *Cell*. 100:57-70.

Hanahan, D., and R.A. Weinberg. 2011. Hallmarks of cancer: the next generation. *Cell*. 144:646-674.

Harper, J.W., S.J. Elledge, K. Keyomarsi, B. Dynlacht, L.H. Tsai, P. Zhang, S. Dobrowolski, C. Bai, L. Connell-Crowley, E. Swindell, and et al. 1995. Inhibition of cyclin-dependent kinases by p21. *Mol Biol Cell*. 6:387-400.

Hart, T., M. Chandrashekhar, M. Aregger, Z. Steinhart, K.R. Brown, G. MacLeod, M. Mis, M. Zimmermann, A. Fradet-Turcotte, S. Sun, P. Mero, P. Dirks, S. Sidhu, F.P. Roth, O.S. Rissland, D. Durocher, S. Angers, and J. Moffat. 2015. High-Resolution CRISPR Screens Reveal Fitness Genes and Genotype-Specific Cancer Liabilities. *Cell*. 163:1515-1526.

Hartman, J.L.t., B. Garvik, and L. Hartwell. 2001. Principles for the buffering of genetic variation. *Science*. 291:1001-1004.

Hartwell, L.H., P. Szankasi, C.J. Roberts, A.W. Murray, and S.H. Friend. 1997. Integrating genetic approaches into the discovery of anticancer drugs. *Science*. 278:1064-1068.

Hartwell, L.H., and T.A. Weinert. 1989. Checkpoints: controls that ensure the order of cell cycle events. *Science*. 246:629-634.

Haupt, Y., R. Maya, A. Kazaz, and M. Oren. 1997. Mdm2 promotes the rapid degradation of p53. *Nature*. 387:296-299.

Hennessy, K.M., A. Lee, E. Chen, and D. Botstein. 1991. A group of interacting yeast DNA replication genes. *Genes & development*. 5:958-969.

Ho, T.H., I.Y. Park, H. Zhao, P. Tong, M.D. Champion, H. Yan, F.A. Monzon, A. Hoang, P. Tamboli, A.S. Parker, R.W. Joseph, W. Qiao, K. Dykema, N.M. Tannir, E.P. Castle, R. Nunez-Nateras, B.T. Teh, J. Wang, C.L. Walker, M.C. Hung, and E. Jonasch. 2016. High-resolution profiling of histone h3 lysine 36 trimethylation in metastatic renal cell carcinoma. *Oncogene*. 35:1565-1574.

Holliday, R., and J.E. Pugh. 1975. DNA modification mechanisms and gene activity during development. *Science*. 187:226-232.

Horlbeck, M.A., L.B. Witkowsky, B. Guglielmi, J.M. Replogle, L.A. Gilbert, J.E. Villalta, S.E. Torigoe, R. Tjian, and J.S. Weissman. 2016. Nucleosomes impede Cas9 access to DNA in vivo and in vitro. *Elife*. 5.

Hotchkiss, R.D. 1948. The quantitative separation of purines, pyrimidines, and nucleosides by paper chromatography. *The Journal of biological chemistry*. 175:315-332.

Hoy, C.A., L.H. Thompson, C.L. Mooney, and E.P. Salazar. 1985. Defective DNA cross-link removal in Chinese hamster cell mutants hypersensitive to bifunctional alkylating agents. *Cancer research*. 45:1737-1743.

Huang, J., M.S. Huen, H. Kim, C.C. Leung, J.N. Glover, X. Yu, and J. Chen. 2009. RAD18 transmits DNA damage signalling to elicit homologous recombination repair. *Nature cell biology*. 11:592-603.

Huber, K.V., K.M. Olek, A.C. Muller, C.S. Tan, K.L. Bennett, J. Colinge, and G. Superti-Furga. 2015. Proteome-wide drug and metabolite interaction mapping by thermal-stability profiling. *Nat Methods*. 12:1055-1057.

Huen, M.S., S.M. Sy, and J. Chen. 2010. BRCA1 and its toolbox for the maintenance of genome integrity. *Nature reviews. Molecular cell biology*. 11:138-148.

Hussain, S.P., and C.C. Harris. 1998. Molecular epidemiology of human cancer: contribution of mutation spectra studies of tumor suppressor genes. *Cancer research*. 58:4023-4037.

Issaeva, N., P. Bozko, M. Enge, M. Protopopova, L.G. Verhoef, M. Masucci, A. Pramanik, and G. Selivanova. 2004. Small molecule RITA binds to p53, blocks p53-HDM-2 interaction and activates p53 function in tumors. *Nature medicine*. 10:1321-1328.

Ito, A., Y. Kawaguchi, C.H. Lai, J.J. Kovacs, Y. Higashimoto, E. Appella, and T.P. Yao. 2002. MDM2-HDAC1-mediated deacetylation of p53 is required for its degradation. *The EMBO journal*. 21:6236-6245.

Jackson, A.L., S.R. Bartz, J. Schelter, S.V. Kobayashi, J. Burchard, M. Mao, B. Li, G. Cavet, and P.S. Linsley. 2003. Expression profiling reveals off-target gene regulation by RNAi. *Nature biotechnology*. 21:635-637.

Joshi, A.A., and K. Struhl. 2005. Eaf3 chromodomain interaction with methylated H3-K36 links histone deacetylation to Pol II elongation. *Molecular cell*. 20:971-978.

Jurkin, J., G. Zupkovitz, S. Lagger, R. Grausenburger, A. Hagelkruys, L. Kenner, and C. Seiser. 2011. Distinct and redundant functions of histone deacetylases HDAC1 and HDAC2 in proliferation and tumorigenesis. *Cell Cycle*. 10:406-412.

Kadoch, C., D.C. Hargreaves, C. Hodges, L. Elias, L. Ho, J. Ranish, and G.R. Crabtree. 2013. Proteomic and bioinformatic analysis of mammalian SWI/SNF complexes identifies extensive roles in human malignancy. *Nature genetics*. 45:592-601.

Kaelin, W.G., Jr. 2005. The concept of synthetic lethality in the context of anticancer therapy. *Nature reviews. Cancer*. 5:689-698.

Kashiyama, K., Y. Nakazawa, D.T. Pilz, C. Guo, M. Shimada, K. Sasaki, H. Fawcett, J.F. Wing, S.O. Lewin, L. Carr, T.S. Li, K. Yoshiura, A. Utani, A. Hirano, S. Yamashita, D. Greenblatt, T. Nardo, M. Stefanini, D. McGibbon, R. Sarkany, H. Fassihi, Y. Takahashi, Y. Nagayama, N. Mitsutake, A.R. Lehmann, and T. Ogi. 2013. Malfunction of nuclease ERCC1-XPF results in diverse clinical manifestations and causes Cockayne syndrome, xeroderma pigmentosum, and Fanconi anemia. *Am J Hum Genet*. 92:807-819.

Kastan, M.B., and J. Bartek. 2004. Cell-cycle checkpoints and cancer. *Nature*. 432:316-323.

Kastan, M.B., O. Onyekwere, D. Sidransky, B. Vogelstein, and R.W. Craig. 1991. Participation of p53 protein in the cellular response to DNA damage. *Cancer research*. 51:6304-6311.

Katsuno, Y., A. Suzuki, K. Sugimura, K. Okumura, D.H. Zineldeen, M. Shimada, H. Niida, T. Mizuno, F. Hanaoka, and M. Nakanishi. 2009. Cyclin A-Cdk1 regulates the origin firing program in mammalian cells. *Proceedings of the National Academy of Sciences of the United States of America*. 106:3184-3189.

Kim, K.H., W. Kim, T.P. Howard, F. Vazquez, A. Tsherniak, J.N. Wu, W. Wang, J.R. Haswell, L.D. Walensky, W.C. Hahn, S.H. Orkin, and C.W. Roberts. 2015. SWI/SNF-mutant cancers depend on catalytic and non-catalytic activity of EZH2. *Nature medicine*. 21:1491-1496.

Kizer, K.O., H.P. Phatnani, Y. Shibata, H. Hall, A.L. Greenleaf, and B.D. Strahl. 2005. A novel domain in Set2 mediates RNA polymerase II interaction and couples histone H3 K36 methylation with transcript elongation. *Molecular and cellular biology*. 25:3305-3316.

Knudsen, E.S., and J.Y. Wang. 1997. Dual mechanisms for the inhibition of E2F binding to RB by cyclin-dependent kinase-mediated RB phosphorylation. *Molecular and cellular biology*. 17:5771-5783.

Knudson, A.G., Jr. 1971. Mutation and cancer: statistical study of retinoblastoma. *Proceedings of the National Academy of Sciences of the United States of America*. 68:820-823.

Knutson, S.K., N.M. Warholic, T.J. Wigle, C.R. Klaus, C.J. Allain, A. Raimondi, M. Porter Scott, R. Chesworth, M.P. Moyer, R.A. Copeland, V.M. Richon, R.M. Pollock, K.W. Kuntz, and H. Keilhack. 2013. Durable tumor regression in genetically altered malignant rhabdoid tumors by inhibition of methyltransferase EZH2. *Proceedings of the National Academy of Sciences of the United States of America*. 110:7922-7927.

Kornberg, R.D. 1974. Chromatin Structure: A Repeating Unit of Histones and DNA. *Science*. 184:868-871.

Krogan, N.J., M. Kim, A. Tong, A. Golshani, G. Cagney, V. Canadien, D.P. Richards, B.K. Beattie, A. Emili, C. Boone, A. Shilatifard, S. Buratowski, and J. Greenblatt. 2003. Methylation of histone H3 by Set2 in Saccharomyces cerevisiae is linked to transcriptional elongation by RNA polymerase II. *Molecular and cellular biology*. 23:4207-4218.

Krokan, H.E., and M. Bjoras. 2013. Base excision repair. *Cold Spring Harb Perspect Biol*. 5:a012583.

Kroll, E.S., K.M. Hyland, P. Hieter, and J.J. Li. 1996. Establishing genetic interactions by a synthetic dosage lethality phenotype. *Genetics*. 143:95-102.

Kubbutat, M.H., S.N. Jones, and K.H. Vousden. 1997. Regulation of p53 stability by Mdm2. *Nature*. 387:299-303.

Kunkel, T.A. 2004. DNA replication fidelity. *The Journal of biological chemistry*. 279:16895-16898.

Kunkel, T.A., and D.A. Erie. 2015. Eukaryotic Mismatch Repair in Relation to DNA Replication. *Annu Rev Genet*. 49:291-313.

Kurashima, K., T. Sekimoto, T. Oda, T. Kawabata, F. Hanaoka, and T. Yamashita. 2018. Poleta, a Y-family translesion synthesis polymerase, promotes cellular tolerance of Myc-induced replication stress. *J Cell Sci*. 131.

Kuscu, C., S. Arslan, R. Singh, J. Thorpe, and M. Adli. 2014. Genome-wide analysis reveals characteristics of off-target sites bound by the Cas9 endonuclease. *Nature biotechnology*. 32:677-683.

Kuzmichev, A., K. Nishioka, H. Erdjument-Bromage, P. Tempst, and D. Reinberg. 2002. Histone methyltransferase activity associated with a human multiprotein complex containing the Enhancer of Zeste protein. *Genes & development*. 16:2893-2905.

Lagger, G., D. O'Carroll, M. Rembold, H. Khier, J. Tischler, G. Weitzer, B. Schuettengruber, C. Hauser, R. Brunmeir, T. Jenuwein, and C. Seiser. 2002. Essential function of histone deacetylase 1 in proliferation control and CDK inhibitor repression. *The EMBO journal*. 21:2672-2681.

Lakin, N.D., B.C. Hann, and S.P. Jackson. 1999. The ataxia-telangiectasia related protein ATR mediates DNA-dependent phosphorylation of p53. *Oncogene*. 18:3989-3995.

Lambert, P.F., F. Kashanchi, M.F. Radonovich, R. Shiekhattar, and J.N. Brady. 1998. Phosphorylation of p53 serine 15 increases interaction with CBP. *The Journal of biological chemistry*. 273:33048-33053.

Lang, T.T., M. Selner, J.D. Young, and C.E. Cass. 2001. Acquisition of human concentrative nucleoside transporter 2 (hcnt2) activity by gene transfer confers sensitivity to fluoropyrimidine nucleosides in drug-resistant leukemia cells. *Molecular pharmacology*. 60:1143-1152.

Leder, A., and P. Leder. 1975. Butyric acid, a potent inducer of erythroid differentiation in cultured erythroleukemic cells. *Cell*. 5:319-322.

Lee, D.H., S.S. Acharya, M. Kwon, P. Drane, Y. Guan, G. Adelmant, P. Kalev, J. Shah, D. Pellman, J.A. Marto, and D. Chowdhury. 2014. Dephosphorylation enables the recruitment of 53BP1 to double-strand DNA breaks. *Molecular cell*. 54:512-525.

Lee, D.Y., J.J. Hayes, D. Pruss, and A.P. Wolffe. 1993. A positive role for histone acetylation in transcription factor access to nucleosomal DNA. *Cell*. 72:73-84.

Lee, H.Z., V.E. Kwitkowski, P.L. Del Valle, M.S. Ricci, H. Saber, B.A. Habtemariam, J. Bullock, E. Bloomquist, Y. Li Shen, X.H. Chen, J. Brown, N. Mehrotra, S. Dorff, R. Charlab, R.C. Kane, E. Kaminskas, R. Justice, A.T. Farrell, and R. Pazdur. 2015. FDA Approval: Belinostat for the Treatment of Patients with Relapsed or Refractory Peripheral T-cell Lymphoma. *Clinical cancer research : an official journal of the American Association for Cancer Research*. 21:2666-2670.

Lees, J.A., K.J. Buchkovich, D.R. Marshak, C.W. Anderson, and E. Harlow. 1991. The retinoblastoma protein is phosphorylated on multiple sites by human cdc2. *The EMBO journal*. 10:4279-4290.

Li, B., L. Howe, S. Anderson, J.R. Yates, 3rd, and J.L. Workman. 2003. The Set2 histone methyltransferase functions through the phosphorylated carboxyl-terminal domain of RNA polymerase II. *The Journal of biological chemistry*. 278:8897-8903.

Li, D., S. Yea, G. Dolios, J.A. Martignetti, G. Narla, R. Wang, M.J. Walsh, and S.L. Friedman. 2005. Regulation of Kruppel-like factor 6 tumor suppressor activity by acetylation. *Cancer research*. 65:9216-9225.

Li, F., G. Mao, D. Tong, J. Huang, L. Gu, W. Yang, and G.M. Li. 2013. The histone mark H3K36me3 regulates human DNA mismatch repair through its interaction with MutSalpha. *Cell*. 153:590-600.

Li, J., D. Moazed, and S.P. Gygi. 2002. Association of the histone methyltransferase Set2 with RNA polymerase II plays a role in transcription elongation. *The Journal of biological chemistry*. 277:49383-49388.

Li, J., J. Pang, Y. Liu, J. Zhang, C. Zhang, G. Shen, and L. Song. 2018. Suppression of RRM2 inhibits cell proliferation, causes cell cycle arrest and promotes the apoptosis of human neuroblastoma cells and in human neuroblastoma RRM2 is suppressed following chemotherapy. *Oncol Rep*. 40:355-360.

Li, M.C., R. Hertz, and D.M. Bergenstal. 1958. Therapy of choriocarcinoma and related trophoblastic tumors with folic acid and purine antagonists. *The New England journal of medicine*. 259:66-74.

Licciardello, M.P., A. Ringler, P. Markt, F. Klepsch, C.H. Lardeau, S. Sdelci, E. Schirghuber, A.C. Muller, M. Caldera, A. Wagner, R. Herzog, T. Penz, M.

Schuster, B. Boidol, G. Durnberger, Y. Folkvaljon, P. Stattin, V. Ivanov, J. Colinge, C. Bock, K. Kratochwill, J. Menche, K.L. Bennett, and S. Kubicek. 2017. A combinatorial screen of the CLOUD uncovers a synergy targeting the androgen receptor. *Nature chemical biology*. 13:771-778.

Lin, C.H., S.Y. Hsieh, I.S. Sheen, W.C. Lee, T.C. Chen, W.C. Shyu, and Y.F. Liaw. 2001. Genome-wide hypomethylation in hepatocellular carcinogenesis. *Cancer research*. 61:4238-4243.

Lin, D., M.T. Shields, S.J. Ullrich, E. Appella, and W.E. Mercer. 1992. Growth arrest induced by wild-type p53 protein blocks cells prior to or near the restriction point in late G1 phase. *Proceedings of the National Academy of Sciences of the United States of America*. 89:9210-9214.

Lin, J., X. Jin, Y. Bu, D. Cao, N. Zhang, S. Li, Q. Sun, C. Tan, C. Gao, and Y. Jiang. 2012. Efficient synthesis of RITA and its analogues: derivation of analogues with improved antiproliferative activity via modulation of p53/miR-34a pathway. *Org Biomol Chem*. 10:9734-9746.

Loechler, E.L., C.L. Green, and J.M. Essigmann. 1984. In vivo mutagenesis by O6-methylguanine built into a unique site in a viral genome. *Proceedings of the National Academy of Sciences of the United States of America*. 81:6271-6275.

Lord, C.J., A.N. Tutt, and A. Ashworth. 2015. Synthetic lethality and cancer therapy: lessons learned from the development of PARP inhibitors. *Annu Rev Med*. 66:455-470.

Lowe, S.W., H.E. Ruley, T. Jacks, and D.E. Housman. 1993a. p53-dependent apoptosis modulates the cytotoxicity of anticancer agents. *Cell*. 74:957-967.

Lowe, S.W., E.M. Schmitt, S.W. Smith, B.A. Osborne, and T. Jacks. 1993b. p53 is required for radiation-induced apoptosis in mouse thymocytes. *Nature*. 362:847-849.

Luco, R.F., Q. Pan, K. Tominaga, B.J. Blencowe, O.M. Pereira-Smith, and T. Misteli. 2010. Regulation of alternative splicing by histone modifications. *Science*. 327:996-1000.

Luger, K., A.W. Mader, R.K. Richmond, D.F. Sargent, and T.J. Richmond. 1997. Crystal structure of the nucleosome core particle at 2.8 A resolution. *Nature*. 389:251-260.

Lukas, C., V. Savic, S. Bekker-Jensen, C. Doil, B. Neumann, R.S. Pedersen, M. Grofte, K.L. Chan, I.D. Hickson, J. Bartek, and J. Lukas. 2011. 53BP1 nuclear bodies form around DNA lesions generated by mitotic transmission of chromosomes under replication stress. *Nature cell biology*. 13:243-253.

Mackey, J.R., R.S. Mani, M. Selner, D. Mowles, J.D. Young, J.A. Belt, C.R. Crawford, and C.E. Cass. 1998. Functional nucleoside transporters are required for gemcitabine influx and manifestation of toxicity in cancer cell lines. *Cancer research*. 58:4349-4357.

Mailand, N., J. Falck, C. Lukas, R.G. Syljuasen, M. Welcker, J. Bartek, and J. Lukas. 2000. Rapid destruction of human Cdc25A in response to DNA damage. *Science*. 288:1425-1429.

Maki, C.G., J.M. Huibregtse, and P.M. Howley. 1996. In vivo ubiquitination and proteasome-mediated degradation of p53(1). *Cancer research*. 56:2649-2654.

Mann, B.S., J.R. Johnson, M.H. Cohen, R. Justice, and R. Pazdur. 2007. FDA approval summary: vorinostat for treatment of advanced primary cutaneous T-cell lymphoma. *Oncologist*. 12:1247-1252.

Marchion, D.C., E. Bicaku, J.G. Turner, M.L. Schmitt, D.R. Morelli, and P.N. Munster. 2009. HDAC2 regulates chromatin plasticity and enhances DNA vulnerability. *Molecular cancer therapeutics*. 8:794-801.

Marteijn, J.A., H. Lans, W. Vermeulen, and J.H. Hoeijmakers. 2014. Understanding nucleotide excision repair and its roles in cancer and ageing. *Nature reviews. Molecular cell biology*. 15:465-481.

Mata, J.F., J.M. Garcia-Manteiga, M.P. Lostao, S. Fernandez-Veledo, E. Guillen-Gomez, I.M. Larrayoz, J. Lloberas, F.J. Casado, and M. Pastor-Anglada. 2001. Role of the human concentrative nucleoside transporter (hCNT1) in the cytotoxic action of 5[Prime]-deoxy-5-fluorouridine, an active intermediate metabolite of capecitabine, a novel oral anticancer drug. *Molecular pharmacology*. 59:1542-1548.

Mazouzi, A., G. Velimezi, and J.I. Loizou. 2014. DNA replication stress: causes, resolution and disease. *Exp Cell Res*. 329:85-93.

McCabe, N., N.C. Turner, C.J. Lord, K. Kluzek, A. Bialkowska, S. Swift, S. Giavara, M.J. O'Connor, A.N. Tutt, M.Z. Zdzienicka, G.C. Smith, and A. Ashworth. 2006. Deficiency in the repair of DNA damage by homologous recombination and sensitivity to poly(ADP-ribose) polymerase inhibition. *Cancer research*. 66:8109-8115.

McHugh, P.J., W.R. Sones, and J.A. Hartley. 2000. Repair of intermediate structures produced at DNA interstrand cross-links in Saccharomyces cerevisiae. *Molecular and cellular biology*. 20:3425-3433.

McKinnon, P.J. 2012. ATM and the molecular pathogenesis of ataxia telangiectasia. *Annu Rev Pathol*. 7:303-321.

McLellan, J.L., N.J. O'Neil, I. Barrett, E. Ferree, D.M. van Pel, K. Ushey, P. Sipahimalani, J. Bryan, A.M. Rose, and P. Hieter. 2012. Synthetic lethality of cohesins with PARPs and replication fork mediators. *PLoS Genet*. 8:e1002574.

Mendes-Pereira, A.M., S.A. Martin, R. Brough, A. McCarthy, J.R. Taylor, J.S. Kim, T. Waldman, C.J. Lord, and A. Ashworth. 2009. Synthetic lethal targeting of PTEN mutant cells with PARP inhibitors. *EMBO Mol Med*. 1:315-322.

Merino, D., S.L. Khaw, S.P. Glaser, D.J. Anderson, L.D. Belmont, C. Wong, P. Yue, M. Robati, B. Phipson, W.D. Fairlie, E.F. Lee, K.J. Campbell, C.J. Vandenberg, S. Cory, A.W. Roberts, M.J. Ludlam, D.C. Huang, and P. Bouillet. 2012. Bcl-2, Bcl-x(L), and Bcl-w are not equivalent targets of ABT-737 and navitoclax (ABT-263) in lymphoid and leukemic cells. *Blood*. 119:5807-5816.

Minami, D., N. Takigawa, H. Takeda, M. Takata, N. Ochi, E. Ichihara, A. Hisamoto, K. Hotta, M. Tanimoto, and K. Kiura. 2013. Synergistic effect of olaparib with combination of cisplatin on PTEN-deficient lung cancer cells. *Mol Cancer Res*. 11:140-148.

Minotti, G., P. Menna, E. Salvatorelli, G. Cairo, and L. Gianni. 2004. Anthracyclines: molecular advances and pharmacologic developments in antitumor activity and cardiotoxicity. *Pharmacol Rev*. 56:185-229.

Mobaraki, R.N., M. Karimi, F. Alikarami, E. Farhadi, A. Amini, D. Bashash, M. Paridar, P. Kokhaei, M.R. Rezvani, A. Kazemi, and M. Safa. 2018. RITA induces apoptosis in p53-null K562 leukemia cells by inhibiting STAT5, Akt, and NF-kappaB signaling pathways. *Anticancer Drugs*. 29:847-853.

Montgomery, R.L., C.A. Davis, M.J. Potthoff, M. Haberland, J. Fielitz, X. Qi, J.A. Hill, J.A. Richardson, and E.N. Olson. 2007. Histone deacetylases 1 and 2 redundantly regulate cardiac morphogenesis, growth, and contractility. *Genes & development*. 21:1790-1802.

Montgomery, R.L., J. Hsieh, A.C. Barbosa, J.A. Richardson, and E.N. Olson. 2009. Histone deacetylases 1 and 2 control the progression of neural precursors to neurons during brain development. *Proceedings of the National Academy of Sciences of the United States of America*. 106:7876-7881.

Morgan, D.O. 1995. Principles of CDK regulation. *Nature*. 374:131-134.

Mounier, N., J. Briere, C. Gisselbrecht, J.F. Emile, P. Lederlin, C. Sebban, F. Berger, A. Bosly, P. Morel, H. Tilly, R. Bouabdallah, F. Reyes, P. Gaulard, and B. Coiffier. 2003. Rituximab plus CHOP (R-CHOP) overcomes bcl-2--associated resistance to chemotherapy in elderly patients with diffuse large B-cell lymphoma (DLBCL). *Blood*. 101:4279-4284.

Moxley, J.H., 3rd, V.T. De Vita, K. Brace, and E. Frei, 3rd. 1967. Intensive combination chemotherapy and X-irradiation in Hodgkin's disease. *Cancer research*. 27:1258-1263.

Moynahan, M.E., J.W. Chiu, B.H. Koller, and M. Jasin. 1999. Brca1 controls homology-directed DNA repair. *Molecular cell*. 4:511-518.

Munoz, D.M., P.J. Cassiani, L. Li, E. Billy, J.M. Korn, M.D. Jones, J. Golji, D.A. Ruddy, K. Yu, G. McAllister, A. DeWeck, D. Abramowski, J. Wan, M.D. Shirley, S.Y. Neshat, D. Rakiec, R. de Beaumont, O. Weber, A. Kauffmann, E.R. McDonald, 3rd, N. Keen, F. Hofmann, W.R. Sellers, T. Schmelzle, F. Stegmeier, and M.R. Schlabach. 2016. CRISPR Screens Provide a Comprehensive Assessment of Cancer Vulnerabilities but Generate False-Positive Hits for Highly Amplified Genomic Regions. *Cancer Discov*. 6:900-913.

Murata-Kamiya, N., and H. Kamiya. 2001. Methylglyoxal, an endogenous aldehyde, crosslinks DNA polymerase and the substrate DNA. *Nucleic acids research*. 29:3433-3438.

Mutskov, V., and G. Felsenfeld. 2004. Silencing of transgene transcription precedes methylation of promoter DNA and histone H3 lysine 9. *The EMBO journal*. 23:138-149.

Negrini, S., V.G. Gorgoulis, and T.D. Halazonetis. 2010. Genomic instability--an evolving hallmark of cancer. *Nature reviews. Molecular cell biology*. 11:220-228.

Newbold, A., J.M. Salmon, B.P. Martin, K. Stanley, and R.W. Johnstone. 2014. The role of p21(waf1/cip1) and p27(Kip1) in HDACi-mediated tumor cell death and

cell cycle arrest in the Emu-myc model of B-cell lymphoma. *Oncogene*. 33:5415-5423.

Newbold, R.F., and K. Mokbel. 2010. Evidence for a tumour suppressor function of SETD2 in human breast cancer: a new hypothesis. *Anticancer research*. 30:3309-3311.

Niedernhofer, L.J., A.S. Lalai, and J.H. Hoeijmakers. 2005. Fanconi anemia (cross)linked to DNA repair. *Cell*. 123:1191-1198.

Niedernhofer, L.J., H. Odijk, M. Budzowska, E. van Drunen, A. Maas, A.F. Theil, J. de Wit, N.G. Jaspers, H.B. Beverloo, J.H. Hoeijmakers, and R. Kanaar. 2004. The structure-specific endonuclease Ercc1-Xpf is required to resolve DNA interstrand cross-link-induced double-strand breaks. *Molecular and cellular biology*. 24:5776-5787.

Niedzwiedz, W., G. Mosedale, M. Johnson, C.Y. Ong, P. Pace, and K.J. Patel. 2004. The Fanconi anaemia gene FANCC promotes homologous recombination and error-prone DNA repair. *Molecular cell*. 15:607-620.

Nieminuszczy, J., R.A. Schwab, and W. Niedzwiedz. 2016. The DNA fibre technique - tracking helicases at work. *Methods*. 108:92-98.

Nieves-Neira, W., M.I. Rivera, G. Kohlhagen, M.L. Hursey, P. Pourquier, E.A. Sausville, and Y. Pommier. 1999. DNA protein cross-links produced by NSC 652287, a novel thiophene derivative active against human renal cancer cells. *Molecular pharmacology*. 56:478-484.

Norton, V.G., K.W. Marvin, P. Yau, and E.M. Bradbury. 1990. Nucleosome linking number change controlled by acetylation of histones H3 and H4. *The Journal of biological chemistry*. 265:19848-19852.

Nurse, P., and P. Thuriaux. 1980. Regulatory genes controlling mitosis in the fission yeast Schizosaccharomyces pombe. *Genetics*. 96:627-637.

Nurse, P., P. Thuriaux, and K. Nasmyth. 1976. Genetic control of the cell division cycle in the fission yeast Schizosaccharomyces pombe. *Molecular & general genetics : MGG*. 146:167-178.

Oliver, T.G., E. Meylan, G.P. Chang, W. Xue, J.R. Burke, T.J. Humpton, D. Hubbard, A. Bhutkar, and T. Jacks. 2011. Caspase-2-mediated cleavage of Mdm2 creates a p53-induced positive feedback loop. *Molecular cell*. 43:57-71.

Olson, E., C.J. Nievera, V. Klimovich, E. Fanning, and X. Wu. 2006. RPA2 is a direct downstream target for ATR to regulate the S-phase checkpoint. *The Journal of biological chemistry*. 281:39517-39533.

Olson, R.D., and P.S. Mushlin. 1990. Doxorubicin cardiotoxicity: analysis of prevailing hypotheses. *FASEB J.* 4:3076-3086.

Oren, M. 1999. Regulation of the p53 tumor suppressor protein. *The Journal of biological chemistry*. 274:36031-36034.

Orthwein, A., A. Fradet-Turcotte, S.M. Noordermeer, M.D. Canny, C.M. Brun, J. Strecker, C. Escribano-Diaz, and D. Durocher. 2014. Mitosis inhibits DNA double-strand break repair to guard against telomere fusions. *Science*. 344:189-193.

Osborn, A.J., S.J. Elledge, and L. Zou. 2002. Checking on the fork: the DNA-replication stress-response pathway. *Trends in cell biology*. 12:509-516.

Osborne, M.R., D.E. Wilman, and P.D. Lawley. 1995. Alkylation of DNA by the nitrogen mustard bis(2-chloroethyl)methylamine. *Chem Res Toxicol*. 8:316-320.

Paddison, P.J., J.M. Silva, D.S. Conklin, M. Schlabach, M. Li, S. Aruleba, V. Balija, A. O'Shaughnessy, L. Gnoj, K. Scobie, K. Chang, T. Westbrook, M. Cleary, R. Sachidanandam, W.R. McCombie, S.J. Elledge, and G.J. Hannon. 2004. A resource for large-scale RNA-interference-based screens in mammals. *Nature*. 428:427-431.

Pai, C.C., K.F. Hsu, S.C. Durley, A. Keszthelyi, S.E. Kearsey, C. Rallis, L.K. Folkes, R. Deegan, S.E. Wilkins, S.X. Pfister, N. De Leon, C.J. Schofield, J. Bahler, A.M. Carr, and T.C. Humphrey. 2019. An essential role for dNTP homeostasis following CDK-induced replication stress. *J Cell Sci*. 132.

Pai, C.C., and S.E. Kearsey. 2017. A Critical Balance: dNTPs and the Maintenance of Genome Stability. *Genes (Basel)*. 8.

Pardee, A.B. 1974. A restriction point for control of normal animal cell proliferation. *Proceedings of the National Academy of Sciences of the United States of America*. 71:1286-1290.

Parker, L.L., and H. Piwnica-Worms. 1992. Inactivation of the p34cdc2-cyclin B complex by the human WEE1 tyrosine kinase. *Science*. 257:1955-1957.

Patnaik, A., A. Tolcher, M. Beeram, J. Nemunaitis, G.J. Weiss, K. Bhalla, M. Agrawal, G. Nichols, S. Middleton, A. Beryozkina, N. Sarapa, R. Peck, and J. Zhi. 2015. Clinical pharmacology characterization of RG7112, an MDM2 antagonist, in patients with advanced solid tumors. *Cancer chemotherapy and pharmacology*. 76:587-595.

Pegg, A.E. 1990. Mammalian O6-alkylguanine-DNA alkyltransferase: regulation and importance in response to alkylating carcinogenic and therapeutic agents. *Cancer research*. 50:6119-6129.

Peng, C.Y., P.R. Graves, R.S. Thoma, Z. Wu, A.S. Shaw, and H. Piwnica-Worms. 1997. Mitotic and G2 checkpoint control: regulation of 14-3-3 protein binding by phosphorylation of Cdc25C on serine-216. *Science*. 277:1501-1505.

Pfister, S.X., S. Ahrabi, L.P. Zalmas, S. Sarkar, F. Aymard, C.Z. Bachrati, T. Helleday, G. Legube, N.B. La Thangue, A.C. Porter, and T.C. Humphrey. 2014. SETD2-dependent histone H3K36 trimethylation is required for homologous recombination repair and genome stability. *Cell reports*. 7:2006-2018.

Pfister, Sophia X., E. Markkanen, Y. Jiang, S. Sarkar, M. Woodcock, G. Orlando, I. Mavrommati, C.-C. Pai, L.-P. Zalmas, N. Drobnitzky, Grigory L. Dianov, C. Verrill, Valentine M. Macaulay, S. Ying, Nicholas B. La Thangue, V. D'Angiolella, Anderson J. Ryan, and Timothy C. Humphrey. 2015. Inhibiting WEE1 Selectively Kills Histone H3K36me3-Deficient Cancers by dNTP Starvation. *Cancer cell*. 28:557-568.

Phelan, M.L., S. Sif, G.J. Narlikar, and R.E. Kingston. 1999. Reconstitution of a core chromatin remodeling complex from SWI/SNF subunits. *Molecular cell*. 3:247-253.

Pines, J. 1991. Cyclins: wheels within wheels. *Cell Growth Differ.* 2:305-310.

Pines, J. 1995. Cyclins and cyclin-dependent kinases: theme and variations. *Adv Cancer Res.* 66:181-212.

Pochampally, R., B. Fodera, L. Chen, W. Shao, E.A. Levine, and J. Chen. 1998. A 60 kd MDM2 isoform is produced by caspase cleavage in non-apoptotic tumor cells. *Oncogene.* 17:2629-2636.

Powers, N.R., E.D. Parvanov, C.L. Baker, M. Walker, P.M. Petkov, and K. Paigen. 2016. The Meiotic Recombination Activator PRDM9 Trimethylates Both H3K36 and H3K4 at Recombination Hotspots In Vivo. *PLoS Genet.* 12:e1006146.

Pruitt, K., R.L. Zinn, J.E. Ohm, K.M. McGarvey, S.H. Kang, D.N. Watkins, J.G. Herman, and S.B. Baylin. 2006. Inhibition of SIRT1 reactivates silenced cancer genes without loss of promoter DNA hypermethylation. *PLoS Genet.* 2:e40.

Rea, S., F. Eisenhaber, D. O'Carroll, B.D. Strahl, Z.W. Sun, M. Schmid, S. Opravil, K. Mechtler, C.P. Ponting, C.D. Allis, and T. Jenuwein. 2000. Regulation of chromatin structure by site-specific histone H3 methyltransferases. *Nature.* 406:593-599.

Rees, M.G., B. Seashore-Ludlow, J.H. Cheah, D.J. Adams, E.V. Price, S. Gill, S. Javaid, M.E. Coletti, V.L. Jones, N.E. Bodycombe, C.K. Soule, B. Alexander, A. Li, P. Montgomery, J.D. Kotz, C.S. Hon, B. Munoz, T. Liefeld, V. Dancik, D.A. Haber, C.B. Clish, J.A. Bittker, M. Palmer, B.K. Wagner, P.A. Clemons, A.F. Shamji, and S.L. Schreiber. 2016. Correlating chemical sensitivity and basal gene expression reveals mechanism of action. *Nature chemical biology.* 12:109-116.

Reichard, P., A. Baldesten, and L. Rutberg. 1961. Formation of deoxycytidine phosphates from cytidine phosphates in extracts from Escherichia coli. *The Journal of biological chemistry.* 236:1150-1157.

Rideout, W.M., 3rd, G.A. Coetzee, A.F. Olumi, C.H. Spruck, and P.A. Jones. 1991. 5-Methylcytosine as an endogenous mutagen in the p53 tumor suppressor gene. *Princess Takamatsu Symp.* 22:207-219.

Riggs, M.G., R.G. Whittaker, J.R. Neumann, and V.M. Ingram. 1977. n-Butyrate causes histone modification in HeLa and Friend erythroleukaemia cells. *Nature.* 268:462-464.

Rivera, M.I., S.F. Stinson, D.T. Vistica, J.L. Jorden, S. Kenney, and E.A. Sausville. 1999. Selective toxicity of the tricyclic thiophene NSC 652287 in renal carcinoma cell lines: differential accumulation and metabolism. *Biochemical pharmacology.* 57:1283-1295.

Roguev, A., S. Bandyopadhyay, M. Zofall, K. Zhang, T. Fischer, S.R. Collins, H. Qu, M. Shales, H.O. Park, J. Hayles, K.L. Hoe, D.U. Kim, T. Ideker, S.I. Grewal, J.S. Weissman, and N.J. Krogan. 2008. Conservation and rewiring of functional modules revealed by an epistasis map in fission yeast. *Science.* 322:405-410.

Rousseau, D., D. Cannella, J. Boulaire, P. Fitzgerald, A. Fotedar, and R. Fotedar. 1999. Growth inhibition by CDK-cyclin and PCNA binding domains of p21

occurs by distinct mechanisms and is regulated by ubiquitin-proteasome pathway. *Oncogene*. 18:4313-4325.

Russell, M.R., K. Levin, J. Rader, L. Belcastro, Y. Li, D. Martinez, B. Pawel, S.D. Shumway, J.M. Maris, and K.A. Cole. 2013. Combination therapy targeting the Chk1 and Wee1 kinases shows therapeutic efficacy in neuroblastoma. *Cancer research*. 73:776-784.

Ruthenburg, A.J., H. Li, D.J. Patel, and C.D. Allis. 2007. Multivalent engagement of chromatin modifications by linked binding modules. *Nature reviews. Molecular cell biology*. 8:983-994.

Saito, S., H. Yamaguchi, Y. Higashimoto, C. Chao, Y. Xu, A.J. Fornace, Jr., E. Appella, and C.W. Anderson. 2003. Phosphorylation site interdependence of human p53 post-translational modifications in response to stress. *The Journal of biological chemistry*. 278:37536-37544.

Sakaguchi, K., J.E. Herrera, S. Saito, T. Miki, M. Bustin, A. Vassilev, C.W. Anderson, and E. Appella. 1998. DNA damage activates p53 through a phosphorylation-acetylation cascade. *Genes & development*. 12:2831-2841.

Sakai, T., J. Toguchida, N. Ohtani, D.W. Yandell, J.M. Rapaport, and T.P. Dryja. 1991. Allele-specific hypermethylation of the retinoblastoma tumor-suppressor gene. *Am J Hum Genet*. 48:880-888.

San-Miguel, J.F., V.T. Hungria, S.S. Yoon, M. Beksac, M.A. Dimopoulos, A. Elghandour, W.W. Jedrzejczak, A. Gunther, T.N. Nakorn, N. Siritanaratkul, P. Corradini, S. Chuncharunee, J.J. Lee, R.L. Schlossman, T. Shelekhova, K. Yong, D. Tan, T. Numbenjapon, J.D. Cavenagh, J. Hou, R. LeBlanc, H. Nahi, L. Qiu, H. Salwender, S. Pulini, P. Moreau, K. Warzocha, D. White, J. Blade, W. Chen, J. de la Rubia, P. Gimsing, S. Lonial, J.L. Kaufman, E.M. Ocio, L. Veskovski, S.K. Sohn, M.C. Wang, J.H. Lee, H. Einsele, M. Sopala, C. Corrado, B.R. Bengoudifa, F. Binlich, and P.G. Richardson. 2014. Panobinostat plus bortezomib and dexamethasone versus placebo plus bortezomib and dexamethasone in patients with relapsed or relapsed and refractory multiple myeloma: a multicentre, randomised, double-blind phase 3 trial. *Lancet Oncol*. 15:1195-1206.

Sandhu, S.K., W.R. Schelman, G. Wilding, V. Moreno, R.D. Baird, S. Miranda, L. Hylands, R. Riisnaes, M. Forster, A. Omlin, N. Kreischer, K. Thway, H. Gevensleben, L. Sun, J. Loughney, M. Chatterjee, C. Toniatti, C.L. Carpenter, R. Iannone, S.B. Kaye, J.S. de Bono, and R.M. Wenham. 2013. The poly(ADP-ribose) polymerase inhibitor niraparib (MK4827) in BRCA mutation carriers and patients with sporadic cancer: a phase 1 dose-escalation trial. *Lancet Oncol*. 14:882-892.

Schlegel, J., I. Peters, S. Orrenius, D.K. Miller, N.A. Thornberry, T.T. Yamin, and D.W. Nicholson. 1996. CPP32/apopain is a key interleukin 1 beta converting enzyme-like protease involved in Fas-mediated apoptosis. *The Journal of biological chemistry*. 271:1841-1844.

Sellers, W.R., and W.G. Kaelin. 1996. RB [corrected] as a modulator of transcription. *Biochimica et biophysica acta*. 1288:M1-5.

Senese, S., K. Zaragoza, S. Minardi, I. Muradore, S. Ronzoni, A. Passafaro, L. Bernard, G.F. Draetta, M. Alcalay, C. Seiser, and S. Chiocca. 2007. Role for histone deacetylase 1 in human tumor cell proliferation. *Molecular and cellular biology*. 27:4784-4795.

Sexl, V., J.A. Diehl, C.J. Sherr, R. Ashmun, D. Beach, and M.F. Roussel. 1999. A rate limiting function of cdc25A for S phase entry inversely correlates with tyrosine dephosphorylation of Cdk2. *Oncogene*. 18:573-582.

Sfeir, A., and L.S. Symington. 2015. Microhomology-Mediated End Joining: A Back-up Survival Mechanism or Dedicated Pathway? *Trends Biochem Sci*. 40:701-714.

Shah, N.P., J.M. Nicoll, B. Nagar, M.E. Gorre, R.L. Paquette, J. Kuriyan, and C.L. Sawyers. 2002. Multiple BCR-ABL kinase domain mutations confer polyclonal resistance to the tyrosine kinase inhibitor imatinib (STI571) in chronic phase and blast crisis chronic myeloid leukemia. *Cancer cell*. 2:117-125.

Shah, N.P., C. Tran, F.Y. Lee, P. Chen, D. Norris, and C.L. Sawyers. 2004. Overriding imatinib resistance with a novel ABL kinase inhibitor. *Science*. 305:399-401.

Shalem, O., N.E. Sanjana, and F. Zhang. 2015. High-throughput functional genomics using CRISPR-Cas9. *Nat Rev Genet*. 16:299-311.

Shin, D., E.H. Kim, J. Lee, and J.L. Roh. 2017. RITA plus 3-MA overcomes chemoresistance of head and neck cancer cells via dual inhibition of autophagy and antioxidant systems. *Redox Biol*. 13:219-227.

Shoemaker, R.H. 2006. The NCI60 human tumour cell line anticancer drug screen. *Nature reviews. Cancer*. 6:813-823.

Slamon, D.J., B. Leyland-Jones, S. Shak, H. Fuchs, V. Paton, A. Bajamonde, T. Fleming, W. Eiermann, J. Wolter, M. Pegram, J. Baselga, and L. Norton. 2001. Use of chemotherapy plus a monoclonal antibody against HER2 for metastatic breast cancer that overexpresses HER2. *The New England journal of medicine*. 344:783-792.

Songyang, Z., S. Blechner, N. Hoagland, M.F. Hoekstra, H. Piwnica-Worms, and L.C. Cantley. 1994. Use of an oriented peptide library to determine the optimal substrates of protein kinases. *Curr Biol*. 4:973-982.

Spanswick, V.J., J.M. Hartley, and J.A. Hartley. 2010. Measurement of DNA interstrand crosslinking in individual cells using the Single Cell Gel Electrophoresis (Comet) assay. *Methods Mol Biol*. 613:267-282.

Stavrovskaya, A.A., and T.P. Stromskaya. 2008. Transport proteins of the ABC family and multidrug resistance of tumor cells. *Biochemistry (Mosc)*. 73:592-604.

Stein, S., Y. Lao, I.Y. Yang, S.S. Hecht, and M. Moriya. 2006. Genotoxicity of acetaldehyde- and crotonaldehyde-induced 1,N2-propanodeoxyguanosine DNA adducts in human cells. *Mutat Res*. 608:1-7.

Strahl, B.D., and C.D. Allis. 2000. The language of covalent histone modifications. *Nature*. 403:41-45.

Strahl, B.D., P.A. Grant, S.D. Briggs, Z.W. Sun, J.R. Bone, J.A. Caldwell, S. Mollah, R.G. Cook, J. Shabanowitz, D.F. Hunt, and C.D. Allis. 2002. Set2 is a

nucleosomal histone H3-selective methyltransferase that mediates transcriptional repression. *Molecular and cellular biology*. 22:1298-1306.

Sun, W.J., H. Huang, B. He, D.H. Hu, P.H. Li, Y.J. Yu, X.H. Zhou, Z. Lv, L. Zhou, T.Y. Hu, Z.C. Yao, M.D. Lu, X. Shen, and Z.Q. Zheng. 2017. Romidepsin induces G2/M phase arrest via Erk/cdc25C/cdc2/cyclinB pathway and apoptosis induction through JNK/c-Jun/caspase3 pathway in hepatocellular carcinoma cells. *Biochemical pharmacology*. 127:90-100.

Sun, X.J., J. Wei, X.Y. Wu, M. Hu, L. Wang, H.H. Wang, Q.H. Zhang, S.J. Chen, Q.H. Huang, and Z. Chen. 2005. Identification and characterization of a novel human histone H3 lysine 36-specific methyltransferase. *The Journal of biological chemistry*. 280:35261-35271.

Suraweera, A., K.J. O'Byrne, and D.J. Richard. 2018. Combination Therapy With Histone Deacetylase Inhibitors (HDACi) for the Treatment of Cancer: Achieving the Full Therapeutic Potential of HDACi. *Front Oncol*. 8:92.

Sy, S.M., M.S. Huen, and J. Chen. 2009. PALB2 is an integral component of the BRCA complex required for homologous recombination repair. *Proceedings of the National Academy of Sciences of the United States of America*. 106:7155-7160.

Szlachta, K., C. Kuscu, T. Tufan, S.J. Adair, S. Shang, A.D. Michaels, M.G. Mullen, N.L. Fischer, J. Yang, L. Liu, P. Trivedi, E.B. Stelow, P.T. Stukenberg, J.T. Parsons, T.W. Bauer, and M. Adli. 2018. CRISPR knockout screening identifies combinatorial drug targets in pancreatic cancer and models cellular drug response. *Nat Commun*. 9:4275.

Tanaka, N., A.A. Patel, L. Tang, N.L. Silver, A. Lindemann, H. Takahashi, R. Jaksik, X. Rao, N.N. Kalu, T.C. Chen, J. Wang, M.J. Frederick, F. Johnson, F.O. Gleber-Netto, S. Fu, M. Kimmel, J. Wang, W.N. Hittelman, C.R. Pickering, J.N. Myers, and A.A. Osman. 2017. Replication Stress Leading to Apoptosis within the S-phase Contributes to Synergism between Vorinostat and AZD1775 in HNSCC Harboring High-Risk TP53 Mutation. *Clinical cancer research : an official journal of the American Association for Cancer Research*. 23:6541-6554.

Torgovnick, A., and B. Schumacher. 2015. DNA repair mechanisms in cancer development and therapy. *Front Genet*. 6:157.

Torrance, C.J., V. Agrawal, B. Vogelstein, and K.W. Kinzler. 2001. Use of isogenic human cancer cells for high-throughput screening and drug discovery. *Nature biotechnology*. 19:940-945.

Tort, F., J. Bartkova, M. Sehested, T. Orntoft, J. Lukas, and J. Bartek. 2006. Retinoblastoma pathway defects show differential ability to activate the constitutive DNA damage response in human tumorigenesis. *Cancer research*. 66:10258-10263.

Tse, C., A.R. Shoemaker, J. Adickes, M.G. Anderson, J. Chen, S. Jin, E.F. Johnson, K.C. Marsh, M.J. Mitten, P. Nimmer, L. Roberts, S.K. Tahir, Y. Xiao, X. Yang, H. Zhang, S. Fesik, S.H. Rosenberg, and S.W. Elmore. 2008. ABT-263: a potent and orally bioavailable Bcl-2 family inhibitor. *Cancer research*. 68:3421-3428.

Tsujimoto, Y. 2003. Cell death regulation by the Bcl-2 protein family in the mitochondria. *J Cell Physiol*. 195:158-167.

Tutt, A., M. Robson, J.E. Garber, S.M. Domchek, M.W. Audeh, J.N. Weitzel, M. Friedlander, B. Arun, N. Loman, R.K. Schmutzler, A. Wardley, G. Mitchell, H. Earl, M. Wickens, and J. Carmichael. 2010. Oral poly(ADP-ribose) polymerase inhibitor olaparib in patients with BRCA1 or BRCA2 mutations and advanced breast cancer: a proof-of-concept trial. *Lancet*. 376:235-244.

van Vugt, M.A., A.K. Gardino, R. Linding, G.J. Ostheimer, H.C. Reinhardt, S.E. Ong, C.S. Tan, H. Miao, S.M. Keezer, J. Li, T. Pawson, T.A. Lewis, S.A. Carr, S.J. Smerdon, T.R. Brummelkamp, and M.B. Yaffe. 2010. A mitotic phosphorylation feedback network connects Cdk1, Plk1, 53BP1, and Chk2 to inactivate the G(2)/M DNA damage checkpoint. *PLoS Biol*. 8:e1000287.

Vassilev, L.T., B.T. Vu, B. Graves, D. Carvajal, F. Podlaski, Z. Filipovic, N. Kong, U. Kammlott, C. Lukacs, C. Klein, N. Fotouhi, and E.A. Liu. 2004. In vivo activation of the p53 pathway by small-molecule antagonists of MDM2. *Science*. 303:844-848.

Verhoef, V., J. Sarup, and A. Fridland. 1981. Identification of the mechanism of activation of 9-beta-D-arabinofuranosyladenine in human lymphoid cells using mutants deficient in nucleoside kinases. *Cancer research*. 41:4478-4483.

Vermeulen, K., D.R. Van Bockstaele, and Z.N. Berneman. 2003. The cell cycle: a review of regulation, deregulation and therapeutic targets in cancer. *Cell Prolif*. 36:131-149.

Vinodhkumar, R., Y.S. Song, and T. Devaki. 2008. Romidepsin (depsipeptide) induced cell cycle arrest, apoptosis and histone hyperacetylation in lung carcinoma cells (A549) are associated with increase in p21 and hypophosphorylated retinoblastoma proteins expression. *Biomed Pharmacother*. 62:85-93.

Vizeacoumar, F.J., R. Arnold, F.S. Vizeacoumar, M. Chandrashekhar, A. Buzina, J.T. Young, J.H. Kwan, A. Sayad, P. Mero, S. Lawo, H. Tanaka, K.R. Brown, A. Baryshnikova, A.B. Mak, Y. Fedyshyn, Y. Wang, G.C. Brito, D. Kasimer, T. Makhnevych, T. Ketela, A. Datti, M. Babu, A. Emili, L. Pelletier, J. Wrana, Z. Wainberg, P.M. Kim, R. Rottapel, C.A. O'Brien, B. Andrews, C. Boone, and J. Moffat. 2013. A negative genetic interaction map in isogenic cancer cell lines reveals cancer cell vulnerabilities. *Mol Syst Biol*. 9:696.

Waddington, C.H. 1942. CANALIZATION OF DEVELOPMENT AND THE INHERITANCE OF ACQUIRED CHARACTERS. *Nature*. 150:563-565.

Wagner, E.J., and P.B. Carpenter. 2012. Understanding the language of Lys36 methylation at histone H3. *Nature reviews. Molecular cell biology*. 13:115-126.

Wali, V.B., C.G. Langdon, M.A. Held, J.T. Platt, G.A. Patwardhan, A. Safonov, B. Aktas, L. Pusztai, D.F. Stern, and C. Hatzis. 2017. Systematic Drug Screening Identifies Tractable Targeted Combination Therapies in Triple-Negative Breast Cancer. *Cancer research*. 77:566-578.

Wang, D., and S.J. Lippard. 2005. Cellular processing of platinum anticancer drugs. *Nature reviews. Drug discovery*. 4:307-320.

Wang, M., E.J. McIntee, G. Cheng, Y. Shi, P.W. Villalta, and S.S. Hecht. 2000. Identification of DNA adducts of acetaldehyde. *Chem Res Toxicol*. 13:1149-1157.

Wang, N., Y. Li, and J. Zhou. 2018. Downregulation of ribonucleotide reductase subunits M2 induces apoptosis and G1 arrest of cervical cancer cells. *Oncol Lett*. 15:3719-3725.

Wang, T., K. Birsoy, N.W. Hughes, K.M. Krupczak, Y. Post, J.J. Wei, E.S. Lander, and D.M. Sabatini. 2015. Identification and characterization of essential genes in the human genome. *Science*. 350:1096-1101.

Wanzel, M., J.B. Vischedyk, M.P. Gittler, N. Gremke, J.R. Seiz, M. Hefter, M. Noack, R. Savai, M. Mernberger, J.P. Charles, J. Schneikert, A.C. Bretz, A. Nist, and T. Stiewe. 2016. CRISPR-Cas9-based target validation for p53-reactivating model compounds. *Nature chemical biology*. 12:22-28.

Ward, J.F. 1988. DNA damage produced by ionizing radiation in mammalian cells: identities, mechanisms of formation, and reparability. *Prog Nucleic Acid Res Mol Biol*. 35:95-125.

Watanabe, N., M. Broome, and T. Hunter. 1995. Regulation of the human WEE1Hu CDK tyrosine 15-kinase during the cell cycle. *The EMBO journal*. 14:1878-1891.

Weilbacher, A., M. Gutekunst, M. Oren, W.E. Aulitzky, and H. van der Kuip. 2014. RITA can induce cell death in p53-defective cells independently of p53 function via activation of JNK/SAPK and p38. *Cell death & disease*. 5:e1318.

Wright, J.A., A.K. Chan, B.K. Choy, R.A. Hurta, G.A. McClarty, and A.Y. Tagger. 1990. Regulation and drug resistance mechanisms of mammalian ribonucleotide reductase, and the significance to DNA synthesis. *Biochemistry and cell biology = Biochimie et biologie cellulaire*. 68:1364-1371.

Wright, W.D., S.S. Shah, and W.D. Heyer. 2018. Homologous recombination and the repair of DNA double-strand breaks. *The Journal of biological chemistry*. 293:10524-10535.

Xie, P., C. Tian, L. An, J. Nie, K. Lu, G. Xing, L. Zhang, and F. He. 2008. Histone methyltransferase protein SETD2 interacts with p53 and selectively regulates its downstream genes. *Cellular signalling*. 20:1671-1678.

Yamaguchi, T., F. Cubizolles, Y. Zhang, N. Reichert, H. Kohler, C. Seiser, and P. Matthias. 2010. Histone deacetylases 1 and 2 act in concert to promote the G1-to-S progression. *Genes & development*. 24:455-469.

Yang, Y., Y. Gao, L. Mutter-Rottmayer, A. Zlatanou, M. Durando, W. Ding, D. Wyatt, D. Ramsden, Y. Tanoue, S. Tateishi, and C. Vaziri. 2017. DNA repair factor RAD18 and DNA polymerase Polkappa confer tolerance of oncogenic DNA replication stress. *The Journal of cell biology*. 216:3097-3115.

Yao, X., K. Panichpisal, N. Kurtzman, and K. Nugent. 2007. Cisplatin nephrotoxicity: a review. *Am J Med Sci*. 334:115-124.

Yoh, S.M., J.S. Lucas, and K.A. Jones. 2008. The Iws1:Spt6:CTD complex controls cotranscriptional mRNA biosynthesis and HYPB/Setd2-mediated histone H3K36 methylation. *Genes & development*. 22:3422-3434.

Yu, H.A., M.E. Arcila, N. Rekhtman, C.S. Sima, M.F. Zakowski, W. Pao, M.G. Kris, V.A. Miller, M. Ladanyi, and G.J. Riely. 2013. Analysis of tumor specimens at the time of acquired resistance to EGFR-TKI therapy in 155 patients with

EGFR-mutant lung cancers. *Clinical cancer research : an official journal of the American Association for Cancer Research*. 19:2240-2247.

Yuan, J., S. Shaham, S. Ledoux, H.M. Ellis, and H.R. Horvitz. 1993. The C. elegans cell death gene ced-3 encodes a protein similar to mammalian interleukin-1 beta-converting enzyme. *Cell*. 75:641-652.

Zawacka-Pankau, J., V.V. Grinkevich, M. Burmakin, A. Vema, K. Ridderstråle, N. Issaeva, V. Andreotti, E.R. Dickinson, E. Hedström, C. Spinnler, A. Inga, L.-G. Larsson, A. Karlén, O. Tarasova, V. Poroikov, S. Lavrenov, M. Preobrazhenskaya, M. Wilhelm, P.E. Barran, A.L. Okorokov, and G. Selivanova. 2018. Novel allosteric mechanism of p53 activation by small molecules for targeted anticancer therapy. *bioRxiv*:384248.

Zbar, B., H. Brauch, C. Talmadge, and M. Linehan. 1987. Loss of alleles of loci on the short arm of chromosome 3 in renal cell carcinoma. *Nature*. 327:721-724.

Zeman, M.K., and K.A. Cimprich. 2014. Causes and consequences of replication stress. *Nature cell biology*. 16:2-9.

Zhan, Q., M.J. Antinore, X.W. Wang, F. Carrier, M.L. Smith, C.C. Harris, and A.J. Fornace, Jr. 1999. Association with Cdc2 and inhibition of Cdc2/Cyclin B1 kinase activity by the p53-regulated protein Gadd45. *Oncogene*. 18:2892-2900.

Zhang, F., J. Ma, J. Wu, L. Ye, H. Cai, B. Xia, and X. Yu. 2009. PALB2 links BRCA1 and BRCA2 in the DNA-damage response. *Curr Biol*. 19:524-529.

Zhang, M., J. Wang, R. Yao, and L. Wang. 2013. Small interfering RNA (siRNA)-mediated silencing of the M2 subunit of ribonucleotide reductase: a novel therapeutic strategy in ovarian cancer. *Int J Gynecol Cancer*. 23:659-666.

Zhao, C.Y., V.V. Grinkevich, F. Nikulenkov, W. Bao, and G. Selivanova. 2010. Rescue of the apoptotic-inducing function of mutant p53 by small molecule RITA. *Cell Cycle*. 9:1847-1855.

Zhao, Y., and B.A. Garcia. 2015. Comprehensive Catalog of Currently Documented Histone Modifications. *Cold Spring Harb Perspect Biol*. 7:a025064.

Zhou, L., Y. Zhang, S. Chen, M. Kmieciak, Y. Leng, H. Lin, K.A. Rizzo, C.I. Dumur, A. Ferreira-Gonzalez, Y. Dai, and S. Grant. 2015. A regimen combining the Wee1 inhibitor AZD1775 with HDAC inhibitors targets human acute myeloid leukemia cells harboring various genetic mutations. *Leukemia*. 29:807-818.

Zou, L., and S.J. Elledge. 2003. Sensing DNA damage through ATRIP recognition of RPA-ssDNA complexes. *Science*. 300:1542-1548.

Zupkovitz, G., R. Grausenburger, R. Brunmeir, S. Senese, J. Tischler, J. Jurkin, M. Rembold, D. Meunier, G. Egger, S. Lagger, S. Chiocca, F. Propst, G. Weitzer, and C. Seiser. 2010. The cyclin-dependent kinase inhibitor p21 is a crucial target for histone deacetylase 1 as a regulator of cellular proliferation. *Molecular and cellular biology*. 30:1171-1181.

# 8. Appendix

## 8.1 List of Top 100 Hits for New Synthetic Lethal Compounds (0.1 μM)

| Drug | Target | RankProd | PFP | Mean ΔZ-score |
|---|---|---|---|---|
| RITA (NSC 652287) | E3 Ligase, p53 | 1.00 | 0.01 | -14.95 |
| AZD7762 | Chk | 3.46 | 0.01 | -9.45 |
| TAK-901 | Aurora Kinase | 10.58 | 0.07 | -7.14 |
| PF-477736 | Chk | 16.88 | 0.17 | -5.63 |
| Dexmedetomidine | Adrenergic Receptor | 17.15 | 0.14 | -5.01 |
| Pravastatin sodium | HMG-CoA Reductase | 17.75 | 0.12 | -4.91 |
| MK-8776 (SCH 900776) | CDK,Chk | 19.49 | 0.14 | -4.70 |
| Pentamidine | PRL Phosphatases, inhibits synthesis of DNA, RNA and protein | 21.07 | 0.14 | -5.30 |
| Triflusal | COX | 29.15 | 0.27 | -4.18 |
| Hydroxyzine 2HCl | Histamine Receptor | 29.33 | 0.25 | -4.20 |
| Amorolfine HCl | Antifungal reagent | 29.39 | 0.22 | -4.34 |
| Betulinic acid | Topoisomerase I | 30.33 | 0.22 | -4.22 |
| Lamotrigine | Sodium Channel, 5-HT Receptor | 33.39 | 0.26 | -4.56 |
| Atomoxetine HCl | 5-HT Receptor | 33.76 | 0.24 | -4.05 |
| Solifenacin succinate | AChR | 34.23 | 0.23 | -4.43 |
| Diclofenac Potassium | Nonsteroidal anti-inflammatory drug | 43.30 | 0.39 | -3.68 |
| Dihydromyricetin | Antioxidant flavonoid | 45.78 | 0.41 | -3.45 |
| Carbimazole | Antithyroid agent | 48.97 | 0.45 | -3.46 |
| Allylthiourea | Ammonia oxidation | 55.94 | 0.55 | -3.34 |
| CEP-32496 | CSF-1R, Raf | 56.19 | 0.53 | -3.39 |
| Norethindrone | Synthetic progestin | 56.44 | 0.51 | -3.34 |
| Ketorolac | COX | 61.58 | 0.58 | -3.00 |
| JTC-801 | Opioid Receptor | 65.86 | 0.63 | -3.31 |
| Reboxetine mesylate | Norepinephrine reuptake inhibitor | 66.63 | 0.63 | -3.12 |
| Alogliptin | DPP-4 | 67.53 | 0.62 | -2.99 |
| AST-1306 | EGFR | 67.57 | 0.59 | -3.41 |
| Acetylcholine Chloride | AChR | 68.15 | 0.58 | -3.08 |
| Nocodazole | Microtubule Associated, Autophagy | 68.63 | 0.57 | -3.85 |

| | | | | |
|---|---|---|---|---|
| Ethynodiol diacetate | Estrogen/progestogen Receptor | 69.35 | 0.56 | -2.93 |
| TAK-901 | Aurora kinases | 69.97 | 0.55 | -3.07 |
| Sulfamethizole | Antibacterial agent | 70.75 | 0.54 | -2.89 |
| Ropivacaine HCl | Sodium Channel | 70.82 | 0.53 | -2.93 |
| Rifaximin | Antibiotic | 73.61 | 0.54 | -2.86 |
| Griseofulvin | Microtubule Associated | 74.24 | 0.53 | -2.92 |
| Atracurium Besylate | Neuromuscular blocking agent | 74.67 | 0.52 | -2.96 |
| Icotinib | EGFR | 75.63 | 0.52 | -2.95 |
| Sirtinol | Sirtuin | 76.11 | 0.51 | -2.78 |
| EMPTY | | 76.72 | 0.51 | -2.89 |
| YO-01027 | Gamma-secretase | 81.59 | 0.54 | -2.90 |
| Rimonabant | Cannabinoid Receptor | 82.58 | 0.54 | -2.79 |
| Ticagrelor | P2 Receptor | 82.78 | 0.53 | -2.62 |
| Crenolanib (CP-868596) | PDGFR | 83.01 | 0.52 | -2.64 |
| Chloroxine | Synthetic antibacterial compound that is effective in the treatment of dandruff and seborrheic dermatitis | 85.25 | 0.53 | -2.64 |
| Milciclib (PHA-848125) | CDK | 87.13 | 0.54 | -2.76 |
| WAY-600 | mTOR | 91.83 | 0.58 | -2.71 |
| TPCA-1 | IκB/IKK | 93.73 | 0.59 | -2.66 |
| Hyodeoxycholic acid (HDCA) | Secondary bile acid, one of the metabolic byproducts of intestinal bacteria. | 95.46 | 0.59 | -2.68 |
| CHIR-124 | Chk | 96.99 | 0.60 | -2.53 |
| RG108 | Transferase, DNA Methyltransferase | 98.59 | 0.61 | -2.48 |
| Deoxyarbutin | Tyrosinase | 98.63 | 0.59 | -2.55 |
| Pidotimod | Immunostimulant | 101.40 | 0.61 | -2.52 |
| Tolcapone | Transferase | 101.65 | 0.60 | -2.55 |
| Tenovin-6 | p53 | 102.76 | 0.61 | -2.50 |
| BMY 7378 | 5-HT Receptor | 105.98 | 0.63 | -2.53 |
| AMG-900 | Aurora Kinase | 106.49 | 0.63 | -2.23 |
| Moguisteine | Novel peripheral non-narcotic antitussive drug | 106.75 | 0.62 | -2.44 |
| ADX-47273 | GluR | 106.95 | 0.61 | -2.49 |
| ONX-0914 (PR-957) | Proteasome | 107.31 | 0.60 | -2.46 |
| SB271046 | 5-HT Receptor | 108.22 | 0.60 | -2.31 |

| | | | | |
|---|---|---|---|---|
| Fenbendazole | Broad spectrum benzimidazole anthelmintic used against gastrointestinal parasites | 112.15 | 0.62 | -2.28 |
| Atglistatin | ATGL | 113.45 | 0.62 | -2.37 |
| AM251 | Cannabinoid Receptor | 113.58 | 0.62 | -2.40 |
| S-Ruxolitinib (INCB018424) | JAK | 115.99 | 0.63 | -1.90 |
| Doxycycline HCl | MMP,Others | 118.00 | 0.64 | -2.40 |
| HMN-214 | PLK | 120.66 | 0.66 | -2.21 |
| Azlocillin sodium salt | Acylampicillin with a broad spectrum against bacteria | 121.19 | 0.65 | -2.35 |
| Semagacestat (LY450139) | Gamma-secretase | 122.39 | 0.65 | -1.72 |
| Bisacodyl | Stimulant laxative drug that works directly on the colon to produce a bowel movement. | 124.74 | 0.67 | -2.16 |
| Caspofungin Acetate | Caspofungin acetate is a lipopeptide antifungal drug. | 127.15 | 0.68 | -2.29 |
| Camostat Mesilate | Trypsin-like protease inhibitor, inhibits airway epithelial sodium channel (ENaC), trypsin, prostasin, and matriptase. | 127.17 | 0.67 | -2.24 |
| OC000459 | GPR | 127.28 | 0.66 | -2.24 |
| PF-4981517 | P450 (e.g. CYP17) | 128.39 | 0.66 | -2.06 |
| CCT137690 | Aurora Kinase | 129.24 | 0.66 | -1.63 |
| Bufexamac | COX | 130.64 | 0.66 | -2.14 |
| Lonafarnib | Transferase | 132.70 | 0.66 | -2.21 |
| Canagliflozin | SGLT | 137.11 | 0.69 | -2.18 |
| GSK1838705A | IGF-1R, ALK | 139.37 | 0.70 | -1.96 |
| Lorcaserin HCl | 5-HT Receptor | 140.41 | 0.70 | -2.01 |
| Otilonium Bromide | AChR | 142.45 | 0.71 | -2.12 |
| Aminothiazole | Aminothiazole can be used as a thyroid inhibitor and it has antibacterial activity. | 146.88 | 0.74 | -1.88 |
| Schisandrin B (Sch B) | Most abundant dibenzocyclooctadiene lignan present in the traditional Chinese medicinal herb Schisandra chinensis (Turcz.) Baill. | 147.36 | 0.73 | -2.02 |
| Darifenacin HBr | AChR | 148.27 | 0.73 | -1.87 |

| | | | | |
|---|---|---|---|---|
| Chlorothiazide | Chlorothiazide is a diuretic and antihypertensive. | 150.24 | 0.74 | -1.75 |
| Torcetrapib | CETP | 150.85 | 0.74 | -2.03 |
| Lithocholic acid | Lithocholic acid is a toxic secondary bile acid, causes intrahepatic cholestasis, has tumor-promoting activity, its toxic effect can be protected after it activates the vitamin D receptor, PXR and FXR. | 151.10 | 0.73 | -2.08 |
| HER2-Inhibitor-1 | HER2, EGFR | 153.45 | 0.74 | -2.02 |
| Carvedilol | Adrenergic Receptor | 154.39 | 0.73 | -1.99 |
| Ornidazole | Ornidazole is a 5-nitroimidazole derivative with antiprotozoal and antibacterial properties against anaerobic bacteria. | 155.95 | 0.74 | -1.99 |
| Nilvadipine | Calcium Channel | 156.69 | 0.73 | -1.97 |
| Nafcillin Sodium | Nafcillin sodium reversibly inhibits β-lactamase with Kd of 33 mM. | 159.41 | 0.74 | -1.90 |
| Anacetrapib (MK-0859) | CETP | 159.73 | 0.74 | -1.92 |
| Phenazopyridine HCl | Phenazopyridine HCl a local analgesic that has been used in urinary tract disorders. | 160.86 | 0.74 | -1.94 |
| WHI-P154 | JAK, EGFR | 160.92 | 0.73 | -1.97 |
| AZD 7762 hydrochloride | Chk1 | 161.25 | 0.73 | -1.84 |
| Aloperine | Aloperine is exhibits anti-inflammatory, antibacterial, antiviral, and anti-tumor properties. | 163.22 | 0.73 | -1.92 |
| SB705498 | TRPV | 163.35 | 0.73 | -1.42 |
| KX2-391 | Src | 165.18 | 0.73 | -1.14 |
| Mexiletine HCl | Mexiletine HCl belongs to Class IB anti-arrhythmic group of medicines, inhibits sodium channels to reduce the inward sodium current. | 167.25 | 0.74 | -1.73 |

## 8.2 List of Top 100 Hits for Synergistic Compounds (0.1 μM)

| Drug | Target | RankProd | PFP | Mean ΔZ-score |
|---|---|---|---|---|
| MK-8776 (SCH 900776) | CDK,Chk | 14.42 | 0.30 | -6.66 |
| LY2603618 | Chk | 22.58 | 0.30 | -5.37 |
| Elesclomol (STA-4783) | HSP (e.g. HSP90) | 27.50 | 0.34 | -8.07 |
| YM155 (Sepantronium Bromide) | Survivin | 28.14 | 0.31 | -7.89 |
| Ondansetron HCl | 5-HT Receptor | 31.08 | 0.36 | -7.43 |
| 17-DMAG (Alvespimycin) HCl | HSP (e.g. HSP90) | 51.61 | 0.69 | -7.31 |
| Manidipine | Calcium Channel | 52.99 | 0.67 | -4.12 |
| JNJ-26854165 (Serdemetan) | p53, E3 Ligase | 53.07 | 0.63 | -4.76 |
| Vincristine | Microtubule Associated, Autophagy | 56.71 | 0.67 | -7.19 |
| Paeonol | Monoamine oxidase | 57.45 | 0.64 | -4.04 |
| AUY922 (NVP-AUY922) | HSP (e.g. HSP90) | 58.16 | 0.62 | -6.92 |
| Mycophenolic acid | Immunosuppressant agent | 59.09 | 0.61 | -6.07 |
| Epothilone A | Microtubule Associated | 60.87 | 0.55 | -7.16 |
| PCI-24781 (Abexinostat) | HDAC | 60.99 | 0.53 | -4.63 |
| PF-477736 | Chk | 61.16 | 0.51 | -2.76 |
| GDC-0941 | PI3K | 65.38 | 0.53 | -5.17 |
| Alprostadil | Alprostadil is used as a drug in the treatment of erectile dysfunction and has vasodilatory properties. | 65.53 | 0.51 | -6.70 |
| 2-Thiouracil | 2-Thiouracil is a thiolated uracil derivative that is a known antihyperthyroid agent. | 68.88 | 0.51 | -3.13 |
| Nepafenac | Nepafenac is a non-steroidal anti-inflammatory agent. | 70.82 | 0.51 | -5.89 |
| Pramiracetam | Pramiracetam is a more potent nootropic drug derived from piracetam. | 71.06 | 0.49 | -3.74 |

| | | | | |
|---|---|---|---|---|
| Nanchangmycin | Nanchangmycin (dianemycin) is a polyether antibiotic with similar structure to dianemycin and is very active against a broad spectrum of harmful nematodes and insects but not for for mammals and plants. | 72.88 | 0.50 | -4.02 |
| Nutlin-3 | E3 Ligase, Mdm2 | 73.89 | 0.50 | -5.23 |
| LY2603618_Rabusertib | Chk2 | 74.67 | 0.49 | -4.02 |
| Levetiracetam | Levetiracetam is an antiepileptic compound. | 77.72 | 0.52 | -5.19 |
| AG-490 (Tyrphostin B42) | JAK, EGFR | 80.56 | 0.55 | -4.64 |
| H 89 2HCl | PKA | 81.85 | 0.55 | 1.13 |
| Tenofovir Disoproxil Fumarate | Reverse Transcriptase | 83.52 | 0.55 | -5.69 |
| Losmapimod (GW856553X) | p38 MAPK | 83.62 | 0.54 | -4.24 |
| Paclitaxel | Microtubule Associated, Autophagy | 84.73 | 0.54 | -6.42 |
| Sorafenib Tosylate | PDGFR, Raf, VEGFR | 84.80 | 0.53 | -4.78 |
| Dioscin | Dioscin is a saponin extracted and isolated from Polygonatum Zanlanscianense Pamp, showing antitumor activities. | 85.32 | 0.52 | -3.55 |
| Amisulpride | Dopamine Receptor | 86.10 | 0.52 | -6.29 |
| Cathepsin Inhibitor 1 | Cathepsin (L, L2, S, K, B) | 86.90 | 0.52 | -3.16 |
| Clofarabine | DNA/RNA Synthesis | 87.91 | 0.52 | -6.29 |
| Thiazovivin | ROCK | 91.46 | 0.54 | -5.51 |
| Lenvatinib (E7080) | VEGFR | 92.07 | 0.54 | -4.61 |
| Geldanamycin | HSP (e.g. HSP90), Autophagy | 93.38 | 0.54 | 0.03 |
| GSK1904529A | IGF-1R | 93.67 | 0.53 | -4.12 |
| Phenytoin | Sodium Channel | 97.21 | 0.55 | -3.33 |
| TSU-68 (SU6668, Orantinib) | VEGFR, PDGFR, FGFR | 97.24 | 0.54 | -5.57 |
| Decitabine | DNA Methyltransferase | 98.94 | 0.55 | -4.94 |

| | | | | |
|---|---|---|---|---|
| Naringin | Naringin is a flavanone glycoside, which exerts a variety of pharmacological effects such as antioxidant activity, blood lipid lowering, anticancer activity, and inhibition of cytochrome P450 enzymes. | 103.96 | 0.58 | -3.06 |
| Ispinesib (SB-715992) | Kinesin | 104.70 | 0.58 | -6.09 |
| Droxinostat | HDAC | 105.94 | 0.58 | -4.79 |
| MK-0752 | Gamma-secretase, Beta Amyloid | 107.09 | 0.59 | -2.94 |
| Daclatasvir (BMS-790052) | HCV Protease | 108.03 | 0.58 | -5.42 |
| TAPI-1 | ADAM17/TACE | 108.93 | 0.58 | -3.20 |
| Ponatinib (AP24534) | PDGFR, FGFR, VEGFR, Bcr-Abl | 109.40 | 0.58 | -5.37 |
| Ganetespib (STA-9090) | HSP (e.g. HSP90) | 110.23 | 0.57 | -5.89 |
| PD184352 (CI-1040) | MEK | 111.84 | 0.58 | -4.01 |
| Epothilone B (EPO906, Patupilone) | Microtubule Associated | 113.10 | 0.58 | -5.67 |
| Ciproxifan | Histamine Receptor | 113.59 | 0.57 | -3.01 |
| Omeprazole | Autophagy,Proton Pump | 114.89 | 0.58 | -3.44 |
| GSK1838705A | IGF-1R, ALK | 115.49 | 0.57 | -3.02 |
| TTNPB (Arotinoid Acid) | RAR agonist, inhibits binding of [3H]tRA with IC50 of 5.1 nM, 4.5 nM, and 9.3 nM for human RARα, β, and γ, respectively. | 122.68 | 0.63 | -2.91 |
| Levonorgestrel | Levonorgestrel(Levonelle) is a synthetic progestogen used as an active ingredient in some hormonal contraceptives. | 125.67 | 0.64 | 3.32 |
| Tolbutamide | Potassium Channel | 125.72 | 0.64 | -3.06 |
| PH-797804 | p38 MAPK | 126.00 | 0.63 | -2.14 |
| 6H05 | Rho | 126.72 | 0.63 | -3.49 |
| Edaravone | Edaravone, a strong novel free radical scavenger, is used for treatment of | 130.11 | 0.65 | -5.36 |

| | | | | |
|---|---|---|---|---|
| | patients with acute brain infarction. | | | |
| Carfilzomib (PR-171) | Proteasome | 132.88 | 0.66 | 0.82 |
| Azithromycin | Autophagy | 134.52 | 0.66 | -2.51 |
| Raltitrexed | DNA/RNA Synthesis | 135.87 | 0.67 | -3.45 |
| Brivanib (BMS-540215) | FGFR, VEGFR | 136.73 | 0.67 | -3.88 |
| Fluorouracil (5-Fluoracil, 5-FU) | DNA/RNA Synthesis | 137.24 | 0.66 | -3.24 |
| VX-680 (Tozasertib, MK-0457) | Aurora Kinase | 139.60 | 0.68 | -5.10 |
| CUDC-907 | PI3K, HDAC | 140.97 | 0.68 | 0.86 |
| Obatoclax Mesylate (GX15-070) | Bcl-2 family | 141.29 | 0.68 | -2.43 |
| Sofosbuvir (PSI-7977, GS-7977) | DNA/RNA Synthesis | 142.05 | 0.66 | -2.57 |
| Daphnetin | DNA/RNA Synthesis | 142.10 | 0.66 | -2.59 |
| Agomelatine | 5-HT Receptor | 144.14 | 0.67 | -3.88 |
| Bufexamac | COX | 146.59 | 0.68 | -2.41 |
| Fluvoxamine maleate | 5-HT Receptor | 147.62 | 0.68 | -4.80 |
| Dinaciclib (SCH727965) | CDK | 148.96 | 0.68 | 1.07 |
| Cladribine | DNA/RNA Synthesis | 150.50 | 0.69 | -4.04 |
| Propafenone HCl | Sodium Channel | 150.75 | 0.68 | -3.32 |
| VUF 10166 | 5-HT Receptor | 155.28 | 0.71 | -2.12 |
| Triptolide (PG490) | Triptolide is a diterpene triepoxide, immunosuppresive agent extracted from the Chinese herb Tripterygium wilfordii. | 156.48 | 0.71 | 1.15 |
| ENMD-2076 | Aurora Kinase, FLT3, VEGFR | 157.11 | 0.71 | -3.95 |
| VX-745 | p38 MAPK | 157.53 | 0.70 | -2.95 |
| AP26113 | ALK | 159.00 | 0.71 | -2.60 |
| Luteolin | PDE | 161.05 | 0.72 | -2.82 |
| XL880 (Foretinib) | cMET, VEGFR2 | 162.11 | 0.72 | -2.21 |
| ZM 336372 | Raf | 162.97 | 0.72 | -2.17 |
| Benidipine HCl | Calcium Channel | 163.22 | 0.71 | -1.64 |